Fertilizer Interactions With Micronutrients In Tropical Volcanic Soils

Róger Armando Fallas Corrales

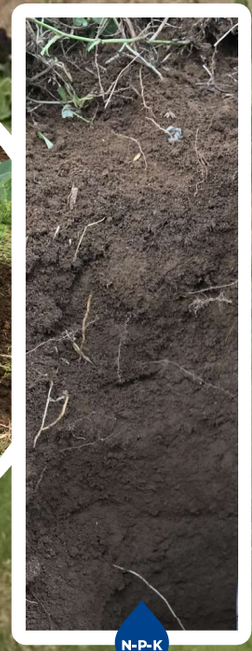

Fertilizer Interactions With Micronutrients In Tropical Volcanic Soils

Róger Armando Fallas Corrales

Propositions

1. The nutrient availability assessment based only on routine soil extraction methods lacks theoretical and experimental support.
   (This thesis)

2. The estimation of retardation factors based on linear adsorption coefficients (Kd) leads to incorrect conclusions about solute transport in soil systems.
   (This thesis)

3. Agricultural scientists must first focus on health issues related to pesticide use before aiming to increasing crop yields.

4. Not using the principle of precaution in agricultural practice may lead to environmental problems that affect society.

5. The short-term economic vision of humanity prevents the effective use of the energy available in the different production systems.

6. What is defined as a good research idea is a matter of temporary and spatial scales.

Propositions belonging to the thesis entitled:
Fertilizer interactions with micronutrients in tropical volcanic soils.

Róger Armando Fallas-Corrales
Wageningen, Tuesday 1 November 2022

Fertilizer interactions with micronutrients in tropical volcanic soils

Roger A. Fallas Corrales

Thesis Committee

Promotors
Prof. Dr V Geissen
Personal chair at the Soil Physics and Land Management Group
Wageningen Universiteit & Research

Prof. Dr SEATM van der Zee
Personal chair at the Soil Physics and Land Management Group
Wageningen Universiteit & Research

Co-promotor:
Dr JCL Meeussen
Senior Scientist, Nuclear Research and Consultancy Group (NRG), Petten
Associate Professor, Faculty of Civil Engineering and Geosciences, Delft University of Technology

Other members
Dr J.J. Dijkstra, TNO Geological Survey of The Netherlands, Utrecht
Dr JJ Stoorvogel, Wageningen Universiteit & Research
Dr A. Alaoui, University of Bern, Switzerland
Dr JE Groenenberg, Wageningen Universiteit & Research

This research was conducted under the auspices of the Graduate School Wageningen Institute for Environment and Climate Research and the Research School for Socio-Economic and Natural Sciences of the Environment (SENSE).

Fertilizer interactions with micronutrients in tropical volcanic soils

Roger A. Fallas Corrales

Thesis

submitted in fulfilment of the requirements for the degree of doctor
at Wageningen University,
by the authority of the Rector Magnificus,
Prof. Dr A.P.J. Mol,
in the presence of the
Thesis Committee appointed by the Academic Board
to be defended in public
on Tuesday 1 November 2022
at 4 p.m. in the Omnia Auditorium.

Roger A. Fallas Corrales
Fertilizer interactions with micronutrients in tropical volcanic soils, 151 pages

PhD thesis, Wageningen University, Wageningen, the Netherlands (2022)
With references, with summary in English

ISBN: 978-94-6447-381-0
DOI: https://doi.org/10.18174/576126

Table of contents

Chapter 1

General Introduction

Background information for the development of this research:

Around the year 2010, we studied nutrient management for papaya (*Carica papaya* L.) production systems in Costa Rica. The main reason to study these production systems was that papaya is principally grown by small farmers in Costa Rica, who generally operated under low input conditions and limited technical assistance. In addition, there was a general lack of essential information about the correct management of this crop. Firstly, we characterized the nutrient uptake for a high-yielding papaya hybrid (Figure 1.1) (Fallas et al., 2014). As a result, we found that papaya absorbed amounts of nutrients that exceed the quantities typically applied by farmers, and the fertilizer amounts previously applied were not compensating for total plant nutrient uptake. The application of lower quantities of fertilizer compared to the plant nutrient uptake have several consequences for growers and for the soil system, for instance low productivity per unit area, and depletion of nutrients. Additionally, the nutrient management in papaya production systems is difficult because of the variation of the nutrient requirements over time. Papaya nutrient uptake is concentrated in short periods of time (Figure 1.1), which complicates the correct supply of highly demanded nutrients according to their uptake by the plant. Excessive input of a specific fertilizer in the soil could produce side effects like competition with other ions and increased leaching rates.

According to previous observations of the high nutrient demand for the papaya production systems, the growers have increased the addition of fertilizer rates (basically N-P-K) considerably, but this decision lacked agronomical and environmental evidence that justify this practice. Consequently, we have developed field experiments to evaluate the agronomical effects (possible decreasing of yield gaps) of the application of increased N and K fertilizer rates in papaya. The results of this experiment for a dystric volcanic soil are shown in Figure 1.2. From these experiments we observed a noticeable increase in the number of fruits per plant when adding high rates of N and K. These results thus support the use of high fertilizer rates in papaya production systems.

The decision to apply increased fertilizer rates for papaya production systems, however, did not consider the environmental consequences of the movement of concentrated solutions through these soils mainly because the possible consequences were not completely understood. Concerned about potential environmental implications due to increased nutrient management in papaya production systems, we realized that the addition of high fertilizer rates is a common practice in other large-scale agricultural production systems and is common for intensive production systems developed in permeable volcanic soils. For instance, more than 43.000 hectares are currently cultivated with bananas in Costa Rica (CORBANA, 2022), receiving high rates of N-P-K fertilizers to account for the high yields required by these intensive production systems. An important fraction of this area is cultivated in permeable volcanic soils. Also, Cattan et al. (2006) mentioned that banana production systems from the Caribbean, Central America, oceanic Asia,

and some parts of Africa are principally concentrated on humid tropical climates, and over young volcanic soils, where runoff and leaching losses could be important. In their study Cattan et al. (2006) found that runoff losses are moderate for the volcanic soil evaluated (runoff coefficients of 5 to 11%); consequently, in volcanic soils with high infiltration capacity, the leaching losses and underground solute transport processes could attain important dimensions.

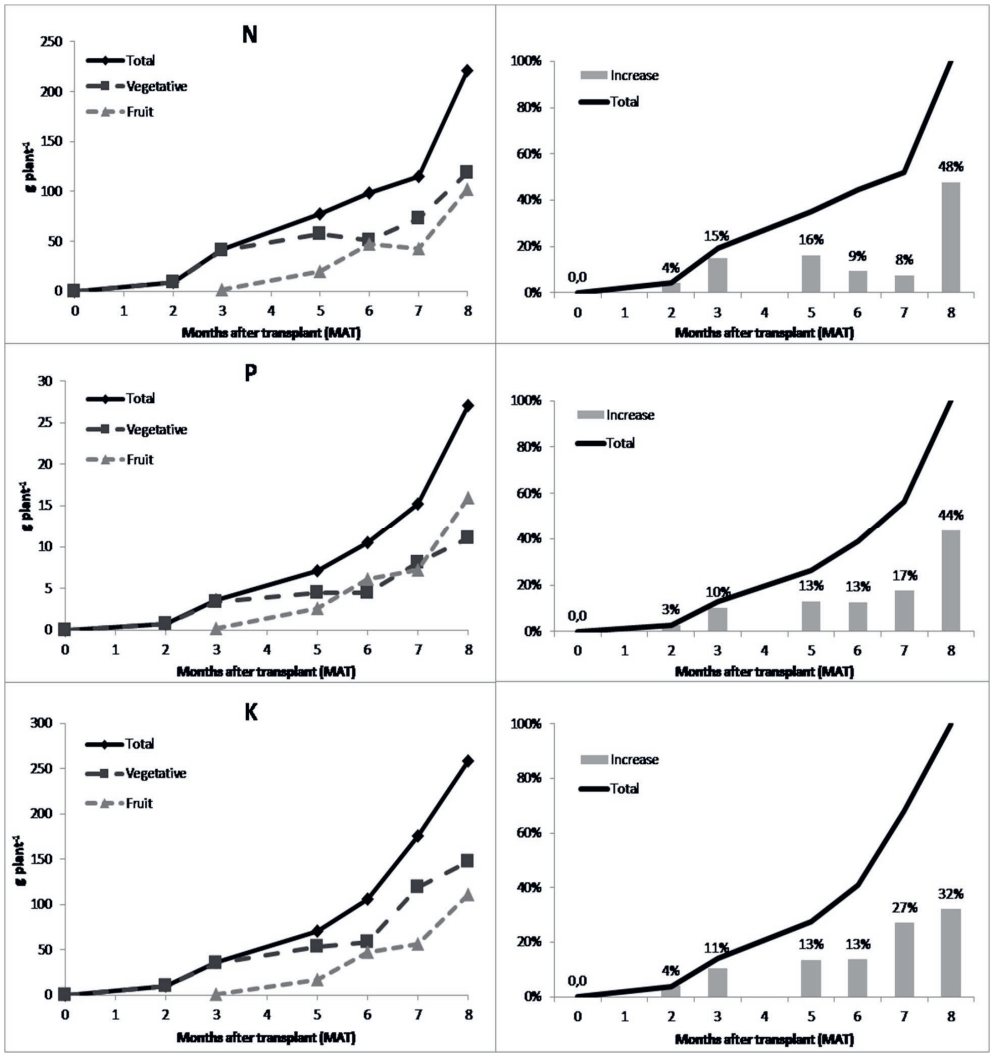

Figure 1.1. Nutrient accumulation (N-P-K) by Carica papaya L. cv. Pococí in the Atlantic Region of Costa Rica for a period of eight months after the transplanting (from Fallas-Corrales and van der Zee, 2020; Fallas et al., 2014).

Because of the specific physical properties of volcanic soils (low bulk density, low penetration resistance, high water storage, and good drainage), these soils are commonly used for intensive agricultural production of nutrient-demanding crops such as papaya, banana and some vegetables (Cattan et al., 2006; Perret and Dorel, 1999; Pinochet et al., 2018). Therefore, the application of high rates of nutrients is a common pattern in these soil systems. For instance, in the lowland areas of tropical volcanic regions, banana is produced at large scales (Cattan et al., 2006; Comte et al., 2018; CORBANA, 2022; Perret and Dorel, 1999; Sansoulet et al., 2007). Therefore, these banana production areas are facing a similar situation as highlighted for papaya –a high nutrient demand and the consequent application of very high fertilizer rates—, which could develop other collateral environmental problems like groundwater contamination, excessive nutrient leaching (including scarce micronutrients), and increased availability of undesired elements like heavy metals.

After observing that papaya yield increased remarkably when applying very high rates of nutrients (N-P-K) and considering the potential environmental issues of adding very high fertilizer rates, some research questions emerged and featured the present Ph.D. dissertation. First, we were curious about the impact of the addition of high quantities of fertilizers in volcanic soil systems, mainly regarding the effect of multi-component adsorption interactions and transport between the added fertilizer and the scarce micronutrients that commonly constrain the plant production in the tropical volcanic soils. Then, regarding the solute transport processes, we investigated the implications of significant changes in the soil solution composition on the hydrodynamic solute transport parameters commonly used for modeling nutrient transport in volcanic soil systems. The latter because the volcanic soils from tropical regions are typically characterized by permeable soils and receive very high precipitation rates (Cattan et al., 2006; Perret and Dorel, 1999), which could result in increased leaching losses.

Volcanic soils characteristics and fertilization related issues

Andosols are an important group of soils derived from volcanic ejecta materials (tephra, ash, glass), which by weathering processes, evolve into nanocrystalline minerals like allophane, imogolite, ferrihydrite, and aluminum-humus complexes. These soils cover around 1% of the earth's surface but support about 10% of the world population (Gonzalez-Rodriguez and Fernandez-Marcos, 2018) and store more than 4 % of the soil organic carbon of the world (Eswaran et al., 1993). Andosols typically have a low content of exchangeable cations; in most cases, these soils are present in humid to per-humid climates. Additionally, andosols have low permanent and high variable charge, a very high phosphate fixation capacity, a very high water retention and infiltration capacity, and high organic carbon contents on the upper soil horizons (Alvarado, 1982; Cattan et al., 2006; Gonzalez-Rodriguez and Fernandez-Marcos, 2018; Montalvo et al., 2015; Nanzyo et al., 1993a, 1993b; Wada, 1985). The clay mineralogy of andosols is typically dominated

by allophane and imogolite in humid environments with low organic matter inputs and periodic deposition of new volcanic materials, while halloysite is present in dryer environments. For instance, the volcanic soils from the alluvial plain in the Caribbean region of Costa Rica are characterized by the frequent depositions of new material (volcanic origin) product of constant flooding and transport of new material from the upper hills to the lowlands, where the material is kept in a moist condition for most of the time.

According to several authors (Alvarado, 1982; Gonzalez-Rodriguez and Fernandez-Marcos, 2018; Hashimoto et al., 2012; Montalvo et al., 2015; Nanzyo et al., 1993a), the major limiting factor for agricultural production in andosols is a very high phosphate fixation capacity. Actually, the percentage of phosphate retention is a classification criterion for defining andosols (Shoji, 1985). In this regard, Hashimoto et al. (2012) found that phosphate retention capacity of andosols principally correlates with the Al content determined in ammonium oxalate extract for allophanic soils and with Al content determined by pyrophosphate extract in non-allophanic soils. The agricultural volcanic soils normally receive high rates of phosphate fertilizer to compensate for the high phosphate fixation, which by multi-component interactions could affect the adsorption of other nutrients like boron. Although Atique-ur-Rehman et al. (2018) highlighted the importance of P-B interactions, these interactions and their mechanisms have not been thoroughly investigated for volcanic soil systems.

Boron deficiencies are common in agricultural production systems developed in volcanic soils (Shorrocks, 1997; Sillanpää, 1982), and boron deficiencies have been reported in more than 80 countries affecting a great variety of crops (more than 130 crops) (Shorrocks, 1997), including woody plants with symptoms like reduction of growing points and deformity of organs (Wang et al., 2015). For andosols of Ecuador, Tollenaar (1969) mentioned that several monocotyledonous crops commonly show boron deficiencies in these cultivated volcanic soils areas, while there are reports of boron deficiencies in papayas cultivated in volcanic soils from Hawaii (Nelson, 2012). This situation agrees with the appearance of boron deficiency symptoms observed for papaya production systems in the Caribbean alluvial plains of Costa Rica (the sampled site for present dissertation). However, as boron solubility and solution pH negatively correlate for pure and multi-surface systems (Goldberg, 2004; Keren and Sparks, 1994; Van Eynde et al., 2020), the appearance of boron deficiencies in low pH volcanic soils is not expected.

The occurrence of boron deficiencies depends on the plant species. For instance, in some plant species boron is immobile in the phloem, while for others is mobile (Shu et al., 1997). Furthermore, boron deficiency symptoms sometimes are observed only during the reproductive stages of the crop development, with symptoms like bumpy fruit in papaya (*Carica papaya* L.) (Nautiyal et al., 1986; Nelson, 2012; Wang and Ko, 1975), abscission and lower number of seeds in green gram (*Vigna radiata*) (Bell et al., 1990), or fruit drop in apple (Zude et al., 1997). On the other hand, there is a small range in concentrations between

boron sufficiency and toxicity (Chapman et al., 1997), which makes necessary a thorough comprehension of boron adsorption mechanisms and processes to correct boron deficiency problems, avoiding the occurrence of toxicity related to an erroneous boron supply.

Consequently, in Chapter 2 the effect of high phosphate solution concentrations on boron adsorption was assessed. By modeling, we increased our understanding of inferred the boron (boric acid) adsorption mechanisms for a volcanic soil system. As volcanic soil systems characterize by high permeability, an increased boron solution concentration under high precipitation regimes could result in increased boron leaching rates. Therefore, if competitive interactions between boric acid and phosphate exist, there could be increased boron losses from these volcanic soil systems. At low pH, the dominant boron species in aqueous solution corresponds to boric acid (Duffin et al., 2011), and plants mostly uptake boron in the form of boric acid (Brdar-Jokanović, 2020), both observations indicate the importance of understanding the adsorption behavior of boric acid in soil systems. We focused on phosphate-boron interactions because phosphate is applied at constant and high rates in tropical volcanic soils, while boron deficiencies are common in acid volcanic soils from different regions. The cause of the B deficiency appearance in these low pH soils is unclear, as boron solubility should increase at low pH.

It is therefore not completely clear whether the observed boron deficiency in acid volcanic soils is caused by very strong adsorption to the soil surfaces (e.g., allophane, ferrihydrite, organic matter) or by increased solubility produced by the low pH and enhanced leaching produced by the strong rainfall rates commonly observed in these volcanic soil regions. Understanding boron adsorption processes in volcanic soils will be helpful to improve management of boron deficiencies in such soils.

Effects of the addition of very high fertilizer rates on intensive agricultural systems:

Optimizing the timing of fertilizer application in intensive agricultural systems with high nutrient-demanding crops is challenging, mainly in the humid or very humid regions where leaching losses can be excessive. Sub-optimal timing between nutrient addition and plant uptake could cause a significant increase of the solution ionic strength, pH changes, and probably ionic competition that potentially affect the nutrient availability and leaching. In intensive production systems, N, P, and K fertilizers are applied at constant high rates to account for the high crop demand (as evidenced in Figure 1.1), and the high phosphate fixation previously highlighted for volcanic soils.

Among these major nutrients (N-P-K), potassium management has special importance as it is the most demanded nutrient for some crops like banana and papaya. Potassium has been applied in large

amounts for decades in some soils (Khan et al., 2013). Many crops require high potassium amounts during short periods of time. For instance, in annual crops like soybean, there is a low potassium accumulation rate during the vegetative phenological stages and a very high accumulation rate during reproductive stages (Fernández et al., 2009). Consequently, high potassium rates are commonly applied at the beginning of reproductive stages. These periods of intensive fertilizer applications do not necessarily match in time with the crop demand. As well, the high potassium demand at reproductive stages it is even more critical for semi-perennial crops like papaya and banana, for these crops concurrently occur the development of vegetative and reproductive tissues once the reproductive stage starts. This generates an extremely high demand for nutrients during these crop development stages. For instance, the total amount of potassium accumulated by the papaya crop from transplanting up to 9 months after transplant was about 415 kg of potassium per hectare (Figure 1.1), but more than 50% of this amount was accumulated between the months 7 to 9 (Fallas-Corrales and van der Zee, 2020; Fallas et al., 2014). This very high demand for potassium is related to the fruit filling plus the production of new vegetative tissue.

For high nutrient-demanding crops like papaya, the crop yield is strongly related to the rate of nutrient supply. In most of these cases, the fertilizer recommendations follow the results of field experiments that evaluate the yield response at different fertilizer rates.

For example, in Costa Rica, we observed a strong dependence of the papaya fruit yield on the potassium and nitrogen fertilizer rates, and a strong interaction between these nutrients and fruit yield (Fallas-Corrales and van der Zee, 2020) (Figure 1.2).

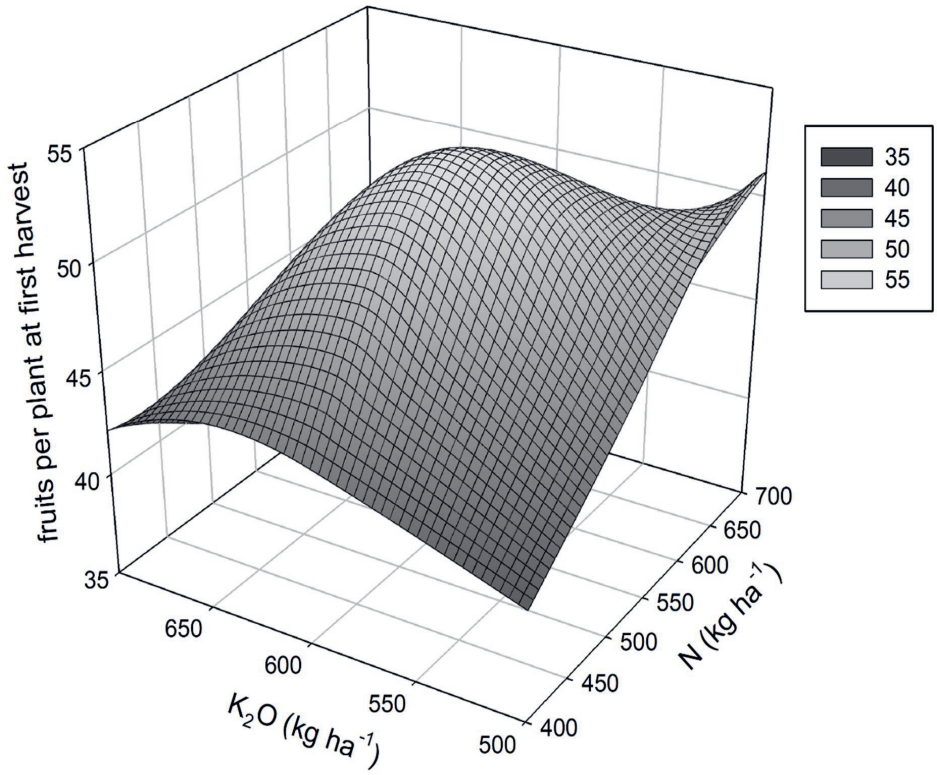

Figure 1.2. Effect of nitrogen and potassium fertilizer rates on the number of fruits per plant at the stage of the first harvest in Carica papaya L. cv. Pococí. The experiment was developed in a commercial papaya plantation field located at La Sonia, Pococí, Costa Rica. The nitrogen and potassium fertilizer rates corresponds to the cumulative amount applied during nine months. From Fallas-Corrales and van der Zee (2020).

The principal disadvantage of recommending fertilizer rates based on regional experiments of nutrient rates is the implicit risk to contaminate groundwater sources, as this approach only considers the agronomical effect of fertilizer additions, but do not take into account the complex interactions and processes of nutrient adsorption and leaching of nutrients from soil systems.

Based on the previous results, improving fertilizer management for intensive production systems requires a precise match between fertilizer application timing and its uptake by the crop. Excessive leaching, nutrient misbalances, and complex nutrient multi-component interactions could occur otherwise, which

affects sustainable production in intensive agricultural systems. A significant concern is the application of very high concentrations of N-P-K, but without the application of extra micronutrients (e.g., Zn and B) or major cations (e.g., Mg and Ca). Furthermore, the implications of the addition of highly concentrated solutions on the soil solution reactions and on nutrient transport parameters in these porous systems are commonly disregarded.

The addition of high rates of potassium chloride (KCl) modifies the soil solution pH (Du et al., 2010), and increases the ionic strength, which could increase the solubilization of nutrients and undesired elements (Boekhold et al., 1993; Lagas et al., 1984; Nunes et al., 2022). Additionally, prolonged potassium overfertilization has been associated with a reduction of Ca and Mg accumulation in the soil and its consequent lower uptake by the plants (Gransee and Führs, 2013; Hogg, 1960; Jakobsen, 1993; Ohno and Grunes, 1985). The types of (mis)management could have serious adverse effects on crop production on volcanic soils.

In Chapter 3, we evaluated the multi-component effect of high potassium chloride applications on zinc solubilization and transport considering the following observations: 1) potassium is required and applied at very high rates in fruit production systems developed in volcanic soils (Fallas et al., 2014; Turner and Barkus, 1983), 2) in general potassium has been excessively applied in agricultural production systems (Khan et al., 2013), and 3) the addition of high rates of potassium to soil systems could modify chemical factors like pH and ionic strength that directly or indirectly affect the zinc adsorption-desorption process. In addition, zinc frequently constrains crop production in the Costa Rican volcanic soils (Mendez and Bertsch, 2012). Therefore, if competitive interactions exist, zinc deficiencies in humid volcanic soil systems could be aggravated by adding high potassium rates.

Nutrient interactions in soil systems

At least two principal mechanisms should be understood for modeling the nutrient availability and transport in soil systems mechanistically. The first corresponds to the chemical processes that nutrients experience in the complex multi-component soil systems, where the adsorption process plays a major role. The second corresponds to complex physical processes that drive the movement of saline solutions in the porous soil systems. The availability, storage, and transport of these nutrients in soils will depend on the relationship between water content and excess water input with sorption and desorption reactions.

The sorption process results from attractive electrostatic forces that keep the ions near the surface or form stronger chemical bonds between the ion and the surface functional groups of (hydr)oxides, clay,

and organic matter (Strawn, 2021). These electrostatic forces present at the different soil surface particles are produced by processes like isomorphic substitution and protonation-deprotonation of functional groups generating a charge that attracts the ions to the surface. For volcanic soils, the presence of variable charge surfaces is related to nanocrystalline minerals like allophane, imogolite, and ferrihydrite (Auxtero et al., 2004; Ishiguro et al., 1992). The presence of these minerals and the changes in solution pH strongly affects the ion adsorption in these soils. Therefore, the pH changes and the ionic strength of the soil solution could modify the adsorption behavior of nutrients in volcanic soil systems.

Different types of complexes can occur during the adsorption process to the (hydr)oxide fraction. For instance, the inner-sphere complex has no water molecules between the surface functional group and the ion or molecule. This surface complex is stable and is the product of ligand exchange reactions which allow the ion approaching closer to the surface (Hiemstra and Van Riemsdijk, 1996). The higher stability of these complexes is related to the nature of the ionic or covalent bonds that create the complex. In contrast, outer-sphere complexes have at least one water or oxygen molecule between the ion and the surface functional group and are created principally by electrostatic forces that keep the ions near the surface (Goldberg, 1997; Hiemstra and Van Riemsdijk, 1996; Sposito, 2008). As a result, outer-sphere complexes are located at a larger distance from the surface than the inner-sphere ones. Consequently, the formation of inner- or outer-sphere complexes have particular importance on the strength of bonding and consequently on the availability and susceptibility of an ion to leach.

Regarding the adsorption to clay minerals (phyllosilicates), the generation of charge at the surfaces occurs by isomorphic substitution of Al^{3+} for Si^{4+} at the tetrahedral sheet (with a charge deficiency spread over four oxygen ligands) or by isomorphic substitution of Mg^{2+} for Al^{3+} at the octahedral sheets, where the charge deficiency is distributed over six oxygen ligands (Strawn et al., 2020). Additionally, the dissociation of protons from the -OH groups could generate a variable charge at the clay edges (Strawn et al., 2020).

Among the most common (hydr)oxides present in soil systems, highlights ferrihydrite by its frequent appearance in volcanic soils (Strawn et al., 2020), probably related to the fast-weathering process and the high content of organic matter that prevents the formation of more crystallized iron oxides. Consequently, the high ferrihydrite abundance in volcanic soils plus its small size offer an opportunity to use this oxide as a proxy to represent the adsorption at nanocrystalline minerals present in volcanic soils.

Soil organic matter also plays an essential role in ion adsorption. These organic particles consist of a variety of molecules with different functional groups that can bind organic and inorganic molecules (Sposito, 2008). Due to the variability and diversity of organic surface functional groups, the organic matter

surface is typically characterized by a range of values for chemical constants (e.g., proton dissociation) (Sposito, 2008). This variability has also been contemplated for the development of geochemical models that predict and explain the interaction of ions with the organic matter (Kinniburgh et al., 1996; Milne et al., 2003; Tipping, 1994).

The implementation of different adsorption models has helped to estimate the adsorbate concentrations in solution, and in some cases the adsorption mechanisms and ionic species can be inferred based on the modeling results. Some adsorption models are empirical, while others are based on the theoretical mechanisms that govern the adsorption process. For the empirical models, the model parameters are simply fitted to the observed data, while for the implementation of a mechanistic model it is necessary to characterize the different adsorption surfaces, their reaction equilibrium equations, the mass balance, and charge balance (Goldberg, 2005; Mendez, 2020). The implementation of both types of models (empirical or mechanistic surface complexation models) most of the time assumes that an equilibrium condition is achieved.

Among these empirical models, the most popular ones are the linear adsorption model, the Freundlich, and the Langmuir model. The simplest model corresponds to the linear adsorption model, commonly applicable to systems with very low and restricted adsorbate concentrations (Goldberg, 2005; Van der Zee and Leijnse, 2013). When assuming equilibrium and at low adsorbate concentrations, the linear adsorption isotherms can be described by the distribution coefficient (Kd), which is fitted according to Equation 1.1

$$Cs = Kd * C \qquad \text{Equation 1.1}$$

where Cs corresponds to the concentration in the adsorbed fraction, Kd the distribution coefficient, and C corresponds to the solution concentration.

On the other hand, the Freundlich and the Langmuir models can be applied for non-linear adsorption data, commonly observed at high adsorbate concentrations. The main conceptual difference between these two non-linear models is that Langmuir isotherm considers a finite number of binding sites, while Freundlich does not (Goldberg, 2005).

Considering that adsorption reactions in the complex soil surfaces depend on a large number of factors (for instance, ionic strength, pH, oxidation-reduction conditions, counter ions, variation of physical-chemical properties related to the impact of the electrostatic field as the adsorption process advance), the implementation of empirical adsorption models is limited to specific conditions that cannot explain the real adsorption under variable conditions. For instance, empirical models lack the flexibility to simulate the

nutrient interactions under different conditions than those used for model calibration. This limitation has been partially solved by developing more flexible mechanistic theoretical models capable to describe ion adsorption under variable pH, variable ionic strength, different concentrations of binding surfaces (e.g., different soils), and different concentrations of adsorbates.

Among the mechanistic surface complexation models, there is a range of sophistication and complexity. For example, the Constant Capacitance model which has been implemented in several studies (Goldberg et al., 2005; Goldberg and Glaubig, 1986, 1985; Ikhsan et al., 2005; Manning and Goldberg, 1996; Schindler et al., 1976) assumes that adsorption occurs only as inner-sphere species and surface complexes exist in a chargeless environment. On the other hand, for the Triple Layer model, adsorption can be expressed as both (inner- or outer-sphere species) (Davis et al., 1978; Goldberg, 2005).

The CD-MUSIC model is a more complex, advanced, and theoretically sound surface complexation model. This model consists of two parts: First, the CD (Charge Distribution) which deals with the electrostatic distribution of charge from the adsorption process. Here the adsorbed molecules are not considered as point charges, instead, there is a distribution of charge over two different electrostatic planes (Hiemstra and Van Riemsdijk, 1996). Second, the MUSIC (MUlti-Site Ion Complexation) which deals with the differences in affinity for proton and oxygen at the different surface groups. This heterogeneity of the surface groups is created by the differences in coordination number of the metal (singly, doubly, and triply-coordinated), which derives in charge differences (Hiemstra et al., 1989).

In the original CD approach, the outer-sphere species are located in the solution side of the Stern layer, while the inner-sphere species are located closer to the surface due to the ligand exchange (Hiemstra and Van Riemsdijk, 1996). Hiemstra and Van Riemsdijk (2006) refined their model by considering an extended Stern layer approach, they defined a second layer that separates the electrolyte ion pairs from the head of the diffuse double layer (DDL). Consequently, this model has three planes (0-, 1-, and 2- plane) to accommodate the distribution of charges. For the CD model, the charge is distributed by CD coefficients (Δz_0, Δz_1, and Δz_2), representing charge changes introduced at the 0-, 1-, and 2-plane.

For the Multi-Site Complexation (MUSIC) approach, each surface group has its affinity constant (K) for the reaction with the adsorbing ion (Hiemstra et al., 1989; Rahnemaie et al., 2007a; Van Eynde et al., 2022b, 2020a), and for the different metal coordinated species (surface groups) different types of complexes can be found. For instance, singly coordinated groups can form monodentate and binuclear bidentate surface complexes with ions like phosphate (Hiemstra and Zhao, 2016).

Applying the CD-MUSIC model to field samples can be challenging because of difficulties in estimating the equivalent reactive surface area (RSA) of the natural oxide fraction, but different methods

like probing the surface with ions appear to be useful. For example, the competitive interaction between the reversibly adsorbed phosphate (R-PO4) and added carbonate at a high concentration (e.g., 0.5 M $NaHCO_3$ solution) showed good results about the estimation of the RSA of the soil (Hiemstra et al., 2010), but ferrihydrite appears to be a better proxy nanocrystalline particle instead of goethite for the RSA estimation (Mendez et al., 2020).

The main disadvantage or limitation for the implementation of surface complexation models in soil adsorption processes description is that they require many parameters, which sometimes are not available at all, or it can be difficult or time-demanding to be obtained, or are obtained by fitting procedures under specific conditions, which limits the generic applicability of the models (Goldberg, 2005). However, the great advance and frequent application of the CD-MUSIC model during the last years has provided most of the necessary parameters for modeling the adsorption of protons, phosphate, zinc, boron, calcium, and magnesium for pure and multi-surface soil systems (e.g., Goli et al., 2011; Hiemstra and Zhao, 2016; Van Eynde et al., 2022, 2020). Furthermore, this significant advance allowed us to use this tool to study and better understand the boron-phosphate interactions in volcanic soil systems, as described in Chapter 2.

The use of mechanistic models to describe adsorption and transport processes has increased during the last years, principally by the implementation of multi-surface models in different codes like ORCHESTRA (Meeussen, 2003), MINTEQA2 (Allison et al., 1991), ECOSAT (Keizer and Van Riemsdijk, 2009) and PHREEQC (Parkhurst and Appelo, 1999). The Multi-Surface Adsorption models consider the additive effect of adsorption to different surfaces such as crystallized and amorphous (hydr)oxides, organic matter, and clay silicates (Peng et al., 2018; Weng et al., 2001), estimating the equilibrium solution concentration of the adsorbate based on the adsorption to individual surfaces

A better understanding of the nutrient adsorption process and its interactions would allow a better description of the transport processes to estimate leaching in soil systems and to propose fertilizer management practices.

Transport processes in soil systems

Once the solutes (e.g., fertilizers) are applied to the environment (e.g., an agricultural soil), their movement through the soil profile is conditioned by the complex interaction of physical, chemical, and biological processes (van Genuchten et al., 2014). These solutes are typically transported by the water that moves into the soil, dissolving and transporting different organic and inorganic solutes. Therefore, factors

that drive the water movement in the soil have particular importance for the solute movement in porous systems.

The solute transport process is typically described by the well-known Convection-Dispersion Equation (CDE) or by non-equilibrium models (e.g., the Mobile-Immobile model (MIM)) (Šimůnek and van Genuchten, 2008; van Genuchten and Wierenga, 1976). For the CDE model, the convective part represents the movement of dissolved particles or ions by water flowing in the vadose zone or the groundwater (Van der Zee and Leijnse, 2013). The theoretical solute movement by uniquely convective transport would be considered as a piston flow process. However, the real transport process typically shows a solute spreading, which is accounted for by the dispersive part of the model. Solute spreading is generated by molecular diffusion and mechanical dispersion, the latter caused by variations in the average pore water velocity (Van der Zee and Leijnse, 2013). On the other hand, for more complex non-equilibrium flow systems, the simulation of solute movement in the soils requires additional parameters (Arora et al., 2012; Šimůnek and van Genuchten, 2008; van Genuchten and Wierenga, 1976).

Implementing the CDE and MIM models generally assume constant values for the model parameters. These parameters can be determined directly by different measuring methods (Diamantopoulos et al., 2015; Hasan et al., 2020; Kumahor, 2017; Kumahor et al., 2015b, 2015a; Weller et al., 2011) or indirectly by fitting to experimental data (Diamantopoulos et al., 2012; Šimůnek et al., 2008; Toride et al., 1995). However, recently, it has been observed that the CDE and MIM parameters might vary with factors like the pore water velocity (Kumahor et al., 2015b), soil water saturation, and flow rates (Chen et al., 2021; Hasan et al., 2020, 2019; Karadimitriou et al., 2017), and therefore the results of fitting procedures (constant values) are not always reliable. Furthermore, the interactions between the physical and chemical processes appear to be even more complex than those typically tackled in solute transport modeling, as some papers show that hydrodynamic parameters could depend on the interactions within the chemical processes, on the reactant, and solution concentration (Caron et al., 2015; Chiogna et al., 2010; Muniruzzaman and Rolle, 2021; Rolle et al., 2013b), but most of the time it is assumed constant values for the hydrodynamic solute transport parameters. Consequently, the high fertilization rates currently applied to high-yielding crops in volcanic soils, could influence the parameters used to simulate the movement of solutes (e.g., fertilizer) in these important soil systems.

How these factors affect the solute transport in highly fertilized volcanic soil systems is still unclear. Consequently, in Chapter 4, we evaluated the effect of flow rate and different concentrations on the parameters commonly implemented to describe the transport of solutes by two of the most commonly used solute transport models (CDE and MIM).

As previously described, volcanic soils have special physical characteristics like high permeability and high water retention and in some cases, can present preferential flow conditions when macropores are activated (Eguchi and Hasegawa, 2008). Consequently, for these soils is compulsory to understand and model appropriately the solute transport processes.

Objectives and thesis outline:

According to the previous information and considering that the application of high rates of N-P-K fertilizer is a common practice in agricultural volcanic soils, the first objective of the present dissertation was to evaluate whether the high inputs of fertilizer (specifically P and K) could create nutrient imbalances by increasing the micronutrient leaching losses. To evaluate this objective, we developed the adsorption and transport experiments presented in chapters 2 and 3.

In Chapter 2, we developed batch adsorption experiments that evaluated the phosphate-boric acid adsorption interactions. The results of the batch adsorption experiments plus the potential formation of surface complexes were interpreted by a state-of-the-art multi-surface adsorption model (CD-MUSIC-NICA-Donnan). The implemented modeling approach considered the most recent advances in the application of the CD-MUSIC model. For instance, the reactive surface area of the soil (RSA) and the reversibly adsorbed phosphate fraction (R-PO4) were determined by probing the surface by the carbonate-phosphate competitive interaction and using the CD-MUSIC model for the estimation (fitting) of both model parameters based on Hiemstra et al. (2010), but considering ferrihydrite as a better proxy nanoparticle to represent the (hydr)oxide fraction of the soil (Mendez et al., 2020). In addition, the CD-MUSIC boron adsorption parameters were recently developed for pure oxide nanoparticles (ferrihydrite) (Van Eynde et al., 2020a), as well as the parameters for the interaction of boron with humic acids (Goli et al., 2019). These recent advances allowed us to model the boron adsorption mechanistically and obtain more information about the boron and phosphate interactions, plus a better comprehension of the boron adsorbed species and binding mechanisms in a volcanic soil system.

In Chapter 3, we also developed batch adsorption experiments to evaluate the competitive interaction between potassium chloride concentrated solutions and zinc adsorption-desorption in alluvial volcanic soils. With this set of experiments, we evaluated two chemical factors modified by the addition of a potassium chloride concentrated solution (the pH and the ionic strength), which potentially affect zinc adsorption in volcanic soils. Both variables showed considerable effects on zinc adsorption. Additionally, we developed column transport experiments using undisturbed volcanic soil cores. These experiments were performed under unsaturated and constant gravitational flow conditions using a modified version of the

Multi-Step Flux Transport device (Kumahor et al., 2015b, 2015a; Weller et al., 2011). The results obtained showed the competitive interactions produced by the addition of high rates of potassium chloride in these volcanic soils, which solubilize substantial quantities of zinc. This second set of K-Zn experiments evaluated the zinc desorption process, not the more commonly studied adsorption process.

On the other hand, **Chapter 4** deals with the effects of highly concentrated fertilizer solution on hydrodynamic solute transport parameters as a first approach to elucidate the effects of chemical and physical interactions for modeling nutrient transport in volcanic soil systems. To develop this set of experiments, we built a modified version of the Multi-Step Flux transport device (Kumahor et al., 2015b, 2015a; Weller et al., 2011). This experimental setup allowed the development of long-time experiments, obtaining data at detailed time-steps, developing solute transport experiments at different flow rates and at different solute concentrations. Our results about hysteresis agreed with the results obtained by Chen et al. (2021) and Erfani et al. (2021), and contribute to elucidate the cause of the breakthrough curve hysteresis observed between loading or unloading the solute to the soil columns. The knowledge of how chemical and physical processes interact is critical for the correct modeling of nutrient transport in volcanic soil systems.

Finally, in **Chapter 5**, I critically discuss and synthesize the principal findings obtained in the experiments of my Ph.D. dissertation, discussing the implications, limitations, and possible future research experiments, and modeling steps to further elaborate on this topic.

References:

Allison, J.D., Brown, D., Novo-Gradac, K., 1991. MINTEQA2 / PRODEFA2 , A Geochemical Assessment Model for Environmental Systems : User Manual Supplement for Version 3 . 0.

Alvarado, A., 1982. Phosphate retention in Andepts from Guatemala and Costa Rica as related to other soil properties. North Carolina State University.

Arora, B., Mohanty, B.P., McGuire, J.T., 2012. Uncertainty in dual permeability model parameters for structured soils. Water Resour. Res. 48, 1–17. https://doi.org/10.1029/2011WR010500

Auxtero, E., Madeira, M., Sousa, E., 2004. Variable charge characteristics of selected Andisols from the Azores, Portugal. Catena 56, 111–125. https://doi.org/10.1016/j.catena.2003.10.006

Bell, R.W., McLay, L., Plaskett, D., Dell, B., Loneragan, J.F., 1990. Internal boron requirements of green gram (Vigna radiata). Plant Nutr. — Physiol. Appl. 275–280. https://doi.org/10.1007/978-94-009-0585-6_46

Boekhold, A.E., Temminghoff, E.J.M., Van Der Zee, S.E.A.T.M., 1993. Influence of electrolyte composition and pH on cadmium sorption by an acid sandy soil. J. Soil Sci. 44, 85–96. https://doi.org/10.1023/A:1004909322206

Brdar-Jokanović, M., 2020. Boron toxicity and deficiency in agricultural plants. Int. J. Mol. Sci. 21. https://doi.org/10.3390/ijms21041424

Caron, J., Létourneau, G., Fortin, J., 2015. Electrical Conductivity Breakthrough Experiment and Immobile Water Estimation in Organic Substrates: Is R = 1 a Realistic Assumption? Vadose Zo. J. 14. https://doi.org/10.2136/vzj2015.01.0014

Cattan, P., Cabidoche, Y.M., Lacas, J.G., Voltz, M., 2006. Effects of tillage and mulching on runoff under banana (Musa spp.) on a tropical Andosol. Soil Tillage Res. 86, 38–51. https://doi.org/10.1016/j.still.2005.02.002

Chapman, V.J., Edwards, D.G., Blamey, F.P.C., Asher, C.J., 1997. Challenging the dogma of a narrow supply range between deficiency and toxicity of boron BT - Boron in Soils and Plants: Proceedings of the International Symposium on Boron in Soils and Plants held at Chiang Mai, Thailand, 7–11 September, 1997, in: Bell, R.W., Rerkasem, B. (Eds.), . Springer Netherlands, Dordrecht, pp. 151–155. https://doi.org/10.1007/978-94-011-5564-9_29

Chen, Y., Steeb, H., Erfani, H., Karadimitriou, N.K., Walczak, M.S., Ruf, M., Lee, D., An, S., Hasan, S., Connolley, T., Vo, N.T., Niasar, V., 2021. Nonuniqueness of hydrodynamic dispersion revealed using fast 4D synchrotron x-ray imaging. Sci. Adv. 7, 1–7. https://doi.org/10.1126/sciadv.abj0960

Chiogna, G., Eberhardt, C., Grathwohl, P., Cirpka, O.A., Rolle, M., 2010. Evidence of compound-dependent hydrodynamic and mechanical transverse dispersion by multitracer laboratory experiments. Environ. Sci. Technol. 44, 688–693. https://doi.org/10.1021/es9023964

Comte, I., Cattan, P., Charlier, J.B., Gentil, C., Mottes, C., Lesueur-Jannoyer, M., Voltz, M., 2018. Assessing the environmental impact of pesticide use in banana cropping systems. Acta Hortic. 1196, 195–202. https://doi.org/10.17660/ActaHortic.2018.1196.24

CORBANA, 2022. CORBANA. URL https://www.corbana.co.cr/banano-de-costa-rica-2/# (accessed 6.24.22).

Davis, J.A., James, R.O., Leckie, J.O., 1978. Surface ionization and complexation at the oxide/water interface. I Computation of electrical double layer properties in simple electrolytes. J. Colloid

Interface Sci. 63, 480–499.

Diamantopoulos, E., Durner, W., Iden, S.C., Weller, U., Vogel, H.J., 2015. Modeling dynamic non-equilibrium water flow observations under various boundary conditions. J. Hydrol. 529, 1851–1858. https://doi.org/10.1016/j.jhydrol.2015.07.032

Diamantopoulos, E., Iden, S.C., Durner, W., 2012. Inverse modeling of dynamic nonequilibrium in water flow with an effective approach. Water Resour. Res. 48, 1–16. https://doi.org/10.1029/2011WR010717

Du, Z., Zhou, J., Wang, H., Chen, X., Wang, Q., 2010. Communications in Soil Science and Plant Analysis Soil pH Changes from Fertilizer Site as Affected by Application of Monocalcium Phosphate and Potassium Chloride Soil pH Changes from Fertilizer Site as Affected by Application of Monocalcium Phosphate and Potassium Chloride. Commun. Soil Sci. Plant Anal. 41, 1779–1788. https://doi.org/10.1080/00103624.2010.492064

Duffin, A.M., Schwartz, C.P., England, A.H., Uejio, J.S., Prendergast, D., Saykally, R.J., 2011. PH-dependent x-ray absorption spectra of aqueous boron oxides. J. Chem. Phys. 134, 1–7. https://doi.org/10.1063/1.3574838

Eguchi, S., Hasegawa, S., 2008. Determination and Characterization of Preferential Water Flow in Unsaturated Subsoil of Andisol. Soil Sci. Soc. Am. J. 72, 320–330. https://doi.org/10.2136/sssaj2007.0042

Erfani, H., Karadimitriou, N.K., Nissan, A., Walczak, M.S., An, S., Berkowitz, B., Niasar, V., 2021. Process-Dependent Solute Transport in Porous Media. Transp. Porous Media 140, 421–435. https://doi.org/10.1007/s11242-021-01655-6

Eswaran, H., Van Den Berg, E., Reich, P., 1993. Organic Carbon in Soils of the World. Soil Sci. Soc. Am. J. 57, 192–194. https://doi.org/10.2136/sssaj1993.03615995005700010034x

Fallas-Corrales, R., van der Zee, S.E.A.T.M., 2020. Diagnosis and management of nutrient constraints in papaya, in: Srivastava, A.K., Chengxiao, H. (Eds.), Fruit Crops. Elsevier Inc., pp. 607–628. https://doi.org/10.1016/b978-0-12-818732-6.00042-3

Fallas, R., Bertsch, F., Barrientos, M., 2014. Curvas de absorción de nutrientes en papaya (Carica papaya L.) CV. "Pococí" en las fases de crecimiento vegetativo, floración e inicio de cosecha. Agron. Costarric. 38, 43–54.

Fernández, F.G., Brouder, S.M., Volenec, J.J., Beyrouty, C.A., Hoyum, R., 2009. Root and shoot growth, seed composition, and yield components of no-till rainfed soybean under variable potassium. Plant Soil 322, 125–138. https://doi.org/10.1007/s11104-009-9900-9

Goldberg, S., 2005. Equations and Models Describing Adsorption Processes in Soils, in: Chemical Processes in Soils. SSSA, pp. 489–517.

Goldberg, S., 2004. Modeling Boron Adsorption Isotherms and Envelopes Using the Constant Capacitance Model. Vadose Zo. J. 3, 676–680. https://doi.org/10.2136/vzj2004.0676

Goldberg, S., 1997. Reactions of boron with soils. Plant Soil 193, 35–48. https://doi.org/10.1023/A:1004203723343

Goldberg, S., Corwin, D.L., Shouse, P.J., Suarez, D.L., 2005. Prediction of Boron Adsorption by Field Samples of Diverse Textures. Soil Sci. Soc. Am. J. 69, 1379–1388. https://doi.org/10.2136/sssaj2004.0354

Goldberg, S., Glaubig, R.A., 1986. Boron Adsorption and Silicon Release by the Clay Minerals Kaolinite, Montmorillonite, and Illite1. Soil Sci. Soc. Am. J. 50, 1442. https://doi.org/10.2136/sssaj1986.03615995005000060013x

Goldberg, S., Glaubig, R.A., 1985. Boron Adsorption on Aluminum and Iron Oxide Minerals. Soil Sci. Soc. Am. J. 49, 1374–1379.

Goli, E., Hiemstra, T., Rahnemaie, R., 2019. Interaction of boron with humic acid and natural organic matter: Experiments and modeling. Chem. Geol. 515, 1–8. https://doi.org/10.1016/j.chemgeo.2019.03.021

Goli, E., Rahnemaie, R., Hiemstra, T., Malakouti, M.J., 2011. The interaction of boron with goethite: Experiments and CD-MUSIC modeling. Chemosphere 82, 1475–1481. https://doi.org/10.1016/j.chemosphere.2010.11.034

Gonzalez-Rodriguez, S., Fernandez-Marcos, M.L., 2018. Phosphate sorption and desorption by two contrasting volcanic soils of equatorial Africa. PeerJ 2018, 1–14. https://doi.org/10.7717/peerj.5820

Gransee, A., Führs, H., 2013. Magnesium mobility in soils as a challenge for soil and plant analysis, magnesium fertilization and root uptake under adverse growth conditions. Plant Soil 368, 5–21. https://doi.org/10.1007/s11104-012-1567-y

Hasan, S., Joekar-Niasar, V., Karadimitriou, N.K., Sahimi, M., 2019. Saturation Dependence of Non-Fickian Transport in Porous Media. Water Resour. Res. https://doi.org/10.1029/2018WR023554

Hasan, S., Niasar, V., Karadimitriou, N.K., Godinho, J.R.A., Vo, N.T., An, S., Rabbani, A., Steeb, H., 2020. Direct characterization of solute transport in unsaturated porous media using fast X-ray synchrotron microtomography. Proc. Natl. Acad. Sci. U. S. A. 117, 23443–23449. https://doi.org/10.1073/pnas.2011716117

Hashimoto, Y., Kang, J., Matsuyama, N., Saigusa, M., 2012. Path Analysis of Phosphorus Retention Capacity in Allophanic and Non-Allophanic Andisols. Soil Sci. Soc. Am. J. 76, 441–448. https://doi.org/10.2136/sssaj

Hiemstra, T., Antelo, J., Rahnemaie, R., Riemsdijk, W.H. va., 2010. Nanoparticles in natural systems I: The effective reactive surface area of the natural oxide fraction in field samples. Geochim. Cosmochim. Acta 74, 41–58. https://doi.org/10.1016/j.gca.2009.10.018

Hiemstra, T., Van Riemsdijk, W.H., 2006. On the relationship between charge distribution, surface hydration, and the structure of the interface of metal hydroxides. J. Colloid Interface Sci. 301, 1–18. https://doi.org/10.1016/j.jcis.2006.05.008

Hiemstra, T., Van Riemsdijk, W.H., 1996. A Surface Structural Approach to Ion Adsorption: The Charge Distribution (CD) Model. J. Colloid Interface Sci. 179, 488–508. https://doi.org/10.1006/jcis.1996.0242

Hiemstra, T., Van Riemsdijk, W.H., Bolt, G.H., 1989. Multisite proton adsorption modeling at the solid/solution interface of (hydr)oxides: A new approach. I.Model description and evaluation of intrinsic reaction constants. J. Colloid Interface Sci. 133, 91–104. https://doi.org/10.1016/0021-9797(89)90284-1

Hiemstra, T., Zhao, W., 2016. Reactivity of ferrihydrite and ferritin in relation to surface structure, size, and nanoparticle formation studied for phosphate and arsenate. Environ. Sci. Nano 3, 1265. https://doi.org/10.1039/c6en00061d

Hogg, D.E., 1960. Magnesium losses from horotiu sandy loam following application of Potassium

Chloride. New Zeal. J. Agric. Res. 3, 377–383. https://doi.org/10.1080/00288233.1960.10418092

Ikhsan, J., Wells, J.D., Johnson, B.B., Angove, M.J., 2005. Surface complexation modeling of the sorption of Zn(II) by montmorillonite. Colloids Surfaces A Physicochem. Eng. Asp. 252, 33–41. https://doi.org/10.1016/j.colsurfa.2004.10.011

Ishiguro, M., Song, K.-C., Yuita, K., 1992. Ion Transport in an Allophanic Andisol under the Influence of Variable Charge. Soil Sci. Soc. Am. J. 56, 1789–1793. https://doi.org/10.2136/sssaj1992.03615995005600060022x

Jakobsen, S.T., 1993. Interaction between Plant Nutrients: III. Antagonism between Potassium, Magnesium and Calcium. Acta Agric. Scand. Sect. B - Soil Plant Sci. 43, 1–5. https://doi.org/10.1080/09064719309410223

Karadimitriou, N.K., Joekar-Niasar, V., Brizuela, O.G., 2017. Hydro-dynamic Solute Transport under Two-Phase Flow Conditions. Sci. Rep. 7, 1–7. https://doi.org/10.1038/s41598-017-06748-1

Keizer, M.G., Van Riemsdijk, W.H., 2009. ECOSAT. A computer program for the calculation of speciation and transport in soil-water systems. https://doi.org/10.1007/SpringerReference_28001

Keren, R., Sparks, D.L., 1994. Effect of pH and Ionic Strength on Boron Adsorption by Pyrophyllite. Soil Sci. Soc. Am. J. 58, 1095. https://doi.org/10.2136/sssaj1994.03615995005800040013x

Khan, S.A., Mulvaney, R.L., Ellsworth, T.R., 2013. The potassium paradox: Implications for soil fertility, crop production and human health. Renew. Agric. Food Syst. 29, 3–27. https://doi.org/10.1017/S1742170513000318

Kinniburgh, D.G., Milne, C.J., Benedetti, M.F., Pinheiro, J.P., Filius, J., Koopal, L.K., Van Riemsdijk, W.H., 1996. Metal Ion Binding by Humic Acid: Application of the NICA-Donnan Model. Environ. Sci. Technol. 30, 1687–1698.

Kumahor, S.K., 2017. Transport in Unsaturated Porous Media. Martin-Luther-Universit¨at Halle-Wittenberg.

Kumahor, S.K., de Rooij, G.H., Schlüter, S., Vogel, H.-J., 2015a. Water Flow and Solute Transport in Unsaturated Sand—A Comprehensive Experimental Approach. Vadose Zo. J. 14, 0. https://doi.org/10.2136/vzj2014.08.0105

Kumahor, S.K., Hron, P., Metreveli, G., Schaumann, G.E., Klitzke, S., Lang, F., Vogel, H.J., 2015b. Transport of citrate-coated silver nanoparticles in unsaturated sand. Sci. Total Environ. 535, 113–121. https://doi.org/10.1016/j.jconhyd.2016.10.001

Lagas, P., Loch, J.P.G., Bom, C.M., Gerringa, L.J.A., 1984. The behavior of barium in a landfill and the underlying soil. Water. Air. Soil Pollut. 22, 121–129. https://doi.org/10.1007/BF00163093

Manning, B.A., Goldberg, S., 1996. Modeling Competitive Adsorption of Arsenate with Phosphate and Molybdate on Oxide Minerals. Soil Sci. Soc. Am. J. 60, 121. https://doi.org/10.2136/sssaj1996.03615995006000010020x

Meeussen, J.C.L., 2003. Orchestra: An object-oriented framework for implementing chemical equilibrium models. Environ. Sci. Technol. 37, 1175–1182. https://doi.org/10.1021/es025597s

Mendez, J.C., 2020. Ion complexation modelling of ferrihydrite : Wageningen University. https://doi.org/doi.org/10.18174/525623

Mendez, J.C., Bertsch, F., 2012. Guía para la interpretación de la fertilidad de los suelos de Costa Rica. Asociación Costarricense de la Ciencia del Suelo, San José, Costa Rica.

Mendez, J.C., Hiemstra, T., Koopmans, G.F., 2020. Assessing the Reactive Surface Area of Soils and the Association of Soil Organic Carbon with Natural Oxide Nanoparticles Using Ferrihydrite as Proxy. Environ. Sci. Technol. 54, 11990–12000. https://doi.org/10.1021/acs.est.0c02163

Milne, C.J., Kinniburgh, D.G., Van Riemsdijk, W.H., Tipping, E., 2003. Generic NICA - Donnan model parameters for metal-ion binding by humic substances. Environ. Sci. Technol. 37, 958–971. https://doi.org/10.1021/es0258879

Montalvo, D., Degryse, F., McLaughlin, M.J., 2015. Natural colloidal P and its contribution to plant P uptake. Environ. Sci. Technol. 49, 3427–3434. https://doi.org/10.1021/es504643f

Muniruzzaman, M., Rolle, M., 2021. Impact of diffuse layer processes on contaminant forward and back diffusion in heterogeneous sandy-clayey domains. J. Contam. Hydrol. 237, 103754. https://doi.org/10.1016/j.jconhyd.2020.103754

Nanzyo, M., Dahlgren, R., Shoji, S., 1993a. Chapter 6 Chemical Characteristics of Volcanic Ash Soils. Dev. Soil Sci. 21, 145–187. https://doi.org/10.1016/S0166-2481(08)70267-8

Nanzyo, M., Shoji, S, Dahlgren, R., 1993b. Chapter 7 Physical Characteristics of Volcanic Ash Soils, in: Shoji, Sadao, Nanzyo, Masami, Dahlgren, R.B.T.-D. in S.S. (Eds.), Volcanic Ash Soils. Elsevier, pp. 189–207. https://doi.org/https://doi.org/10.1016/S0166-2481(08)70268-X

Nautiyal, B.D., Sharma, C.P., Agarwala, S.C., 1986. Iron, zinc and boron deficiency in papaya. Sci. Hortic. (Amsterdam). 29, 115–123. https://doi.org/10.1016/0304-4238(86)90037-3

Nelson, S., 2012. Boron Deficiency of Papaya. Plant Dis. CTAHR Univ. Hawaii Manoa.

Nunes, E.A., Kiyota, E., Andrade, S.A.L., 2022. Cadmium Accumulation in a Tropicalized Lettuce Variety Under Overfertilization Simulation. Clean - Soil, Air, Water 50, 1–13. https://doi.org/10.1002/clen.202100065

Ohno, T., Grunes, D.L., 1985. Potassium-Magnesium Interactions Affecting Nutrient Uptake by Wheat Forage. Soil Sci. Soc. Am. J. 49, 685–690.

Parkhurst, D., Appelo, C.A.J., 1999. User's guide to PHREEQC (version 2) - A computer program for speciation, batch-reaction, one-dimensional transport, and inverse geochemical calculations. Water Investig. Rep. 99-4259 312.

Peng, S., Wang, P., Peng, L., Cheng, T., Sun, W., Shi, Z., 2018. Predicting Heavy Metal Partition Equilibrium in Soils: Roles of Soil Components and Binding Sites. Soil Sci. Soc. Am. J. 839–849. https://doi.org/10.2136/sssaj2014.07.0299

Perret, S., Dorel, M., 1999. Relationships between land use, fertility and Andisol behaviour: Examples from volcanic islands. Soil Use Manag. 15, 144–149. https://doi.org/10.1111/j.1475-2743.1999.tb00080.x

Pinochet, D., Clunes, J., Gauna, C., Contreras, A., 2018. Reasoned fertilization of potato in response to nitrogen supply in andisols. J. Soil Sci. Plant Nutr. 18, 790–803. https://doi.org/10.4067/S0718-95162018005002301

Rahnemaie, R., Hiemstra, T., van Riemsdijk, W.H., 2007. Carbonate adsorption on goethite in competition with phosphate. J. Colloid Interface Sci. 315, 415–425. https://doi.org/10.1016/j.jcis.2007.07.017

Rolle, M., Muniruzzaman, M., Haberer, C.M., Grathwohl, P., 2013. Coulombic effects in advection-dominated transport of electrolytes in porous media: Multicomponent ionic dispersion. Geochim.

Cosmochim. Acta 120, 195–205. https://doi.org/10.1016/j.gca.2013.06.031

Sansoulet, J., Cabidoche, Y.M., Cattan, P., 2007. Adsorption and transport of nitrate and potassium in an Andosol under banana (Guadeloupe, French West Indies). Eur. J. Soil Sci. 58, 478–489. https://doi.org/10.1111/j.1365-2389.2007.00904.x

Schindler, P.W., Fürst, B., Dick, R., Wolf, P.U., 1976. Ligand properties of surface silanol groups. I. surface complex formation with Fe3+, Cu2+, Cd2+, and Pb2+. J. Colloid Interface Sci. 55, 469–475. https://doi.org/10.1016/0021-9797(76)90057-6

Shoji, S., 1985. Genesis and properties of non-allophanic andisols in Japan. Appl. Clay Sci. 1, 83–88. https://doi.org/10.1016/0169-1317(85)90564-2

Shorrocks, V.M., 1997. The occurrence and correction of boron deficiency. Plant Soil 193, 121–148. https://doi.org/10.1007/978-94-011-5580-9_9

Shu, Z.-H., Oberly, G.H., Cary, E.E., 1997. Absorption, movement and distribution of boron applied to peach (Prunus persica L. Batsch) fruits BT - Boron in Soils and Plants: Proceedings of the International Symposium on Boron in Soils and Plants held at Chiang Mai, Thailand, 7–11 September, 1997, in: Bell, R.W., Rerkasem, B. (Eds.), . Springer Netherlands, Dordrecht, pp. 209–212. https://doi.org/10.1007/978-94-011-5564-9_41

Sillanpää, M., 1982. Micronutrients and the nutrient status of soils: a global study. FAO soils bulletin 48. FAO, Rome, Italy.

Simunek, J., Jacques, D., Ramos, T.B., Leterme, B., 2014. The use of multicomponent solute transport models in environmental analyses, in: Geraldes Texeira, W., Basis Ceddia, M., Vasconcelos Ottoni, M., Kangussu Donnagema, G. (Eds.), Application of Soil Physics in Environmental Analyses: Measuring, Modelling and Data Integration. pp. 377–402. https://doi.org/10.1007/978-3-319-06013-2

Šimůnek, J., van Genuchten, M.T., 2008. Modeling Nonequilibrium Flow and Transport Processes Using HYDRUS. Vadose Zo. J. 7, 782–797. https://doi.org/10.2136/vzj2007.0074

Šimůnek, J., van Genuchten, M.T., Šejna, M., 2008. Development and Applications of the HYDRUS and STANMOD Software Packages and Related Codes. Vadose Zo. J. 7, 587. https://doi.org/10.2136/vzj2007.0077

Sposito, G., 2008. The chemistry of soils, 2nd ed. Oxford University Press.

Strawn, D.G., 2021. Sorption mechanisms of chemicals in soils. Soil Syst. 5, 1–22. https://doi.org/10.3390/soilsystems5010013

Strawn, D.G., Bohn, H.L., O'Connor, G.A., 2020. Chemistry of soil clays. Soil Chem. 379.

Tipping, E., 1994. WHAM- A chemical equilibrium model and computer code for waters, sediments, and soils incorporating a discrete site/electrostatic model of ion-binding by humic substances. Comput. Geosci. 20, 973–1023.

Tollenaar, D., 1969. Boron deficiency in sugar cane, oil palm and other monocotyledons on volcanic soils of Ecuador. Netherlands J. Agric. Sci. 17, 81–91. https://doi.org/10.18174/njas.v17i2.17378

Toride, N., Leij, F.J., van Genuchten, M.T.., 1995. The CXTFIT code for estimating transport parameters from laboratory or field tracer experiments. Version 2.0, Research Report No. 137.

Turner, D.W., Barkus, B., 1983. The uptake and distribution of mineral nutrients in the banana in response to supply of K, Mg and Mn. Fertil. Res. 4, 89–99. https://doi.org/10.1007/BF01049669

Van der Zee, S.E.A.T.M., Leijnse, A., 2013. Solute Transport in Soil, in: Hernández-Soriano, M.C. (Ed.), Soil Processes and Current Trends in Quality Assessment. IntechOpen, pp. 33–86. https://doi.org/http://dx.doi.org/10.5772/54557

Van Eynde, E., Hiemstra, T., Comans, R.N.J., 2022. Interaction of Zn with ferrihydrite and its cooperative binding in the presence of PO4. Geochim. Cosmochim. Acta 320, 223–237. https://doi.org/10.1016/j.gca.2022.01.010

Van Eynde, E., Mendez, J.C., Hiemstra, T., Comans, R.N.J., 2020. Boron Adsorption to Ferrihydrite with Implications for Surface Speciation in Soils: Experiments and Modeling. ACS Earth Sp. Chem. 4, 1269–1280. https://doi.org/10.1021/acsearthspacechem.0c00078

van Genuchten, M.T., Naveira-Cotta, C., Skaggs, T.H., Raoof, A., Pontedeiro, E.M., 2014. The Use of Numerical Flow and Transport Models in Environmental Analyses BT - Application of Soil Physics in Environmental Analyses: Measuring, Modelling and Data Integration, in: Teixeira, W.G., Ceddia, M.B., Ottoni, M.V., Donnagema, G.K. (Eds.), . Springer International Publishing, Cham, pp. 349–376. https://doi.org/10.1007/978-3-319-06013-2_15

van Genuchten, M.T., Wierenga, P.J., 1976. Mass Transfer Studies in Sorbing Porous Media I. Analytical Solutions. Soil Sci. Soc. Am. J. 40, 473–480. https://doi.org/10.2136/sssaj1976.03615995004000040011x

Wada, K., 1985. The Distinctive Properties of Andosols, in: Stewart, B.A. (Ed.), Advances in Soil Science. Springer New York, New York, NY, pp. 173–229.

Wang, D., Ko, W., 1975. Relationship between deformed fruit disease of papaya and boron deficiency.pdf. Phytopathology 65, 445–447.

Wang, N., Yang, C., Pan, Z., Liu, Y., Peng, S., 2015. Boron deficiency in woody plants: Various responses and tolerance mechanisms. Front. Plant Sci. 6, 1–14. https://doi.org/10.3389/fpls.2015.00916

Weller, U., Ippisch, O., Köhne, M., Vogel, H.-J., 2011. Direct Measurement of Unsaturated Conductivity including Hydraulic Nonequilibrium and Hysteresis. Vadose Zo. J. 10, 654. https://doi.org/10.2136/vzj2010.0074

Weng, L., Temminghoff, E.J.M., Van Riemsdijk, W.H., 2001. Contribution of individual sorbents to the control of heavy metal activity in sandy soil. Environ. Sci. Technol. 35, 4436–4443. https://doi.org/10.1021/es010085j

Zude, M., Alexander, A., Lüdders, P., 1997. Influence of boron spray on boron concentration, fruit set and calcium related disorders in apple (Malus domestica) cv. 'Elstar'/M26 BT - Boron in Soils and Plants: Proceedings of the International Symposium on Boron in Soils and Plants held at Chiang Ma, in: Bell, R.W., Rerkasem, B. (Eds.), . Springer Netherlands, Dordrecht, pp. 139–143. https://doi.org/10.1007/978-94-011-5564-9_27

Chapter 2

Boron adsorption and competition with phosphate in a tropical volcanic ash-derived soil

Róger A. Fallas-Corrales[a], Juan C. Mendez[b], Johannes C.L. Meeussen[c,d], Sjoerd E. A. T. M. van der Zee[a]

Submitted.

Abstract

Boron deficiency management in volcanic ash-derived soil systems from humid regions is a general issue for the agricultural production of susceptible crops (e.g., papaya crop). Boron availability/deficiency in soils depends on adsorption, desorption, and competition with other nutrients. Hence this relationship needs to be understood for good boron management. We studied boric acid adsorption in a volcanic ash-derived soil system by performing batch adsorption experiments. We interpreted the results using a state-of-the-art multi-component adsorption model to simulate boron adsorption to ferrihydrite using the CD-MUSIC model, and the NICA-Donnan model for boric acid adsorption to humic acids. The measured data and model simulations (in a fully predictive scheme) had a remarkable agreement even at very low micromolar boron concentrations. Phosphate had an almost imperceptible effect on boron adsorption at low boron concentrations in soil solution, and modest effects at high boron concentrations. For the Al-(hydr)oxide dominated soil, the adsorption interaction between boron and phosphate is effectively modeled using nanocrystalline ferrihydrite as a proxy for the overall reactive oxide fraction. The information from these experiments provides new awareness of how to deal with boron deficiency in volcanic systems with high phosphate inputs and high phosphate immobilization.

Keywords: Andosols, boron adsorption, phosphate, CD-MUSIC, NICA-Donnan, ORCHESTRA.

2.1 Introduction

Boron is an essential plant nutrient, and boron deficiency is widespread around the world, particularly present but not limited to high pH and arid regions. Boron deficiency affects crops, with an important impact on fruit production systems, as it reduces the quantity and quality of harvested and marketable products from agricultural fields. Therefore, the understanding of boron dynamics in the soil-plant systems is essential for the correct crop management. Adsorption/desorption plays an important role in these dynamics.

Boron availability depends on soil pH (Goldberg and Glaubig, 1985; Suarez et al., 2012), with lower adsorption and higher plant uptake at low pH values, stronger adsorption, and lower plant uptake under alkaline soil conditions. According to Goldberg & Glaubig (1985) and Keren & Mezuman (1981), maximum boron adsorption in soils occurs around pH 9. Consequently, B adsorption and availability have been investigated principally for high pH soils.

The cause of boron deficiency is unclear for acid and volcanic acid soils, as the low pH should promote higher boron solubility.

Two contrasting situations could explain the low boron concentrations observed in soil solution from tropical volcanic acid soils. First, the high contents of (hydr)oxides and aluminosilicates like allophane, ferrihydrite, and halloysite, and in some cases, the high organic matter contents present in volcanic acid soils adsorb boron, limiting its availability and leaching. Second, the high solubility of boron at low pH plus the high rainfall rates observed in tropical regions could result in the depletion of boron from the root zone area. Which of these contrasting situations is limiting boron availability in tropical volcanic acid soils is not clear.

Additionally, the effect of anionic fertilizers applications (e.g., phosphate) on the boron ads/desorption in these systems is unclear, and its consequences for boron leaching. The allophanic volcanic soils typically receive high rates of oxyanions such as phosphate due to the characteristic of high anion fixation normally present in these soils (Kurokawa and Kamura, 2018; Parfitt, 2009, 1990). In the case of competition between phosphate and boron, the high application rates of phosphate could derive to enhanced boron losses from volcanic soil systems.

Considering the very high affinity of phosphate for adsorption to hydroxides and the low affinity of boron for these surfaces, plus the high inputs of phosphate applied to volcanic soils, one could assume an enhanced displacement of boron from the root zone related to the application of phosphate fertilizer. However, phosphate and boric acid competition experiments showed inconsistent results.

For example, Bloesch, Bell, & Hughes (1987) and Rashid (1971) reported different degrees of competition between phosphate and borate adsorption in soils, while Bingham & Page (1971), working on allophanic soils suggest specific adsorption of boron (at 4.8 mM), which was unaffected by the presence of phosphate at concentrations of 0.1 M. The results obtained by Goldberg, Forster, Lesch, & Heick, (1996), also indicate a lack of interaction between other anions and boron, they suggested specificity in the boron adsorption to explain the absence of interaction.

Recently, Van Eynde, Mendez, et al. (2020) found adsorption competition between phosphate and boric acid in a pure ferrihydrite suspension system when keeping boron amounts constant and increasing the phosphate concentrations. Furthermore, Van Eynde, Mendez, et al. (2020) inferred the mechanisms of boric acid adsorption to the pure ferrihydrite by modeling and its agreement with the spectroscopic results of Su and Suarez (1997, 1995). These studies suggested the formation of tetrahedral bidentate complexes for high pH and trigonal inner-sphere bidentate complexes plus outer-sphere complexes for low to neutral pH values.

The competition of boron with other elements for adsorption sites could occur only at specific species (e.g., only for inner-sphere species). Consequently, distinguishing between the different boron adsorbed species could help to understand the mobility, availability, and sorption of B in volcanic soils.

For mono-component boron systems, the inner-sphere mechanism appears to be an important or even the principal mechanism for boron adsorption; for example, Goli et al. (2011) suggest a B adsorption process by inner-sphere species for adsorption to Goethite pure suspension system, Su & Suarez (1995) also suggest inner-sphere for boron adsorption to amorphous aluminum hydroxides, allophane, and kaolinite.

Van Eynde, Mendez et al. (2020) reported that the trigonal inner-sphere species of boron are important for acid to neutral pH values. The results of Van Eynde, Mendez, et al. (2020) suggest that these inner-sphere species vanish as phosphate concentrations increase. Consequently, only outer-sphere trigonal complexes remain important for describing boric acid adsorption to ferrihydrite at low pH and high phosphate concentrations.

The results about the dominance of outer-sphere adsorption of boric acid under high phosphate concentrations (Van Eynde et al., 2020a) contrast with the presupposed specific-adsorption mechanism suggested by Kurokawa & Kamura (2018) to explain the higher adsorption of borate as the concentration of the other anions increased for volcanic soils. The modeling simulations conducted by Van Eynde, Mendez, et al. (2020) predict competition for specifically adsorbed species (the inner-sphere adsorbed species).

Bingham & Page (1971) and Goldberg et al. (1996) mentioned that the lack of competition between other anions and boron could be related to the specificity of the boron adsorption sites. From the results of Van Eynde, Mendez et al. (2020), this specificity for boron adsorption could be represented by the outer-sphere sites.

Understanding the different mechanisms of boron adsorption to (hydr)oxide soil particles – inner sphere and outer sphere – is crucial to predict boron adsorption in natural soil systems accurately. In addition, understanding these mechanisms will allow us to predict the effect of oxy-anion competition with boron in real soil systems and comprehend the contribution of the different soil surfaces to the boron adsorption process.

Geochemical models could enhance understanding of the different mechanisms of boron binding to the different soil surfaces, and if well parameterized, these models could also predict boron availability

and leaching from soil systems. In the past, different geochemical models predicted boron adsorption and concentrations in solution for both pure and multi-surface systems.

Among the geochemical models used to describe boron adsorption in soils and clay minerals, the Constant Capacitance is the most commonly applied model (Goldberg, 2004; Goldberg et al., 2005, 2000; Goldberg and Glaubig, 1986, 1985; Meyer and Bloom, 1997; Vaughan and Suarez, 2003). This model described with relatively good precision the boron adsorption in soils and clay minerals, but it has several limitations for the description of boron adsorption in soils:

First, the Constant Capacitance model considers the soil as a single surface plane in which adsorption reactions occur; consequently, the Constant Capacitance model only describes inner-sphere adsorption. This limitation disagrees with the results of spectroscopic data obtained by Su & Suarez (1995), which revealed the presence of outer-sphere species in an acid to neutral pH and under the presence of phosphate in low pH pure ferrihydrite suspension systems (Van Eynde et al., 2020a).

Second, the binding constants (model parameters) are specific to the soil conditions and experiments in which they were determined. This situation limits the applicability of the Constant Capacitance model for generic soils and generic conditions.

A more advanced and mechanistically sound model is the Charge Distribution (CD) model (Hiemstra & Van Riemsdijk, 1996), which in combination with the Multi-site Ion Complexation (MUSIC) model (Hiemstra et al., 1989) successfully described boron adsorption to pure Goethite and Ferrihydrite suspension systems. While the NICA-Donnan model (Kinniburgh et al., 1996) effectively described adsorption to organic matter. In combination, these models (NICA-Donnan and CD-MUSIC) can simulate adsorption processes under multi-surface conditions, for example, natural soil systems.

The parameters for describing boron adsorption employing the CD-MUSIC model were derived for pure Goethite suspension systems by Goli et al. (2011) and more recently, for pure Ferrihydrite suspension systems by Van Eynde, Mendez, et al. (2020), while Goli et al. (2019) obtained the model parameters for boron adsorption to humic acids. The combination of these recent approaches allows for the simulation of boron adsorption to a multi-surface system.

The CD-MUSIC-NICA-Donnan modeling approach has several advantages over other boron adsorption models. For example, it includes adsorption of both species – inner and outer-sphere –, the modeling can be executed by a fully predictive scheme leaving aside the fitting of specific equilibrium

reaction constants for each soil, it considers the multi-component interaction between ions, as the distribution of charges in the different adsorption planes is taken into account.

Van Eynde, Weng, & Comans (2020) estimated by the CD-MUSIC-NICA-Donnan model the contribution of the different soil surfaces to the boron adsorption for temperate and tropical (Ferralsols) soils; they showed the importance of the different surfaces in boron adsorption varies with pH with more adsorption to the organic matter as the pH increases and higher importance of the (hydr)oxide fraction at low pH values. For volcanic soils, it is not clear whether the oxide fractions or the organic matter (both are abundant in volcanic soils) play a principal role in boron adsorption.

Van Eynde et al. (2020) also modeled the reactive boron fraction determined by three different boron extractants in temperate and tropical soils (multi-surface systems), employing the NICA-Donnan model with the generic parameters set of Milne et al. (2003) and the boric acid parameters developed by Goli et al. (2019). They implemented the CD-MUSIC model to describe boron adsorption to ferrihydrite with the parameters developed by Van Eynde, Mendez, et al. (2020).

As far as the authors are concerned, this newly available modeling approach (NICA-Donnan model with the parameters developed by Goli et al. (2019) plus the CD-MUSIC with model parameters developed for ferrihydrite (Van Eynde et al., 2020a)) has not been used to evaluate the interaction of boron with other nutrients in a multi-component system, has not been applied to describe boron adsorption to volcanic soils, and has not been implemented for the description of boron adsorption isotherms in multi-surface soil systems.

This approach will enable now to evaluate which reactive surfaces are more important for controlling B availability in this type of soil and evaluate the competition of anions such as phosphate, which could improve the boron management in volcanic acid soil systems.

This chapter aims to identify the binding mechanisms and adsorption surfaces that play a principal role in boron adsorption for volcanic ash-derived soils. Also, to test whether the high inputs of phosphate applied to volcanic soils could compete with boric acid sorption. Finally, to evaluate the performance of a state-of-the-art Multi-Surface Adsorption Model as a tool for predicting boron adsorption and its competition with phosphate in a volcanic ash-derived soil.

2.2 Materials and methods:

2.2.1 Soil characterization and experiments:

Soil characterization:

The soil sample used in this study has a volcanic origin. We collected the soil samples from a papaya plantation located in San Bosco, Pococí, Costa Rica (10.279290 N, -83.802527 W) at an altitude of 110 m.a.s.l. The georeferenced coordinates classify this soil as Aluandic Dystric Andosol (Fluvic) (World Reference Base soil classification system).

We conducted chemical analyses as needed for the Multi-Surface Model with soil samples collected from 0-20 cm depth. All the samples were oven-dried (50 ºC) for 48 hours and sieved (<2mm) prior to chemical analyses. The soil-pH was determined in ultrapure water and 0.01 M $CaCl_2$, using a soil/solution ratio of 1/10 w/v. We performed selective dissolution extractions of Fe and Al using Dithionite-Citrate-Bicarbonate (DC) and acid ammonium oxalate (AO) extractants as described by Burt (2004). Total soil organic C was determined by a dry combustion analyzer (Elementar vario Macro cube). We assumed the lack of carbonates in the soil samples due to the low carbonate composition of the parent material, plus the high precipitation regime for the sampled region (mean of 4500 mm per year). Dissolved organic carbon (DOC) was determined in a TOC analyzer using the method 5310 B (Baird et al., 2017) for DOC extractions developed in ultrapure water (18.2 MΩ, <5 ppb TOC), mixing 2.5 grams of soil with 25 mL of water.

Boron adsorption isotherms:

For the adsorption experiments, we mixed 3 g of soil sample with 30 mL of a solution that contained the background electrolyte (0.01 M of either $CaCl_2$ and $NaNO_3$), the boron, and the phosphate solutions. The phosphate solution corresponded to a freshly prepared +1.6 mM P (with phosphate), or +0 mM P (without phosphate), using KH_2PO_4 as a chemical reagent.

The boron solutions prepared for each specific batch adsorption experiment consisted of 0, 15, 30, 60, and 120 µmol B L^{-1}, using boric acid as a chemical reagent. For all the experiments, we used p.a. chemical reagents and ultrapure water to prepare the solutions, and all the solutions were prepared in plastic material to avoid contamination by borosilicates. For the background electrolyte solution, we used $CaCl_2$ or $NaNO_3$ p.a. chemical reagents.

We developed the adsorption experiments in 50 ml polystyrene centrifuge tubes (1/10 soil/solution ratio(w/v)). Complying with Lemarchand, Schott, & Gaillardet (2007), all the samples were shaken for five days in darkness to obtain B adsorption equilibrium.

The pH of the solutions was measured by a calibrated pH meter (Mettler Toledo Seven Excellence Multiparameter). During the development of the isotherm, we controlled the pH by adding either NaOH or HCl 0.01M solutions using a micropipette. The final pH for the isotherms developed in 0.01M $CaCl_2$ and 0.01M $NaNO_3$ background solutions was 4.98±0.06 and 5.48±0.1, respectively. Although the chosen pH is not at the optimal value for the highest boron sorption, these pH values are common for the volcanic soils from this region, so we evaluated the boron adsorption at pH values similar to those observed in the field plots. The chosen pH for each background solution corresponded to the mean pH of the samples after the addition of the respective background solution plus the boron and phosphate treatments, which also agreed with typical pH values observed for these volcanic soils.

The equilibrium boron concentrations were determined by an ICP-MS (Thermo Scientific iCAP RQ) for the batch adsorption experiments.

2.2.2 Multi-surface ion adsorption modeling:

We implemented a multi-surface ion adsorption model to describe the binding interaction of B and phosphate. This approach allowed us to obtain insights into the boron binding mechanisms and its surface speciation in our volcanic soil. The present multi-surface modeling comprises the description of ion adsorption to the reactive oxide surfaces and to the natural organic matter.

We did not consider an electrostatic model for describing ion adsorption in clay minerals (e.g., the Donnan ion exchange model) in this multi-surface model because: First, the boron is present in solution predominantly as a neutral $B(OH)_3^0$ species. Second, the interaction of boron and phosphate with clay minerals (if any) would be mainly via specific adsorption at the edge faces with oxide properties.

The following sections explain the implemented modeling details. The modeling calculations were done with the chemical speciation software ORCHESTRA.

Adsorption to reactive oxide surfaces:

We described the adsorption of boron and phosphate to the reactive metal (hydr)oxides fraction of the soil with the charge distribution (CD) model (Hiemstra and Van Riemsdijk, 1996), in combination with a recent multisite ion complexation model (MUSIC) for ferrihydrite (Hiemstra and Zhao, 2016). This approach is based on a structural analysis of the surface of ferrihydrite to determine the types of reactive groups and their corresponding densities. The solid-solution interface of ferrihydrite is described using an extended Stern Layer approach (Hiemstra and Van Riemsdijk, 2006), and the primary charging behavior of ferrihydrite is described using the parameters set given by Mendez & Hiemstra (2020). The adsorption

of phosphate (Hiemstra and Zhao, 2016; Mendez and Hiemstra, 2020b) and boron (Van Eynde et al., 2020a) has been described using an internally consistent thermodynamic database with intrinsic CD model parameters recently developed for ferrihydrite. Table S.2.2 presents the complete set of CD model parameters implemented in our model calculations.

We assessed the reactive surface area (RSA) of the oxide fraction by a probe ion methodology based on measuring the competitive interaction of carbonate on the adsorption of native soil phosphate. For this, a series of soil extractions with 0.5 M $NaHCO_3$ solution (pH = 8.5) are performed at different soil-to-solution ratios (SSR). For our soil, we measured the desorption of phosphate at five SSR values, ranging from 0.067 to 0.05 kg/L. To derive the value of RSA, we interpreted the results of the probe ion method with the CD model using parameters calibrated previously for a reference oxide material, e.g., goethite or ferrihydrite. This approach enables the simultaneous calculation of the total amount of phosphate that is reversibly bound to the oxide surfaces (R-PO_4). Details about the experimental procedure and the modeling calculation are given elsewhere (Hiemstra et al., 2010; Mendez et al., 2020). The RSA and R-PO_4 were used as independent model inputs for describing the adsorption isotherms of boron in interaction with phosphate.

Presently, we chose nanocrystalline ferrihydrite as a proxy for describing the overall reactivity of the natural fraction of oxides in our soil. This nanocrystalline material was shown to be a better reference material than well-crystallized goethite for representing the overall reactivity of the natural metal (hydr)oxide fraction in agricultural topsoils from the Netherlands (Mendez et al., 2020) and in weathered tropical topsoils from sub-Saharan countries (Mendez et al., 2022). Furthermore, due to the volcanic origin of our soil, the estimated RSA might also include a significant contribution of reactive $AlOH^{-0.5}$ groups present at the surfaces of allophane nanoparticles. However, no CD model parameters are presently available in the literature for this type of allophanic material. In addition, the oxidic edges of phyllosilicate clay minerals might also contribute to the overall reactivity of the natural oxide fraction in soils. Recently, Van Eynde, Weng, & Comans (2020) showed that the pH-dependent boron adsorption of illite and kaolinite can be described effectively using CD model parameters calibrated for ferrihydrite. Therefore, all reactive surfaces that exhibit oxidic properties have been generically represented in the modeling only by using the ion binding behavior of ferrihydrite as a reference.

Adsorption to soil organic matter:

The boron adsorption to the natural organic matter, both solid and dissolved, was described with the NICA-Donnan model (Kinniburgh et al., 1996). In this approach, two reactive sites are defined to

represent the major types of functional groups present in the reactive organic matter, i.e., carboxylic (S_1) and phenolic (S_2) groups. In our model descriptions, we used generic parameters reported by Milne et al. (2003) for humic acids, including the sites densities ($S_{T,1}$ and $S_{T,2}$) and the heterogeneity parameters (p_1 and p_2) for the sites S_1 and S_2, as well as the corresponding logK values and non-ideality parameters (n values) for describing the specific adsorption of H^+ and Ca^{2+} to these reactive groups. In addition, we used a recent parameter set (logK and n values) reported by Goli et al. (2019) to model specific boron adsorption to organic matter. Presently, a consistent set of NICA-Donnan parameters is only available for describing boron adsorption on humic acids (Goli et al., 2019). Therefore, we assumed that all the reactive organic matter, solid and dissolved, behaves as humic substances. Table S.2.3 presents the complete set of NICA-Donnan parameters used in our modeling.

For the dissolved organic matter, we assumed that 50% of the measured DOC is present as humic acids, as implemented in previous studies (Dijkstra et al., 2009; Groenenberg et al., 2017). Furthermore, we assumed that 35% of the total SOC is present as reactive carbon for the solid organic matter, in line with estimations done in earlier multi-surface adsorption studies (Duffner et al., 2014; Weng et al., 2001). This assumption is also supported by recent experimental data reported by Van Eynde, Weng, et al. (2020), showing that on average ~36% of the total SOC is present as humic substances in a series of agricultural topsoils. In addition, we assumed that the reactive organic matter contains 50% of C, as a rough generalization implemented by Dijkstra et al. (2009) and as suggested by Pribyl (2010).

Description of the solid-solution partitioning of B in $CaCl_2$ and $NaNO_3$ media:

The above multi-surface model with intrinsic adsorption parameters was used to describe the boron adsorption isotherms performed in electrolyte media with 0.01 M solutions of either $CaCl_2$ or $NaNO_3$. The RSA of the oxide fraction and the R-PO_4 values, both derived with the probe ion method, were used as independent model inputs. The natural organic matter (NOM) present at the oxide-solution interfaces affects the adsorption of phosphate due to the competition for the same reactive sites at oxide surfaces. This interaction might also affect the binding of boron to the oxide surfaces. To account for this effect of the interfacial NOM, we implemented a NOM-CD model approach (Hiemstra et al., 2013), which estimates the effective surface density of NOM (i.e., Fe-NOM in μmol/m^2) that competes with PO_4 for the binding in the oxide surface. We fitted the Fe-NOM density to explain the experimental concentration of PO_4 measured in a 0.01 M $CaCl_2$ extraction, which we determined according to a standard procedure (Houba et al., 2000). Table S.2.2 presents the model parameters used for describing this interaction. The so derived Fe-NOM value (FeNOM= 1.98 μmol/m^2) was used as a model input in the description of the boron adsorption

isotherms. A basic assumption is that the Fe-NOM value does not change upon addition of extra phosphate and that this value is the same for $CaCl_2$ and $NaNO_3$ media. However, changes in Fe-NOM density may occur at changing solution conditions.

For the modeling of the boron adsorption isotherms, the native fraction of reactive boron initially present in the soil was estimated in advance by multi-surface modeling, using as a validation criterion the concentration of B measured in an independent 0.01 M $CaCl_2$ extraction (Houba et al., 2000). The thus calculated fraction of reactive boron ($R\text{-}B_{model}$ = 23 µmol/kg soil) is slightly lower than the fraction of boron measured in 0.43 HNO_3 extractions ($R\text{-}B_{HNO3}$ = 26 ± 1 µmol/kg soil, n = 3). This result differs from data presented by Van Eynde, Weng, et al. (2020), showing that the values of $R\text{-}B_{model}$ are on average ~50% lower than the corresponding values of $R\text{-}B_{HNO3}$ measured in a series of soil samples from temperate and tropical regions. Using either the $R\text{-}B_{model}$ or $R\text{-}B_{HNO3}$ value for our soil had little impact on the model description of the adsorption isotherms.

2.3 Results:

2.3.1 Characterization of the soil:

The Andosol used for this experiment is a very permeable soil with a sandy loam texture, low bulk density (0,9 g cm^{-3}), and high total porosity (0.6 cm^3 cm^{-3}), which in combination with the low pH and the high annual precipitation is physically and chemically prone to boron leaching from the root zone. However, the soil also has high metal (hydr)oxides, principally related to the nanocrystalline fraction as shown by the high Al and Fe contents determined by the Ammonium Oxalate extract, which would decrease the boron leaching hazard.

As mentioned by Borggaard (1992); Burt (2004); Parfitt (1989); Schwertmann, Schulze, & Murad (1982); and Simonsson, Berggren, & Gustafsson (1999), the Ammonium Oxalate extract is used to selectively dissolve nanocrystalline materials (i.e., ferrihydrite, allophane, and imogolite), and additionally extracts aluminum and iron complexed with organic substances (Mizota and Reeuwijk, 1989), while, the Dithionite-Citrate extractant is supposed to dissolve all iron and aluminum oxides (well crystallized and nanocrystalline).

The assumptions about the fractions determined by the selective extractions (DC and AO) have been used for the estimation of the nanocrystalline and crystalline fractions for modeling purposes (Dijkstra et al., 2004; Van Eynde et al., 2020b) and translated into specific surface area (SSA) and reactive surface area (RSA) for these soils. However, for our soil, it was not possible to discern between the nanocrystalline

and crystalline fractions based on these selective extraction methods because of the large quantity of Al determined in ammonium oxalate, probably due to the presence of Al monomers complexed by organic matter (Table 2.1).

Table 2.1. Characteristics of the Aluandic Dystric Andosol from San Bosco, Pococí, Costa Rica.

Textural classification			**pH H_2O**	**Fe_{DC}**	**Al_{DC}**	**Fe_{AO}**	**Al_{AO}**	**Mn_{AO}**	**Particulate OC**	**DOC**
Sandy Loam				mmol kg^{-1} soil					%	mg C L^{-1}
Clay %	**Silt %**	**Sand %**	5,85	173,7	248,2	151,9	1112,9	10	2,9	3,6
15	5	80								

DC=Dithionite-Citrate extract, AO=Ammonium oxalate extract.

We applied the probe ion method developed by Hiemstra et al. (2010) to estimate the reactive oxide surface area (RSA (m^2 g^{-1} soil) of our soil. This method appears to be more appropriate than the estimations of the RSA based on selective extractions. The RSA estimations based on selective extractions present substantial uncertainties to estimate the size of the nanocrystalline and crystalline fractions. Additionally, there is no standard specific surface area (SSA (m^2 g^{-1} oxide)) value for all the soils (Mendez et al., 2020).

The probe ion method fitted the RSA of the soil by the implementation of CD-MUSIC modeling with a representation of the (hydr)oxide particle; we used ferrihydrite instead of goethite as a better model particle for the estimation of the RSA of the hydroxide fraction of our volcanic soil, in agreement with the observations of Hiemstra et al. (2010) and Mendez et al. (2020).

The RSA of the soil needed to explain the phosphate concentrations in equilibrium with 0.5 M $NaHCO_3$ solution applied at different soil to solution ratios resulted in 37.6 ± 4.1 m^2 g^{-1}, and the fitted reversibly adsorbed phosphate (R-PO_4) in 18.5 ± 1.8 mmol kg^{-1}. The latter information was subsequently used as independent modeling input for describing the boron adsorption isotherms.

2.3.2 Boron adsorption isotherms and modeling results:

Despite the low pH of our Andosol, in which it is expected boron becomes soluble, 32 % of the applied boron adsorbed to the soil surfaces. This result probably relates to the high RSA of our soil, which derives from the high contents of Al and Fe (hydr)oxides.

The (hydr)oxide fraction acquires more relevance for boron adsorption at low pH values; this situation was reported by Van Eynde, Mendez et al. (2020) and is also suggested by our modeling data (see details in section 2.3.4).

The broad range of boron concentrations evaluated in our experiments was based on the results compiled by Sillanpää (1982) from different countries around the world. They determined the boron concentrations by the hot water extractant for soil areas ranging from boron deficiency to toxicity.

Boron adsorption was similar for the two different background electrolytes in our Andosol.

The effect of the pH differences between both background solutions (ΔpH= 0.5) had a minor repercussion on the adsorption process in our experiments. As it is shown in Figure 2.3 by modeling simulations, there is little change in the soluble B concentrations for the typical pH values of this soil (i.e., from pH 4.0 to 6.0).

Additionally, the ionic strength effect and the counter ion (monovalent or divalent cation) hardly affected the amount of boron adsorbed and the shapes of the adsorption isotherms. These results are discussed further in Section 2.3.5.

For the case of no phosphate addition, boron adsorption was almost linear for the complete boron concentration range. In case phosphate was added, the isotherm became slightly nonlinear, particularly due to the deviation for the highest boron concentration (Figure 2.1).

The implementation of the CD-MUSIC-NICA-Donnan modeling approach produced an excellent agreement between modeled and measured data. This situation is remarkable because our modeling approach did not include any fitting of equilibrium reaction constants (our approach is a fully predictive scheme), and because the implementation of this fully predictive approach correctly predicted the boron concentrations in solution despite such small micromolar boron concentrations observed for this volcanic soil. Furthermore, the good performance of this modeling approach by pure prediction gives the confidence to implement the model for other conditions, for example, different soil pH, counter ions, and soils dominated by Fe or Al (hydr)oxides.

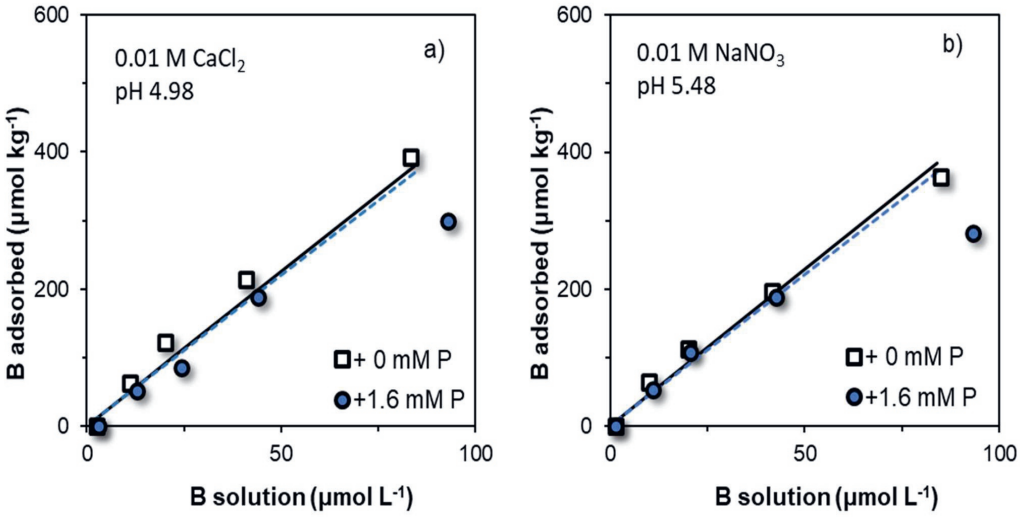

Figure 2.1. Adsorption isotherms of boron (B) for conditions with no extra P and 1.6 mM P added to an Aluandic Dystric Andosol (Fluvic) from Costa Rica. The left (a) and right (b) panels are for systems in 0.01 M $CaCl_2$ and 0.01 M $NaNO_3$ as background solutions, respectively. The symbols are experimental data and lines (solid= +0.0mM P, and dashed= +1.6 mM P) are the multi-surface complexation model predictions (CD-MUSIC-NICA-Donnan).

2.3.2.1 Multi-surface modeling description and boron binding mechanisms:

The multi-surface model (CD-MUSIC-NICA-Donnan), based only on pure predictions, described very well the boron adsorption data (Figure 2.1). The CD-MUSIC accounts for the adsorption to oxide surfaces, while the NICA model describes the adsorption to organic matter.

In the CD-MUSIC approach, using ferrihydrite as a reference oxide material, the formation of inner-sphere boron complexes is assumed to occur only in a fraction of singly coordinated groups that form binuclear bidentate complexes with ions (FeOH(b)) (van Eynde et al. 2020), according to the structural model of the ferrihydrite surface (Hiemstra and Zhao 2016).

The deviation from linearity (competition) at high boron concentrations observed only under the presence of phosphate could be related to the reduction of inner-sphere complexation induced by phosphate, which is evident only at high boron loadings in the system. While the process of outer-sphere adsorption is assumed to be unaffected by phosphate additions due to the neutral nature of the trigonal boric acid molecule, the trigonal species predominate at the pH values of our experiments.

It is clear from our modeling results (Table S.2.4 and Section 2.3.4) and by literature that boron adsorption at the pH values of our experiments occurs principally onto the hydroxide surfaces and mainly as an outer-sphere species when phosphate is present in the system.

For the +0 mM P system, the boric acid adsorbed linearly principally to the (hydr)oxide surfaces, which probably includes the participation of both -- inner-sphere and outer-sphere species--; this assumption is supported by literature about pure Goethite and Ferrihydrite systems (Goli et al., 2011; Van Eynde, Mendez, et al., 2020).

The model performed very well for the +1.6 mM P system up to boron solution concentrations close to 45 μmol L^{-1}. The deviation from linearity observed at the highest boron concentration evaluated could be related to the reduction of the participation of inner-sphere species. Van Eynde et al. (2020), considering a pure Ferrihydrite system, observed that at P concentrations of 0.1 mM, the inner-sphere species of boron are practically negligible. These differences between modeled and measured data for the highest boron concentration could be related to differences between parameter values derived for clean pure systems and its application to a “dirty” natural soil material, which will not match perfectly.

We also tested by modeling other synthetic scenarios to explore the mechanisms that could affect the accuracy between our modeled and measured data. The objective of adding this extra set of adsorption modeling results (Figure S.2.1 of Supplementary information) was not to predict P-B adsorption and competition with a new parameterized model. It was only to explore the different mechanisms that could explain the deviation between the measured and modeled data when applying only the parameters obtained for pure systems available in the literature.

The effect of varying the log K for the formation of outer-sphere species (i.e., $\Delta \log K = -0.20$) and increasing the contribution of inner-sphere complexation (i.e., by increasing the site density of reactive groups that form inner-sphere with boron) (Figure S.2.1), described the phosphate-boric acid competition observed at high B concentrations. Additionally, this explorative scenario predicted reasonably well the boron adsorption isotherm without the addition of phosphate.

Despite these differences between modeled and measured data, the approach that uses only consistent, intrinsic, and previously determined parameters from pure systems showed to be functional for predicting boron adsorption and soluble concentrations in volcanic soils. The good agreement between pure prediction and measured data gives confidence in the model and model assumptions and supports extrapolation to other soils and variable chemical conditions of the soil solution (e.g., electrolyte background).

The advantages of the CD-MUSIC-NICA-Donnan model to other modeling approaches are:

a) adsorption is described with the application of only consistent, intrinsic, and previously determined parameters in pure systems (Ferrihydrite and humic acids for our case), so fitting specific logK constants for each soil is not required.

b) this approach allows for the study of adsorption to different soil reactive surfaces (i.e., boron surface speciation).

c) implementing the CD approach for boron and phosphate adsorption can consider the distribution of charges at different planes and describe outer-sphere adsorption from a mechanistic point of view. Outer-sphere adsorption appears to be an important process for boron adsorption in volcanic soils. Furthermore, the mechanistic description of the boron adsorption process through the CD-MUSIC model allows for extrapolating the model to other soils and other conditions once the parameters are available.

2.3.3 P-B adsorption competition:

As shown in Figure 2.1, adding phosphate to the system showed no effect on the total boron adsorption at low boron concentrations. According to measured data (not modeled), the phosphate additions do not affect the equilibrium boron concentrations observed in the solution for the native boron concentrations (Figure 2.2). The red point in Figure 2.2 represents the “native” soil, i.e., no extra P added. The amount of R-PO_4 was determined by the probe ion method in $NaHCO_3$ 0.5 M extractions, and it corresponded to 18.5 mmol kg^{-1} according to modeling calculations. So, we evaluated the phosphate effect at almost two folds compared to the natural reactive phosphate fraction. The results suggest that under the natural boron concentrations for this soil system, the addition of phosphate does not promote additional boron desorption.

The lack of relationship between boric acid adsorption and phosphate loading in the system at natural boron loading is probably related to the mechanisms of phosphate and boric acid adsorption (see sections 2.3.2.1 and 2.3.5). Phosphate adsorbs with a higher affinity than boron as an inner-sphere species. This phosphate adsorption introduces negative charges to the 1-plane (Hiemstra and Van Riemsdijk, 2006), and the reduction of extra anion adsorption related to electrostatic repulsion and site competition is expected. However, the boric acid at the low natural loadings can adsorb as both inner-sphere and outer-sphere complexes, and due to its neutral electrostatic behavior, the outer-sphere complexes are not affected by these negative charges present at the 1-plane derived from the inner-sphere phosphate adsorption.

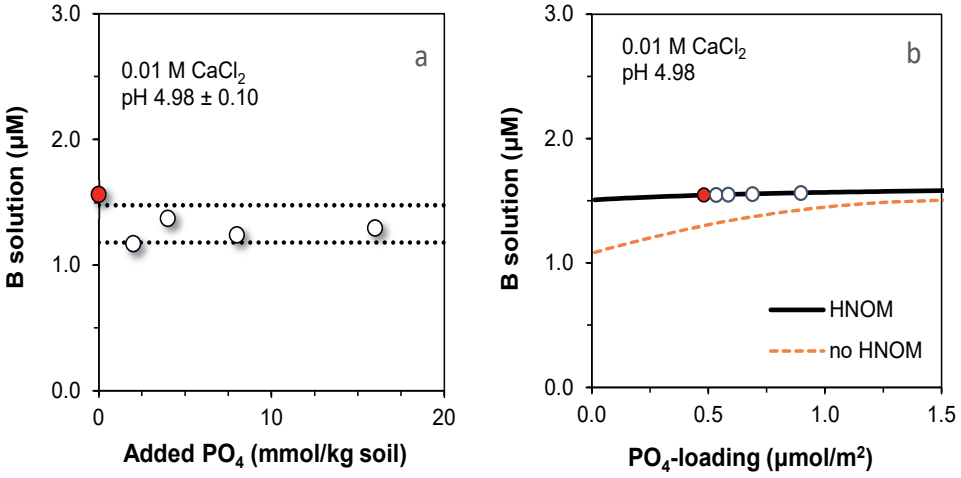

Figure 2.2. Experimental "native" boron solution concentrations as a function of added phosphate concentrations obtained in a $CaCl_2$ 0.01M system (a). The dotted lines represent ±10% of the mean value of all the data points. The right panel (b) presents model lines for the relationship between P-loading and B concentration in solution. Model lines were developed for systems considering the effect of interfacial SOM (HNOM) and without considering it (no HNOM).

Van Eynde et al. (2020a) suggest that boron adsorption under the presence of phosphate occurs principally as an outer-sphere species. However, at high boron concentrations for this soil, part of the boron is adsorbed as inner-sphere complexes, as it was affected by the presence of phosphate (Figure 2.1).

In soil systems, there is also present interfacial SOM adsorbed at the surfaces of metal oxides. The interfacial SOM could compete with boron and phosphate for adsorption sites at the surfaces of metal oxides.

For our soil without boron addition, the expected competitive effect of phosphate additions on the adsorption of B is masked effectively by the SOM already adsorbed to the oxide surfaces. An example of this interaction with SOM is shown in Figure 2.2.b through model calculation.

Considering in the modeling the presence of soil organic matter interacting with the oxide surfaces at an effective density of 1.19 site/nm^{-2} (as found for our soil), almost no effect is predicted for the solution B concentration when the phosphate loading is increased over the range of ~0.5 to 1.5 µmol/m^2.

Conversely, if no interfacial soil organic matter is included in the modeling, an increase in the B concentration in solution is predicted when the phosphate loading increases over the indicated range of

values. In this case, boron solution concentrations achieve similar values at high phosphate loadings compared to the observed values for the condition in which it is considered the effect of the SOM.

For our modeling approach (considering the SOM), most of the boron was adsorbed as an outer-sphere species, which is not affected by phosphate adsorption, while under the absence of SOM (no-HNOM simulations), part of the boron could adsorb as an inner-sphere species and consequently this fraction could be affected by the phosphate loadings. This situation does not occur for the natural condition of our Andosol due to the presence of organic matter.

2.3.4 Modeling the pH dependence of boron sorption:

Figure 2.3 simulates the distribution of the reactive boron fractions at different pH. The modeling was conducted using the intrinsic parameters found for our soil at $CaCl_2$ and $NaNO_3$ background electrolytes (Figure 2.3.a and 2.3.b, respectively), and by implementing the same model parameters, but varying the RSA and the R-PO_4 to lower values (Figure 2.3.c and 2.3.d).

The modeling speciation suggests that most of the boric acid is present as a soluble fraction at the typical pH values found in volcanic soils of this region (4.5 to 6.0). For this pH range, about 31% of the boron is adsorbed to the soil particles for both background electrolytes (Figure 2.3.a, 2.3.b, and Table S.2.4).

The predicted boron adsorption showed an increase with increasing the pH; this increase in boron adsorption was principally related to the more important role of the organic matter for boron adsorption at high pH.

According to the boron adsorption modeling results (Figure 2.3), a reduction of the oxide fraction of the soil (e.g., a volcanic soil with lower oxide contents) is not fully compensated by the increased boron adsorption to the organic fractions. The increase of boron adsorption with the increase of pH was more significant for the Ca-dominated background solution.

A possible reason for the more important role of the organic fractions in boron binding as the soil pH increases could be the increased difficulty of forming (hydr)oxide protonated species (such as $\equiv FeOH_2^{+0.5}$) as the soil pH increases. As mentioned before, boric acid adsorption for this soil was significantly related to outer-sphere adsorption, and the higher pH values could affect the formation of protonated species that adsorb boric acid as an outer-sphere species.

Additionally, at higher pH, the deprotonation of the organic matter binding sites (as shown in section 2.3.5, (Equation 2.3)) could increase the importance of the organic matter for boric acid binding.

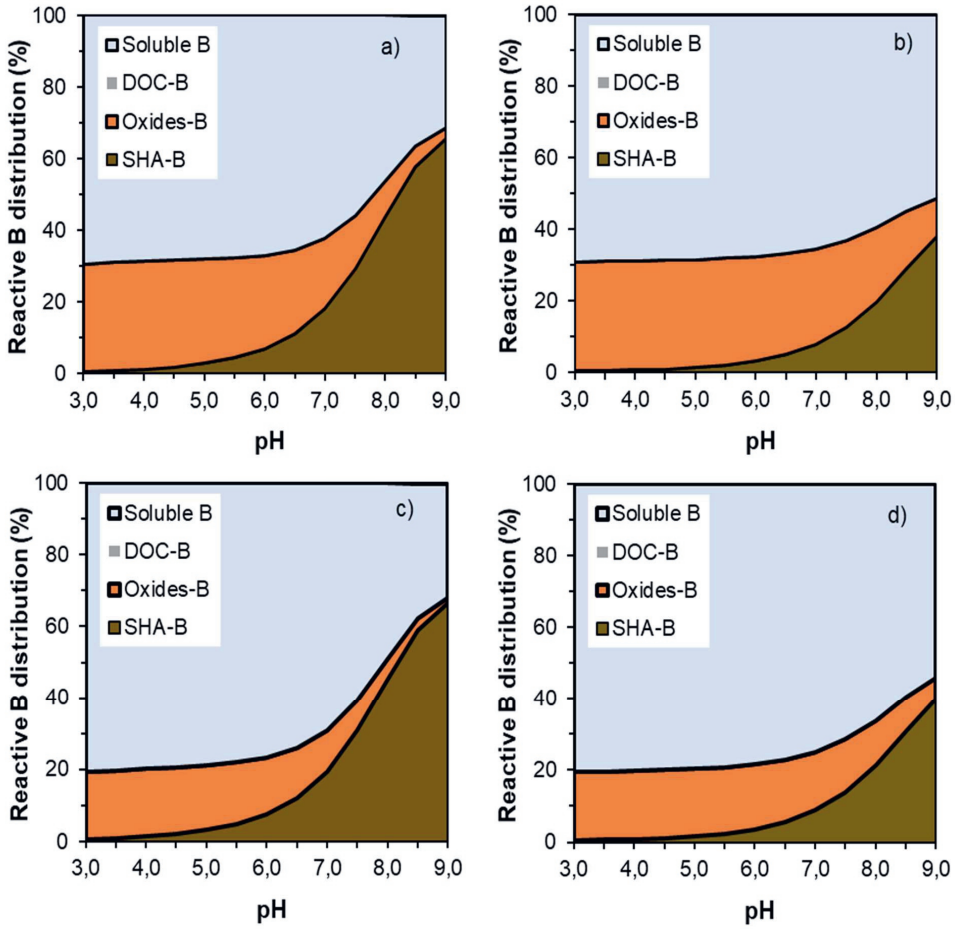

Figure 2.3. Distribution of reactive B in the soil. Left panels (a, c) are for 0.01 M $CaCl_2$ systems and right panels are for 0.01 $NaNO_3$ systems (b, d). The upper panels (a, b) are for the RSA and R-PO_4 loading conditions determined by our soils using the probe-ion method with $NaHCO_3$, fitted HNOM of 1.19 nm^{-2}. The lower panels (c, d) are for conditions where both RSA and R-PO_4 are lower (RSA=20 m^2 g^{-1}, R-PO4=9.8 mmol kg^{-1}), while the same P-loading and HNOM.

For our Andosol in a Ca-dominated system (Figure 2.3.a), the simulation also suggests a more important role of the organic fractions as the soil pH increases. These results appear to be related to the better screening of the charge in Ca systems that promotes the proton desorption and facilitates the boric acid binding to the organic fractions, as described in Section 2.3.5 and explained in detail by Goli et al. (2019).

Our modeling suggests that for a condition with a lower RSA and lower R-PO_4, while keeping the same P-loading and HNOM, more boron will be present in the solution (a more prone to leaching condition).

The latter means that under the reduction of the importance of the (hydr)oxide fraction (e.g., volcanic soils with lower content of (hydr)oxides), at low pH, the organic matter could not compensate for the reduction in the boric acid adsorption. However, the compensation effect is more evident for high pH and Ca-dominated systems and less perceptible for Na-dominated systems.

2.3.5 Boron binding mechanisms in Ca vs Na systems:

Model simulations of boron adsorption for the pure reactive surfaces of our soil (i.e., either oxides or humic acids modeled by separate) showed differences regarding the effect of the charge of the electrolyte cation in the background solution (monovalent or divalent cations).

The model results (Figure 2.4) suggest an effect of the electrolyte cation for the boron adsorption to the organic matter fractions (humic acids) and no effect on boron adsorption to the soil's (hydr)oxides fraction. The latter is related to the mechanisms of boron adsorption to the organic (humic acids), which according to Goli et al. (2019), the trigonal species at pH values below 9.24 require the deprotonation of the sites for the boric acid binding, as shown in Equation 2.3.

$$SitesH^{r} + B(OH)_3^0(aq) \leftrightarrow SitesH_{1-q}^{r-q} - B(OH)_3 + qH^+(aq) \quad \text{(Equation 2.3)}$$

(Goli et al., 2019)

Also, as found by Goli et al. (2019) and supported by our modeling data (Figure 2.4.a), there is more adsorption of boric acid for the organic surfaces (represented as humic acids) of our soil in $CaCl_2$ 0.01M than in NaCl 0.01M systems, this result is a combination of both, the counter ion effect and the ionic strength effect on boric acid adsorption, as it was discussed in depth by Goli et al. (2019).

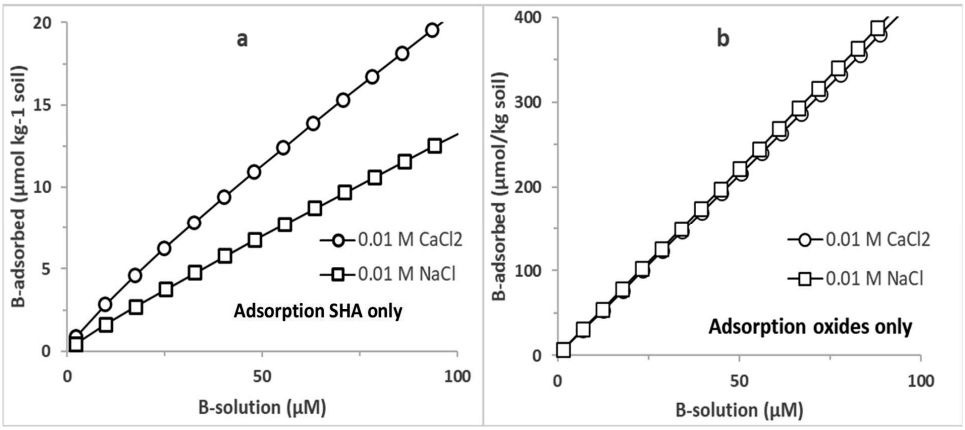

Figure 2.4. Boron adsorption in Ca and Na electrolyte systems. The model data shows the comparison if B would be adsorbed only in HA (a) and oxide fraction (b). For the modeling, the conditions were kept as for the original soil sample, i.e., RSA, R-PO4, SSR, and pH was fixed to 5.0 for both reactive surfaces

The increase of the ionic strength produces a reduction in the electrostatic potential of the Donnan phase; as a consequence, it reduces the local proton concentration and boric acid binding is facilitated by a weaker proton competition.

The effect of changing from a monovalent cation to a divalent cation also favors the deprotonation of the humic acids, as the Ca^{2+} ions better screen the charge of the humic acids reducing the competition of the protons with the boric acid. At the same time, and as mentioned by Goli et al. (2019), the calcium can compete with B for specific adsorption to humic acids. However, this competition effect is compensated by the effect of Ca in decreasing the electrostatic potential compared to the Na systems.

On the other hand, when we applied the same modeling exercise to the (hydr)oxide fraction, it showed no effect of neither the ionic strength nor the change in the cation valence of the electrolyte solution (Figure 2.4.b).

For our Andosol, there were no considerable differences in boron adsorption for different background solutions (NaCl 0.01 M and $CaCl_2$ 0.01 M), which suggest that for this soil under the conditions of the experiments, the adsorption is principally dominated by the oxide fraction (Table S.2.4), and as modeling suggest predominantly as an outer-sphere process.

2.4 Conclusions:

The main conclusion of this work is that under the natural boron condition of the volcanic soil, phosphate applications are not affecting the boron adsorption process.

Therefore, we do not expect that phosphate applications will lead to increased boron leaching,

At high application rates of boric acid and phosphate, we observed reduced boric acid adsorption, so the application of both nutrients simultaneously to the soil should be avoided.

For the Andosol evaluated in this experiment, boric acid adsorption is predicted to be dominated by the (hydr)oxide fraction.

The organic matter fraction could acquire more relevance for boric acid adsorption in soils with smaller (hydr)oxide fraction, high pH, and for Ca-dominated systems.

A multi-surface adsorption model using ferrihydrite as a model oxide nanocrystalline particle can describe the boron adsorption for a low pH Al-dominated volcanic soil. However, model predictions may be further improved by developing model parameters to describe ion adsorption to Al nanocrystalline particles such as allophane, imogolite, and halloysite, which may improve model predictions for P-B competition at high boron concentrations.

It is also necessary to further develop adsorption parameters for other chemical forms of boron, as for the moment, the parameters are only available for the boric acid, but other boron sources such as sodium borates are commonly used in agriculture. Therefore, the availability of model parameters for these other chemical forms of boron could improve boron management for different systems where higher or lower adsorption is necessary.

Data statement:

The dataset related to this chapter is available at the 4TU.ResearchData repository

DOI: 10.4121/19552585

2.5 References:

Baird, R., Eaton, A., Rice, E. (Eds.), 2017. Standard Methods, 23rd ed, Standard Methods for the Examination of Water and Wastewater. https://doi.org/10.1016/B978-0-12-382165-2.00237-3

Bingham, F., Page, A., 1971. Specific character of boron adsorption by amorphous soil. Soil Sci. Soc. Am. J. 35, 892–893.

Bloesch, P.M., Bell, L.C., Hughes, J.D., 1987. Adsorption and desorption of boron by goethite. Aust. J. Soil Res. 25, 377–390.

Borggaard, O.K., 1992. Dissolution of Poorly Crystalline Iron Oxides in Soils by EDTA and Oxalate. J. Plant Nutr. Soil Sci. 155, 431–436. https://doi.org/10.1002/jpln.19921550513

Burt, R., 2004. Soil Survey Laboratory Methods Manual. Soil Survey Investigations report No.42, Version 4.0.

Dijkstra, J.J., Meeussen, J.C.L., Comans, R.N.J., 2009. Evaluation of a Generic Multisurface Sorption Model for Inorganic Soil Contaminants. Environ. Sci. Technol. 43, 6196–6201. https://doi.org/10.1021/es900555g

Dijkstra, J.J., Meeussen, J.C.L., Comans, R.N.J., 2004. Leaching of heavy metals from contaminated soils: An experimental and modeling study. Environ. Sci. Technol. 38, 4390–4395. https://doi.org/10.1021/es049885v

Duffner, A., Weng, L., Hoffland, E., Van Der Zee, S.E.A.T.M., 2014. Multi-surface modeling to predict free zinc ion concentrations in low-zinc soils. Environ. Sci. Technol. 48, 5700–5708. https://doi.org/10.1021/es500257e

Goldberg, S., 2004. Modeling Boron Adsorption Isotherms and Envelopes Using the Constant Capacitance Model. Vadose Zo. J. 3, 676–680. https://doi.org/10.2136/vzj2004.0676

Goldberg, S., Corwin, D.L., Shouse, P.J., Suarez, D.L., 2005. Prediction of Boron Adsorption by Field Samples of Diverse Textures. Soil Sci. Soc. Am. J. 69, 1379–1388. https://doi.org/10.2136/sssaj2004.0354

Goldberg, S., Forster, H.S., Lesch, S.M., Heick, E.L., 1996. Influence of anion competition on Boron adsorption by clays and soils. Soil Sci. 161, 99–103. https://doi.org/10.1097/00010694-199602000-00003

Goldberg, S., Glaubig, R.A., 1986. Boron Adsorption and Silicon Release by the Clay Minerals Kaolinite,

Montmorillonite, and Illite1. Soil Sci. Soc. Am. J. 50, 1442. https://doi.org/10.2136/sssaj1986.03615995005000060013x

Goldberg, S., Glaubig, R.A., 1985. Boron Adsorption on Aluminum and Iron Oxide Minerals. Soil Sci. Soc. Am. J. 49, 1374–1379.

Goldberg, S., Lesch, S.M., Suarez, D.L., 2000. Predicting boron adsorption by soils using soil chemical parameters in the Constant Capacitance Model. Soil Sci. Soc. Am. J. 64, 1356–1363. https://doi.org/10.2136/sssaj2004.7950

Goli, E., Hiemstra, T., Rahnemaie, R., 2019. Interaction of boron with humic acid and natural organic matter: Experiments and modeling. Chem. Geol. 515, 1–8. https://doi.org/10.1016/j.chemgeo.2019.03.021

Goli, E., Rahnemaie, R., Hiemstra, T., Malakouti, M.J., 2011. The interaction of boron with goethite: Experiments and CD-MUSIC modeling. Chemosphere 82, 1475–1481. https://doi.org/10.1016/j.chemosphere.2010.11.034

Groenenberg, J.E., Römkens, P.F.A.M., Zomeren, A. Van, Rodrigues, S.M., Comans, R.N.J., 2017. Evaluation of the Single Dilute (0.43 M) Nitric Acid Extraction to Determine Geochemically Reactive Elements in Soil. Environ. Sci. Technol. 51, 2246–2253. https://doi.org/10.1021/acs.est.6b05151

Hiemstra, T., Antelo, J., Rahnemaie, R., Riemsdijk, W.H. va., 2010. Nanoparticles in natural systems I: The effective reactive surface area of the natural oxide fraction in field samples. Geochim. Cosmochim. Acta 74, 41–58. https://doi.org/10.1016/j.gca.2009.10.018

Hiemstra, T., De Wit, J.C.M., Van Riemsdijk, W.H., 1989. Multisite proton adsorption modeling at the solid/solution interface of (hydr)oxides: A new approach. II. Application to various important (hydr)oxides. J. Colloid Interface Sci. 133, 105–117. https://doi.org/10.1016/0021-9797(89)90285-3

Hiemstra, T., Mia, S., Duhaut, P.-B., Molleman, B., 2013. Natural and Pyrogenic Humic Acids at Goethite and Natural Oxide Surfaces Interacting with Phosphate. Environ. Sci. Technol. 47, 9182–9189. https://doi.org/10.1021/es400997n

Hiemstra, T., Van Riemsdijk, W.H., 2006. On the relationship between charge distribution, surface hydration, and the structure of the interface of metal hydroxides. J. Colloid Interface Sci. 301, 1–18. https://doi.org/10.1016/j.jcis.2006.05.008

Hiemstra, T., Van Riemsdijk, W.H., 1996. A Surface Structural Approach to Ion Adsorption: The Charge

Distribution (CD) Model. J. Colloid Interface Sci. 179, 488–508. https://doi.org/10.1006/jcis.1996.0242

Hiemstra, T., Zhao, W., 2016. Reactivity of ferrihydrite and ferritin in relation to surface structure, size, and nanoparticle formation studied for phosphate and arsenate. Environ. Sci. Nano 3, 1265. https://doi.org/10.1039/c6en00061d

Houba, V.J.G., Temminghoff, E.J.M., Gaikhorst, G.A., van Vark, W., 2000. Soil analysis procedures using 0.01 M calcium chloride as extraction reagent. Commun. Soil Sci. Plant Anal. 31, 1299–1396. https://doi.org/10.1080/00103620009370514

Keren, R., Mezuman, U., 1981. Boron Adsorption By Clay Minerals Using a Phenomenological Equation I. Clays Clay Miner. 29, 198–204. https://doi.org/10.1346/CCMN.1981.0290305

Kinniburgh, D.G., Milne, C.J., Benedetti, M.F., Pinheiro, J.P., Filius, J., Koopal, L.K., Van Riemsdijk, W.H., 1996. Metal Ion Binding by Humic Acid: Application of the NICA-Donnan Model. Environ. Sci. Technol. 30, 1687–1698.

Kurokawa, R., Kamura, K., 2018. Adsorption of Boron by Volcanic Ash Soils Distributed in Japan. Soil Sci. Soc. Am. J. 82, 671. https://doi.org/10.2136/sssaj2017.12.0427

Lemarchand, E., Schott, J., Gaillardet, J., 2007. How surface complexes impact boron isotope fractionation: Evidence from Fe and Mn oxides sorption experiments. Earth Planet. Sci. Lett. 260, 277–296. https://doi.org/10.1016/j.epsl.2007.05.039

Mendez, J.C., Hiemstra, T., 2020a. Surface area of ferrihydrite consistently related to primary surface charge, ion pair formation, and specific ion adsorption. Chem. Geol. 532, 119304. https://doi.org/10.1016/j.chemgeo.2019.119304

Mendez, J.C., Hiemstra, T., 2020b. Ternary Complex Formation of Phosphate with Ca and Mg Ions Binding to Ferrihydrite: Experiments and Mechanisms. ACS Earth Sp. Chem. 4, 545–557. https://doi.org/10.1021/acsearthspacechem.9b00320

Mendez, J.C., Hiemstra, T., Koopmans, G.F., 2020. Assessing the Reactive Surface Area of Soils and the Association of Soil Organic Carbon with Natural Oxide Nanoparticles Using Ferrihydrite as Proxy. Environ. Sci. Technol. 54, 11990–12000. https://doi.org/10.1021/acs.est.0c02163

Mendez, J.C., Van Eynde, E., Hiemstra, T., Comans, R.N.J., 2022. Surface reactivity of the natural metal (hydr)oxides in weathered tropical soils. Geoderma 406, 115517. https://doi.org/10.1016/j.geoderma.2021.115517

Meyer, M.L., Bloom, P.R., 1997. Boric and Silicic Acid Adsorption and Desorption by a Humic Acid. J. Environ. Qual. 26, 63–69. https://doi.org/10.2134/jeq1997.00472425002600010010x

Milne, C.J., Kinniburgh, D.G., Van Riemsdijk, W.H., Tipping, E., 2003. Generic NICA - Donnan model parameters for metal-ion binding by humic substances. Environ. Sci. Technol. 37, 958–971. https://doi.org/10.1021/es0258879

Mizota, C., Reeuwijk, L. Van, 1989. Clay mineralogy and chemistry of soils formed in volcanic material in diverse climatic regions. ISM Monogr.

Parfitt, R.L., 2009. Allophane and imogolite: role in soil biogeochemical processes. Clay Miner. 44, 135–155. https://doi.org/10.1180/claymin.2009.044.1.135

Parfitt, R.L., 1990. Allophane in new zealand—a review. Aust. J. Soil Res. 28, 343–360. https://doi.org/10.1071/SR9900343

Parfitt, R.L., 1989. Optimum conditions for extraction of Al, Fe, and Si from soils with acid oxalate. Commun. Soil Sci. Plant Anal. 20, 801–816. https://doi.org/10.1080/00103628909368118

Pribyl, D.W., 2010. A critical review of the conventional SOC to SOM conversion factor. Geoderma 156, 75–83. https://doi.org/10.1016/j.geoderma.2010.02.003

Rashid, N.M.A., 1971. A Comparative Study of Boron Adsorption By a Calcareous and an Acid Soil. Utah State University.

Schwertmann, U., Schulze, D.G., Murad, E., 1982. Identification of Ferrihydrite in Soils by Dissolution Kinetics, Differential X-ray Diffraction, and Mössbauer Spectroscopy. Soil Sci. Soc. Am. J. 46, 869–875. https://doi.org/10.2136/sssaj1982.03615995004600040040x

Sillanpää, M., 1982. Micronutrients and the nutrient status of soils: a global study. FAO soils bulletin 48. FAO, Rome, Italy.

Simonsson, M., Berggren, D., Gustafsson, J.P., 1999. Solubility of Aluminum and Silica in Spodic Horizons as Affected by Drying and Freezing. Soil Sci. Soc. Am. J. 63, 1116–1123. https://doi.org/10.2136/sssaj1999.6351116x

Su, C., Suarez, D.L., 1997. Boron Sorption and Release by Allophane. Soil Sci. Soc. Am. J. 61, 61–77. https://doi.org/10.2136/sssaj1997.03615995006100010012x

Su, C., Suarez, D.L., 1995. Coordination of Adsorbed Boron: A FTIR Spectroscopic Study. Environ. Sci. Technol. 29, 302–311. https://doi.org/10.1021/es00002a005

Suarez, D.L., Wood, J.D., Taber, P.E., 2012. Adsorption and Desorption of Boron in Column Studies as Related to pH: Results and Model Predictions. Vadose Zo. J. 11, 0. https://doi.org/10.2136/vzj2011.0073

Van Eynde, E., Mendez, J.C., Hiemstra, T., Comans, R.N.J., 2020a. Boron Adsorption to Ferrihydrite with Implications for Surface Speciation in Soils: Experiments and Modeling. ACS Earth Sp. Chem. 4, 1269–1280. https://doi.org/10.1021/acsearthspacechem.0c00078

Van Eynde, E., Weng, L., Comans, R.N.J., 2020b. Boron speciation and extractability in temperate and tropical soils: A multi-surface modeling approach. Appl. Geochemistry 123, 104797. https://doi.org/10.1016/j.apgeochem.2020.104797

Vaughan, P.J., Suarez, D.L., 2003. Constant Capacitance Model Computation of Boron Speciation for Varying Soil Water Content. Methods 253–258. https://doi.org/10.2113/2.2.253

Weng, L., Temminghoff, E.J.M., Van Riemsdijk, W.H., 2001. Contribution of individual sorbents to the control of heavy metal activity in sandy soil. Environ. Sci. Technol. 35, 4436–4443. https://doi.org/10.1021/es010085j

2.6 Supplementary Information (SI):

Table S.2.1. Formation reactions and logK values for the aqueous species considered in the multi-surface modeling calculations.

Aqueous species	Reaction	logK	Reference
$B(OH)_4^-$	$B(OH)_3^0 + H_2O \leftrightarrow B(OH)_4^- + H^+$	-9.24	(Bassett, 1980)
$B_2O(OH)_5^-$	$2B(OH)_3^0 \leftrightarrow B_2O(OH)_5^- + H^+$	-9.31	(Bassett, 1980)
$B_3O_3(OH)_4^-$	$3B(OH)_3^0 \leftrightarrow B_3O_3(OH)_4^- + H^+ + 2H_2O$	-7.31	(Bassett, 1980)
$B_4O_5(OH)_4^{2-}$	$4B(OH)_3^0 \leftrightarrow B_4O_5(OH)_4^{2-} + 2H^+ + 3H_2O$	-15.06	(Bassett, 1980)
$NaB(OH)_4^0$	$Na^+ + B(OH)_3^0 + H_2O \leftrightarrow NaB(OH)_4^0 + H^+$	-8.96	(Pokrovski et al., 1995)
$CaB(OH)_4^+$	$B(OH)_3^0 + Ca^{2+} + H_2O \leftrightarrow CaB(OH)_4^+ + H^+$	-7.41	(Bassett, 1980)
$CaPO_4^-$	$PO_4^{3-} + Ca^{2+} \leftrightarrow CaPO_4^-$	6.46	(Lindsay, 1979)
$CaHPO_4$	$PO_4^{3-} + H^+ + Ca^{2+} \leftrightarrow CaHPO_4$	15.09	(Lindsay, 1979)
$CaH_2PO_4^+$	$PO_4^{3-} + 2H^+ + Ca^{2+} \leftrightarrow CaH_2PO_4^+$	20.95	(Lindsay, 1979)
HPO_4^{2-}	$PO_4^{3-} + H^+ \leftrightarrow HPO_4^{2-}$	12.35	(Lindsay, 1979)
$H_2PO_4^-$	$PO_4^{3-} + 2H^+ \leftrightarrow H_2PO_4^-$	19.55	(Lindsay, 1979)
H_3PO_4	$PO_4^{3-} + 3H^+ \leftrightarrow H_3PO_4$	21.70	(Lindsay, 1979)
$NaOH^0$	$Na^+ + OH^- \leftrightarrow NaOH^0$	-0.20	(Lindsay, 1979)
$NaNO_3^0$	$Na^+ + NO_3^- \leftrightarrow NaNO_3^0$	-0.60	(Lindsay, 1979)
$NaHPO_4^-$	$PO_4^{3-} + Na^+ + H^+ \leftrightarrow NaHPO_4^-$	13.40	(Rahnemaie et al., 2007b)
$NaPO_4^{2-}$	$PO_4^{3-} + Na^+ \leftrightarrow NaPO_4^{2-}$	2.05	(Rahnemaie et al., 2007b)
$CaOH^+$	$Ca^{2+} + OH^- \leftrightarrow CaOH^+$	1.30	(Lindsay, 1979)
$Ca(OH)_2^0$	$Ca^{2+} + 2OH^- \leftrightarrow Ca(OH)_2^0$	0.01	(Lindsay, 1979)
$CaNO_3^+$	$Ca^{2+} + NO_3^- \leftrightarrow CaNO_3^+$	0.70	(De Robertis et al., 1995)
$Ca(NO_3)_2^0$	$Ca^{2+} + 2NO_3^- \leftrightarrow Ca(NO_3)_2^0$	-4.50	(Lindsay, 1979)
$CaCl^+$	$Ca^{2+} + Cl^- \leftrightarrow CaCl^+$	-1.0	(Lindsay, 1979)

Table S.2.2. Surface complexation reactions, logK values, and charge distribution (CD) coefficients for the complete set of surface species implemented in the CD model, using ferrihydrite as reference metal (hydr)oxide material. The surface site densities are taken from Hiemstra and Zhao (2016) with ≡FeOH(a) = 3.0 nm^{-2}, ≡FeOH(b) = 2.8 nm^{-2} and ≡Fe$_3$O = 1.4 nm^{-2}. Two types of ≡FeOH(b) groups were defined to account for site heterogeneity: ≡FeOH(bl) for low and ≡FeOH(bh) for high-affinity sites for the adsorption of Ca^{2+}and B(OH)$_3$. The site densities of these groups were defined respectively to 2.50 and 0.3 nm^{-2}, in line with the densities reported by Mendez & Hiemstra (2020b) *and* Van Eynde, Mendez, et al. (2020) *for these types of groups. The interaction between the metal (hydr)oxide surfaces and natural organic matter is described with the NOM-CD approach described by* Hiemstra et al. (2013). *The capacitance values for the electrostatic model that describes the solid-solution interface (i.e., the extended Stern layers approach) are C$_1$ = 1.15 F m^{-2} and C$_2$ = 0.90 F m^{-2}, as reported by Mendez and Hiemstra (2020) for ferrihydrite nanoparticles with a mean diameter of 2.3 nm.*

Species	Adsorption reaction	Surface group [a]	Δz_0	Δz_1	Δz_2	logK	Reference
$\equiv FeOH_2$	$\equiv FeOH^{-0.5} + H^+ \leftrightarrow \equiv FeOH_2^{+0.5}$	S(a, bl, bh)*	1	0	0	8.10*	Hiemstra & Zhao (2016)
$\equiv Fe_3OH$	$\equiv Fe_3O^{-0.5} + H^+ \leftrightarrow \equiv Fe_3OH^{+0.5}$	T*	1	0	0	8.10*	
$\equiv FeOH\text{--}Na$	$\equiv FeOH^{-0.5} + Na^+ \leftrightarrow \equiv FeOH^{-0.5}\text{--}Na^+$	S(a, bl, bh)*	0	1	0	-0.60±0.02**	Mendez & Hiemstra (2020a)
$\equiv Fe_3O\text{--}Na$	$\equiv Fe_3O^{-0.5} + Na^+ \leftrightarrow \equiv Fe_3O^{-0.5}\text{--}Na^+$	T	0	1	0	-0.60±0.02**	
$\equiv FeOH_2\text{--}NO_3$	$\equiv FeOH^{-0.5} + H^+ + NO_3^- \leftrightarrow \equiv FeOH_2^{+0.5}\text{--}NO_3^-$	S(a, bl, bh)*	1	-1	0	7.42±0.02	Mendez & Hiemstra (2020a)
$\equiv Fe_3OH\text{--}NO_3$	$\equiv Fe_3O^{-0.5} + H^+ + NO_3^- \leftrightarrow \equiv Fe_3OH^{+0.5}\text{--}NO_3^-$	T	1	-1	0	7.42±0.02	
$\equiv (FeO)_2\,Ca$	$2\equiv FeOH^{-0.5} + Ca^{2+} \leftrightarrow \equiv FeO^{-0.06}Ca^{+1.06}$	S(bl)	0.94	1.06	0	2.64±0.03	

Species	Adsorption reaction	Surface group [a]	Δz_0	Δz_1	Δz_2	logK	Reference
$\equiv (FeO)_2\, Ca$	$2\equiv \mathrm{FeOH}^{-0.5} + Ca^{2+} \leftrightarrow \equiv FeO^{-0.06}Ca^{+1.06}$	S(bh)	0.94	1.06	0	5.13±0.02	Mendez & Hiemstra (2020b)
$\equiv FeOH_2 - - Cl$	$\equiv \mathrm{FeOH}^{-0.5} + H^+ + Cl^- \leftrightarrow \equiv FeOH_2{}^{+0.5} - - Cl^-$	S(a, bl, bh)*	1	-1	0	7.74±0.04	Mendez & Hiemstra (2020a)
$\equiv Fe_3OH - - Cl$	$\equiv Fe_3O^{-0.5} + H^+ + Cl^- \leftrightarrow \equiv Fe_3OH^{+0.5} - - Cl^-$	T	1	-1	0	7.74±0.04	
$\equiv FeOPO_2OH$	$\equiv \mathrm{FeOH}^{-0.5} + PO_4{}^{3-} + 2H^+ \leftrightarrow \equiv FeO^{-0.22}PO_2OH^{-1.28} + H_2O$	S(a, bl, bh)*	0.28	-1.28	0	26.36±0.20*	Hiemstra & Zhao (2016)
$\equiv FeOPO(OH)_2$	$\equiv \mathrm{FeOH}^{-0.5} + PO_4{}^{3-} + 3H^+ \leftrightarrow \equiv FeO^{-0.17}PO(OH)_2{}^{-0.33} + H_2O$	S(a, bl, bh)*	0.33	-0.33	0	29.84±0.23*	
$(\equiv FeO)_2PO_2$	$2 \equiv \mathrm{FeOH}^{-0.5} + PO_4{}^{3-} + 2H^+ \leftrightarrow \equiv (FeO)_2{}^{-0.54}PO_2{}^{-1.46} + 2H_2O$	S(bl, bh)*	0.46	-1.46	0	28.31±0.04*	
$(\equiv FeO)_2POOH$	$2 \equiv \mathrm{FeOH}^{-0.5} + PO_4{}^{3-} + 3H^+ \leftrightarrow \equiv (FeO)_2{}^{-0.35}POOH^{-0.65} + 2H_2O$	S(bl, bh)*	0.65	-0.65	0	33.52±0.13	
$\equiv FeOPO_3Ca$	$\equiv \mathrm{FeOH}^{-0.5} + PO_4{}^{3-} + Ca^{2+} + H^+ \leftrightarrow \equiv FeO^{-0.26}PO_3{}^{-1.30}Ca^{+1.06} + H_2O$	S(a, bl, bh)	0.24	-1.30	1.06	22.27±0.12	Mendez & Hiemstra (2020b)
$(\equiv FeO)_2PO_2Ca$	$2\equiv FeOH^{-0.5} + PO_4{}^{3-} + Ca^{2+} + 2H^+ \leftrightarrow (\equiv FeO)_2{}^{-0.38}PO_2{}^{-1.08}Ca^{+1.46} + 2H_2O$	S(bl,bh)	0.62	-1.08	1.46	30.09±0.12	
$\equiv (FeO)_2B(OH)$	$2\equiv FeOH^{-0.5} + B(OH)_3{}^0 \leftrightarrow \equiv (FeO)_2{}^{-0.82}B(OH)^{-0.18} + 2H_2O$	S(bh)	0.18	-0.18	0	3.39±0.18	(Van Eynde et

Species	Adsorption reaction	Surface group [a]	Δz_0	Δz_1	Δz_2	logK	Reference
$\equiv (FeO)_2B(OH)_2$	$2\equiv FeOH^{-0.5} + B(OH)_3{}^0 \leftrightarrow \equiv (FeO)_2{}^{-0.82}B(OH)_2{}^{-0.18} + H_2O + H^+$	S(bh)	-0.25	-0.75	0	-4.68±0.20	al., 2020a)
$\equiv Fe_3OH\text{--}B(OH)_3$	$\equiv Fe_3O^{-0.5} + H^+ + B(OH)_3{}^0 \leftrightarrow \equiv Fe_3OH^{+0.5}\text{--}B(OH)_3{}^0$	T	1	0	0	9.32±0.07	
$\equiv FeOH_2\text{--}B(OH)_3$	$\equiv \mathrm{FeOH}^{-0.5} + H^+ + B(OH)_3{}^0 \leftrightarrow \equiv FeOH_2{}^{+0.5}\text{--}B(OH)_3{}^0$	S(a, bl, bh)	1	0	0	9.32±0.07	
$\equiv FeNOM$	$\equiv \mathrm{FeOH}^{-0.5} + \equiv HNOM^{-1} \leftrightarrow \equiv Fe^0NOM^{-1,-0.5} + \mathrm{H2O}$	S(a, bl, bh) + HNOM	1.5	-1	-0.5	0	
$\underline{\equiv FeOH_2NOM}$	$\underline{\equiv \mathrm{FeOH}^{-0.5} + HNOM^{-1} \leftrightarrow \equiv FeOH_2{}^{+0.5}NOM^{-1.5,-0.5}}$	<u>S(a, bl, bh) +HNOM</u>	<u>2</u>	<u>-1.5</u>	<u>-0.5</u>	<u>0.6</u>	Hiemstra et al. (2013)
$\underline{\equiv \mathrm{Fe}NOMH}$	$\underline{\equiv \mathrm{FeOH}^{-0.5} + HNOM^{-1} + H^+ \leftrightarrow \equiv \mathrm{Fe}^0NOMH^{-0.5,0} + H_2O}$	<u>S(a, bl, bh) + HNOM</u>	<u>1.5</u>	<u>-0.5</u>	<u>0</u>	<u>3.5</u>	

[a] *Type of reactive surface group that can take part in the corresponding adsorption reaction. S and T stand for singly and triply coordinated groups, respectively. For the S, two types are distinguished: the type a form single corner (^{1}C) monodentate and single edge (^{1}E) bidentate complexes, and the type b forms single corner (^{1}C) monodentate and bidentate double-corner (^{2}C) complexes. For type b of singly coordinated groups, high and low-affinity sites are represented respectively by (bh) and (bl) for describing Ca^{2+} adsorption* (Mendez and Hiemstra, 2020a). *For boron, the formation of inner-sphere complexes occurs only with the high-affinity sites (bh), according to the approach presented by* Van Eynde, Mendez, et al. (2020).

Table S.2.3. NICA-Donnan parameters for humic acids implemented in our modeling approach. Boron adsorption parameters were taken from Goli et al. (2019)*, whereas the adsorption parameters for* Ca^{2+} *and* H^{+} *(logK and* n_i*) and the structural parameters related to sites heterogeneity (*p_1 *and* p_2*), site densities (*$S_{T,1}$ *and* $S_{T,2}$*), and Donnan volume were taken from* Milne et al. (2003).

$S_{T,1}$	$S_{T,2}$	p_1	p_2	*Donnan volume*	
3.15 mol kg^{-1}	*2.55 mol* kg^{-1}	*0.62*	*0.41*	$logV_D=b(1-log\ I)-1$	*b=0.49*

Species	**S_1**		**S_2**	
	logK	**n_1**	**logK**	**n_2**
H^+	2.93	0.81	8.00	0.63
Ca^{2+}	-1.37	0.78	-0.43	0.75
$B(OH)_3^0$	-0.23	0.91	1.35	0.61

Table S.2.4. Distribution of boron for the different treatments evaluated in the batch adsorption experiments in 0.01 M $CaCl_2$ and 0.01 M $NaNO_3$ background electrolytes, the results are multi-surface model (CD-MUSIC-NICA-Donnan) predictions.

B solution concentration (µmol L-1)	Background electrolyte	P treatment	Boron distribution		Sub-distribution of adsorbed boron	
			% Total B-Solution	% Total B-adsorbed	%B-Humic	%B-(Hydr)oxides
1.57	0.01M $CaCl_2$	+0mM P	68	32	8,3	91,7
11.87			69	31	6,0	94,0
22.21			69	31	5,4	94,6
42.90			69	31	4,9	95,1
84.36			69	31	4,6	95,4
1.58		+1.6 mM P	69	31	8,7	91,3
11.97			69	31	6,2	93,8
22.39			69	31	5,7	94,3
43.26			69	31	5,3	94,7
85.05			70	30	4,9	95,1
1.79	0.01M $NaNO_3$	+0mM P	68,1	32	6,5	93,5
11.98			68,4	32	5,0	95,0
22.23			68,5	31	4,6	95,4
42.5			68,6	31	4,3	95,7
83.64			68,7	31	4,1	95,9
1.8		+1.6 mM P	68,7	31	6,9	93,1
12.07			69,1	31	5,2	94,8
22.38			69,2	31	4,9	95,1
43.06			69,3	31	4,6	95,4
84.73			69,3	31	4,3	95,7

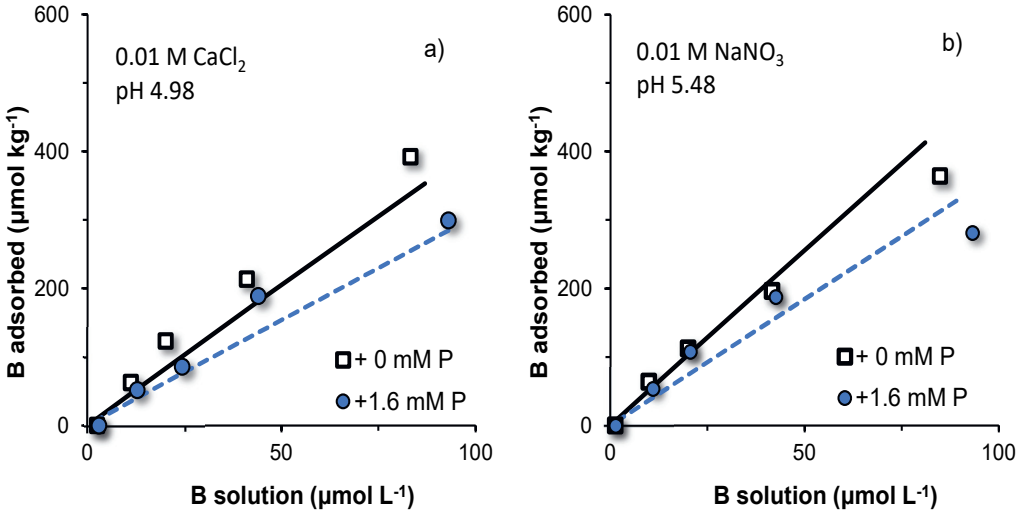

Figure S.2.1. *Boron (B) adsorption isotherms for conditions with no extra P and 1.6 mM P added to an Aluandic Dystric Andosol (Fluvic) from Costa Rica with an explorative modeling approach to test the cause of non-linearity observed at high boron concentrations under the presence of phosphate in the system. Model results correspond to the implementation of a lower log K for the formation of outer-sphere species (Δ logk= -0.20) and with adjusted number of sites for the formation of inner-sphere species (2.8 nm^{-2} for high affinity sites). The left (a) and right (b) panels are for systems in 0.01 M $CaCl_2$ and 0.01 M $NaNO_3$ as background solutions. respectively. The symbols are experimental data and lines (solid= +0.0mM P. and dashed= +1.6 mM P) are the multi-surface complexation model predictions.*

Additional references for supplementary material:

Bassett, R.L., 1980. A critical evaluation of the thermodynamic data for boron ions, ion pairs, complexes, and polyanions in aqueous solution at 298.15 K and 1 bar. Geochim. Cosmochim. Acta 44, 1151–1160. https://doi.org/10.1016/0016-7037(80)90069-1

De Robertis, A., Di Giacomo, P., Foti, C., 1995. Ion-selective electrode measurements for the determination of formation constants of alkali and alkaline earth metals with low-molecular-weight ligands. Anal. Chim. Acta 300, 45–51. https://doi.org/10.1016/0003-2670(94)00421-H

Goli, E., Hiemstra, T., Rahnemaie, R., 2019. Interaction of boron with humic acid and natural organic matter: Experiments and modeling. Chem. Geol. 515, 1–8. https://doi.org/10.1016/j.chemgeo.2019.03.021

Hiemstra, T., Mia, S., Duhaut, P.-B., Molleman, B., 2013. Natural and Pyrogenic Humic Acids at Goethite and Natural Oxide Surfaces Interacting with Phosphate. Environ. Sci. Technol. 47, 9182–9189. https://doi.org/10.1021/es400997n

Hiemstra, T., Zhao, W., 2016. Reactivity of ferrihydrite and ferritin in relation to surface structure, size, and nanoparticle formation studied for phosphate and arsenate. Environ. Sci. Nano 3, 1265. https://doi.org/10.1039/c6en00061d

Lindsay, W.L., 1979. Chemical equilibria in soils. Wiley, New York, NY.

Mendez, J.C., Hiemstra, T., 2020a. Ternary Complex Formation of Phosphate with Ca and Mg Ions Binding to Ferrihydrite: Experiments and Mechanisms. ACS Earth Sp. Chem. 4, 545–557. https://doi.org/10.1021/acsearthspacechem.9b00320

Mendez, J.C., Hiemstra, T., 2020b. Surface area of ferrihydrite consistently related to primary surface charge, ion pair formation, and specific ion adsorption. Chem. Geol. 532, 119304. https://doi.org/10.1016/j.chemgeo.2019.119304

Milne, C.J., Kinniburgh, D.G., Van Riemsdijk, W.H., Tipping, E., 2003. Generic NICA - Donnan model parameters for metal-ion binding by humic substances. Environ. Sci. Technol. 37, 958–971. https://doi.org/10.1021/es0258879

Pokrovski, G.S., Schott, J., Sergeyev, A.S., 1995. Experimental determination of the stability constants of NaSO4- and NaB (OH)40 in hydrothermal solutions using a new high-temperature sodium-selective glass electrode - Implications for boron isotopic fractionation. Chem. Geol. 124, 253–265. https://doi.org/10.1016/0009-2541(95)00057-S

Rahnemaie, R., Hiemstra, T., Van Riemsdijk, W.H., 2007. Geometry, charge distribution, and surface speciation of phosphate on goethite. Langmuir 23, 3680–3689. https://doi.org/10.1021/la062965n

Van Eynde, E., Mendez, J.C., Hiemstra, T., Comans, R.N.J., 2020. Boron Adsorption to Ferrihydrite with Implications for Surface Speciation in Soils: Experiments and Modeling. ACS Earth Sp. Chem. 4, 1269–1280. https://doi.org/10.1021/acsearthspacechem.0c00078

Chapter 3

Multi-component interactions and effects of potassium fertilizer additions on zinc availability in tropical volcanic soils

Róger Fallas-Corrales, Johannes C.L. Meeussen, Sjoerd E. A. T. M. van der Zee

Submitted.

Abstract

Applying fertilizers can have significant secondary effects on the availability of essential trace metals in soils. In this work, the potential effects of adding high rates of potassium chloride (KCl) on the availability and leaching of zinc for two volcanic ash-derived soils were evaluated by combining batch adsorption experiments and undisturbed column transport experiments. Adding fertilizers such as KCl affects the ionic strength and the soil solution pH. We performed batch adsorption experiments at a range of pH's and ionic strengths to test this effect. The results demonstrate that pH has a primary role in the zinc partition between the adsorption surfaces and solution, with lower zinc adsorption at low pH. Furthermore, the ionic strength has an additional effect on the partition of zinc between the solution and surface. Additionally, we carried out potassium transport experiments using undisturbed soil columns, applying KCl solution (0.064 M) during several pore volumes, and evaluating zinc concentrations in the leachate. These experiments revealed an increased zinc leaching related to the higher KCl concentration in soil solution. For "La Sonia" soil (high reactive surface area), the increased zinc leaching showed a strong correlation with the pH and ionic strength of the solution, while for "San Bosco" soil (low reactive surface area), this correlation was less clear. This work indicates that in the case of KCl fertilization strategies, the secondary effect of this fertilizer on Zn availability and leaching should be considered, especially in intensive agricultural systems where significant amounts of potassium fertilizer are applied.

Keywords:

Potassium, fertilizer, zinc, adsorption isotherms, pH, ionic strength, breakthrough curves.

3.1 Introduction

Alluvial volcanic ash-derived soils are commonly used in the tropics to produce high nutrient-demanding fruit crops such as banana, pineapple, and papaya (Arias et al., 2010; Cattan et al., 2006; Ndayiragije and Delvaux, 2004; Rallos et al., 2017). Consequently, these volcanic soils typically receive high rates of N-P-K fertilizer additions that, under specific conditions, could contaminate groundwater sources and, by multi-component nutrient interactions, could produce nutrient imbalance.

Moreover, some of these tropical and subtropical volcanic regions are characterized by high precipitation regimes, for instance, the Caribbean region of Costa Rica, Hawaii, Japan, Philippines, and Guadeloupe, typically in combination with highly permeable volcanic soils (Cattan et al., 2006). Therefore, the combination of high precipitation, permeable soils, and an increased application rate of fertilizers and pesticides in intensive production systems represents a constraint to environmentally friendly and

sustainable agricultural production (Castillo et al., 2000; Comte et al., 2018; Hernández-Hernández et al., 2007; Megchún-García et al., 2019).

A better understanding of the complex multi-component nutrient interactions under volcanic soil production systems from humid regions could help predict nutrient solubility, availability, and transport in these soil systems, reducing the risk of adverse environmental impact from intensive agricultural systems.

In this paper, we focus on the multi-component effect of potassium fertilizer on zinc availability and transport for the following reasons:

i) Potassium is the most demanded nutrient for fruit crops like papaya (Fallas-Corrales and van der Zee, 2020; Fallas et al., 2014) and banana (Turner and Barkus, 1983). **ii)** The excessive potassium application in agriculture dates from the 1970s (Khan et al., 2013). **iii)** The addition of high rates of potassium to soil systems could modify chemical factors that directly and indirectly affect the zinc adsorption-desorption process. Therefore, if competitive interactions exist, zinc deficiencies in humid volcanic soil systems could be exacerbated by adding high potassium rates. **iv)** Low zinc availability is a common constraint for plant production in Costa Rican volcanic soils (Mendez and Bertsch, 2012), where the production from this region is mainly used for export, generating a significant economic impact. **v)** Zinc deficiencies are present in more than one-third of the world-arable land (Sillanpää, 1982), and zinc deficiencies in agricultural soils correlate with human zinc deficiencies (Cakmak and Hoffland, 2012), thus, understanding the zinc interactions with a commonly applied fertilizer for agriculture (such as KCl) could be important for other world regions.

Among the chemical properties that could potentially influence the solubility of the reactive fraction of Zn^{2+} from highly fertilized soils highlights the increase of the ionic strength, the complexation reactions with counter ions (e.g., Cl^-), and the pH changes (Shuman, 1986). All of them could result in different zinc solubility, availability, and leaching.

The primary role of the pH in Zn adsorption/desorption has been extensively documented for pure systems (e.g., ferrihydrite, goethite, or humic acids systems) and for multi-surface soil systems, with higher adsorption as the pH increases and a substantial variation in the adsorbed amounts between pH 4.5 to pH 7 (Arias et al., 2005; Barrow, 1993; Casagrande et al., 2008, 2004; Fest et al., 2005; Kooner, 1993; Nachtegaal and Sparks, 2004; Nomaan et al., 2021; Shuman, 1986; Singh et al., 2008; Trivedi et al., 2004; Van Eynde, 2021; Van Eynde et al., 2022b). The pH also affects the zinc adsorption to the organic matter, as described by Fest et al. (2005), who showed by model calculations that reducing pH also decreases the participation of the soil organic matter for zinc adsorption. The effect of pH on zinc adsorption has also been observed

for analog organic materials like biochar, where functional carboxyl and hydroxyl groups deprotonate at high pH, increasing the organic matter surface charge (Zhao et al., 2020).

On the other hand, the ionic strength has a less strong effect on Zn adsorption to (hydr)oxides (e.g., ferrihydrite) (Trivedi et al., 2004; Van Eynde et al., 2022b), which could be related to the principal zinc-binding mechanism to the (hydr)oxide fraction, suggesting potential chemisorption, which is not significantly affected by salt concentrations (Trivedi et al. (2004)). Regarding the effect of ionic strength on zinc sorption under more heterogeneous natural systems, Casagrande et al. (2008) did not find differences in zinc adsorption for two weathered soils (Oxisol and Alfisol) when pH was below 5.0. However, they observed a more pronounced effect for higher pH, with lower adsorption as the ionic strength increases. Casagrande et al. (2008) related the more notorious effect of the ionic strength observed at higher pH values (above 5) to zinc adsorption to the organic matter present in these soils.

From these results, it appears that for soils with high contents of organic matter and pH values above 5.0, the changes in the ionic strength of the soil solution could also affect the availability and transport of zinc. In this regard, the volcanic soils from tropical regions usually have high contents of organic matter and low pH values (Arias et al., 2010; Nanzyo et al., 1993a). Therefore, it can provide insight to conduct experiments to determine whether the ionic strength modifies the zinc adsorption in volcanic soils.

Furthermore, experiments with other divalent metals (e.g., Cd^{2+}) suggest that metals could experience an increase in complexation reactions when increasing the ionic strength, especially under specific anions like chloride (Boekhold et al., 1993; Temminghoff et al., 1995). However, the effect of complexation reactions at different ionic strengths for zinc is unclear. For instance, Lumsdon et al. (1995) found no effect of chloride complexation reactions on Zn^{2+} adsorption for two Humaquepts soils, which could be related to the low logK (0.43) for the formation of $ZnCl^{+}$ species (U.S. EPA, 1999). On the other hand, Kaur et al. (2010) found higher Zn^{2+} adsorption for chloride-based electrolyte systems than for nitrate-based ones.

The addition of high rates of N-P-K fertilizer to soil systems could modify the pH values (Du et al., 2010; Janke et al., 2020; Qaswar et al., 2020; Tkaczyk et al., 2020), becoming an important factor to consider for zinc deficiencies/toxicities management and for reducing the zinc leaching from agricultural fields. Regarding papaya and banana production systems, most of the potassium required by the crop is typically applied in a clearly defined area around the plant using KCl sources, which according to Du et al. (2010), adding KCl to calcareous and acid soils reduces the pH around the fertilizer application site, and this reduction of pH spreads over time. Therefore, for agricultural production systems developed in volcanic

soils, the application of very high rates of KCl fertilizer could reduce the soil solution pH and modify the availability, transport, and leaching of zinc.

Based on the aspects mentioned above, we hypothesize a possible role of KCl applications in continuous and high quantities for zinc adsorption/desorption and leaching in volcanic soils:

First, changes in the solution pH induced by the H^+ desorption when large amounts of K^+ are present in the solution could modify the Zn^{2+} sorption. We expect that more desorption of Zn^{2+} occurs under high doses of KCl in the system due to the lower pH of the soil solution. Second, we expect the increased ionic strength and the presence of more chloride in the system also modifies the Zn complexation and the zinc adsorption. Third, the lower pH (De Troyer et al., 2014) and adsorption of monovalent cations to soil organic matter (Kalinichev et al., 2011; Skyllberg and Magnusson, 1995; Xu et al., 2019) could indirectly increase the concentration of dissolved organic matter (DOM) and in that way promote the mobility of attached Zn^{2+}.

From the above, it becomes clear that it is relevant to elucidate the possible role of potassium fertilizer applications on volcanic soil systems to better understand the dynamics of micronutrients like zinc and to improve its management. The objectives of this paper are: i) to experimentally evaluate changes in the zinc sorption patterns in two volcanic soils related to variations of pH and ionic strength of the solution, and ii) to determine via transport experiments whether KCl additions modify the zinc transport and leaching patterns for undisturbed volcanic soil columns.

3.2 Materials and Methods:

3.2.1 Sampling and characterization of the soils:

We collected soil samples from alluvial volcanic ash-derived soils in the Atlantic Region of Costa Rica at two locations: San Bosco (10.279290 N, 83.802527 W) and La Sonia (10.276015 N, 83.793851 W), Pococí, Costa Rica. Both fields are located at 110 meters above sea level. According to the georeferenced coordinates, the soils classify as Aluandic Dystric Andosol (Fluvic) (World Reference Base soil classification system).

All soil samples taken were oven-dried (50 ºC) for 48 hours and sieved (<2mm) prior to chemical analyses. Soil organic C content was determined by a dry combustion analyzer (Elementar Vario Macro cube), assuming the lack of carbonates in the samples. Dissolved organic carbon (DOC) was determined in a total organic carbon (TOC) analyzer using the method 5310 B (Baird et al., 2017).

Soil-pH was determined in ultrapure water and 0.01 M $CaCl_2$, using a soil/solution ratio of 1/10 (weight/volume). Selective dissolution extractions of Fe and Al were performed using Dithionite-Citrate-Bicarbonate (DC) and acid Ammonium Oxalate (AO) extractants as described by Burt (2004).

In addition, zinc extractions were performed using deionized water (DW), $CaCl_2$ 0.01 M solution (Houba et al., 2000), HNO_3 0.43M solution (Groenenberg et al., 2017), and the total zinc content was determined by the HNO_3+HCl (aqua regia) digestion as specified by Burt (2004) (method 4H1). For all the extractions and digestions performed, we used soil to solution ratios of 1:10.

3.2.2 Batch adsorption experiments developed at different pH and ionic strengths:

For the batch adsorption isotherms, 4 grams of soil were mixed with 40 mL of a solution that contained the background electrolyte (0.005 M KCl solution), plus the freshly prepared Zn solutions using "pro analysi" (p.a.) grade $ZnCl_2$ as a zinc source. The adsorption isotherms were performed at two pH values (final pH= 4.7 and 5.6) for both soils. The solution pH was initially adjusted using either 0.02 M HCl or NaOH solution using a micropipette (100-1000 µL). Then, samples were shaken for 19 hours at 120 rpm, using a Tecnal orbital shaker (Tecnal, Piracicaba, Brasil), and right after, the pH was re-adjusted by adding 1M HCl or 1M NaOH solution with a micropipette (10-100 µL). After the second pH adjustment, the samples were shaken in the orbital shaker for one additional hour at 120 rpm, and then a final pH measurement was done, which corresponds to the pH reported for the adsorption isotherms. For all the experiments, we used p.a. chemical reagents.

The batch adsorption experiments consisted of individual soil samples where applications of increasing doses of Zn were conducted, adding one specific Zn dose to one soil sample. These increasing doses consisted in adding 40 ml of a solution with a total zinc concentration of 0, 0.6, 1.2, 1.8, 2.4, and 3 mg Zn per liter of solution (0, 9.18, 18.35, 27.5, 36.7, and 45.8 µmol Zn L^{-1}).

The highest concentration evaluated in our adsorption experiments (45.8 µmol Zn L^{-1}) applied 2.5 times the highest concentration of zinc observed in the leachate of San Bosco column experiment under high solubility conditions (low pH and high KCl concentration), as further described in section 3.2.3. Additionally, the evaluated solution concentrations reached values between typical Zn fertilizer recommendations rates (assuming a volumetric water content near saturation for our soils) (Liu et al., 2019).

After the final pH measurement, we centrifuged the samples for 5 minutes at 3750 x g and filtered the supernatant with a 0.20 µm syringe PTFE membrane filter. The zinc equilibrium concentrations in the extracts were determined by inductively coupled plasma mass spectroscopy (ICP-MS) using a Thermo Scientific iCAP RQ ICP-MS.

An additional adsorption isotherm experiment was conducted for both soils, but this time, varying the ionic strength of the solution from 0.005 to 0.05 M (also using a KCl background solution) and applying the same zinc concentrations. These last adsorption isotherms were developed only at pH=5.6. The concentrations for the background electrolyte solutions (0.005 M and 0.05 M) were defined according to a previous exploratory sampling of the soil solution in the root zone area of papaya (*Carica papaya* L.) production plots, which resulted in a 0.001 M ionic strength for an unfertilized area and 0.064 M for the fertilized area (one day after the fertilizer application, and after a heavy rain event).

For this additional adsorption experiment, the samples followed the same previously described shaking and pH adjustment process. Later, we centrifuged the samples for 5 minutes at 3750 x g, and the supernatant was filtered with a 0.20 µm syringe PTFE membrane filter.

The exploratory soil solution samples collected from the field used to define the ionic strength of the solutions for the batch adsorption experiments were collected using non-adsorbing membrane Rhizon samplers (Rhizosphere®) coupled to newly and acid clean 20 ml plastic syringes. These soil solution samples taken from the field were analyzed by inductively coupled plasma optical emission spectroscopy (ICP-OES) using a Perkin-Elmer Corp Optima 8300 ICP-OES.

For the batch adsorption experiment, the total zinc concentration in the extracts was analyzed by inductively coupled plasma mass spectroscopy using a Thermo Scientific iCAP RQ ICP-MS. Additionally, we took one mixed sample for each combination between soil, pH, and ionic strength, to analyze dissolved organic carbon through the method 5310 B (Baird et al., 2017) in a TOC analyzer.

Also, we estimated the retardation factor (R) considering linear adsorption for each adsorption isotherm as follows (Equation 3.1):

$$R = 1 + \frac{1-n}{n} * \rho s * Kd \qquad \text{Equation 3.1}$$

Where ρs and n are, respectively, the bulk density and the mean volumetric water content observed for the undisturbed samples of the column transport experiments, and Kd is the linear adsorption coefficient obtained for each specific isotherm.

3.2.3 Transport experiments developed in undisturbed soil columns

Undisturbed soil core samples (14.7 cm length and 8.3 cm internal diameter for San Bosco and La Sonia soils) were collected to conduct KCl transport experiments that simulated the effect of potash (KCl) fertilization applied at high rates.

Previously, a Multi-Step Flux Transport device was built as specified by Kumahor et al. (2015), but with a modification in the upper boundary of the system. This modification consisted of adding a thin polyurethane sponge placed over the soil column, which received the input solution from the peristaltic pump via needles. This modification aimed to provide a more homogeneous application and distribution of the solute along the upper boundary of the soil column. Solute transport experiments were conducted with this device under unsaturated conditions and gravitational flow. The peristaltic pump (input solution) applied a mean constant flux of 0.286 and 0.198 cm h^{-1} for La Sonia and San Bosco soil columns, respectively. For these experiments, the mean value of one pore volume (mean weight of (soil + solution) - dry weight of the soil) corresponded to 382.5 and 417.5 cm^3 for La Sonia and San Bosco, respectively.

The undisturbed soil column used for the transport experiments of La Sonia soil had a soil bulk density of 0.82 g cm^{-3} and total porosity of 0.64 cm^3 cm^{-3}, while San Bosco had a soil bulk density of 0.885 g cm^{-3} and total porosity of 0.615 cm^3 cm^{-3}.

Initially, the soil columns were saturated with tap water and later equilibrated with a background solution of $CaCl_2$ 0.001M, flushing five pore volumes of 0.001M $CaCl_2$ solution to the columns in the Multi-Step Flux Transport device. After this equilibration process, potassium transport experiments were started, applying sequentially the solutions specified in Table 3.1. The leachate was collected at different time steps during the experiment development. For each sample, pH was measured in a calibrated pH meter (Mettler Toledo SevenExcellence Multiparameter). At the same time, the total potassium concentration was determined in a Perkin-Elmer Corp Optima 8300 ICP-OES, and the total zinc concentration was determined in a Thermo Scientific iCAP RQ ICP-MS.

The mean volumetric water content for the experiments was 0.48 cm^3 cm^{-3} for “La Sonia” soil column and 0.57 cm^3 cm^{-3} for San Bosco.

Table 3.1. The sequence of solutions applied to increase or reduce the potassium chloride concentrations for the solute transport experiments developed in two undisturbed volcanic soil columns from La Sonia and San Bosco, Pococí, Costa Rica.

ID	Mean flow rate cm h^{-1}	Soil	Experiment	Applied pore volumes	Solution applied
1_LS	0.286	La Sonia	Loading KCl	4.3	0.001M $CaCl_2$ + 0.064 M KCl
2_LS		La Sonia	Unloading KCl	8.7	0.001M $CaCl_2$
3_LS		La Sonia	Loading KCl	7.2	0.001M $CaCl_2$ + 0.064 M KCl
4_LS		La Sonia	Unloading KCl	4.4	0.001M $CaCl_2$
1_SB	0.198	San Bosco	Loading KCl	3.1	0.001M $CaCl_2$ + 0.064 M KCl
2_SB		San Bosco	Unloading KCl	4.3	0.001M $CaCl_2$
3_SB		San Bosco	Loading KCl	4.6	0.001M $CaCl_2$ + 0.064 M KCl
4_SB		San Bosco	Unloading KCl	4.0	0.001M $CaCl_2$

3.3 Results and discussion:

3.3.1 Characterization of the soils:

Both volcanic ash-derived soils presented contrasting characteristics that could influence zinc adsorption and availability. For instance, La Sonia soil had a lower pH value than San Bosco soil, which according to literature, a lower pH could result in a higher zinc solubility (Arias et al., 2005; Casagrande et al., 2004; Van Eynde et al., 2022a; Zhao et al., 2020). However, La Sonia had more adsorption surfaces than San Bosco soil, evidenced by the higher (hydr)oxides, organic matter, and clay content, resulting in a higher reactive surface area (Table 3.2). This high amount of (hydr)oxides, organic matter content, and clay content in La Sonia soil (Table 3.2) adsorb significant quantities of zinc, as evidenced in Table 3.3.

La Sonia soil had a higher total zinc content in Aqua regia and in HNO_3 0.43 M solution (Table 3.3) and a lower pH than San Bosco soil, supposing a higher zinc solution content for La Sonia soil. However, the high amount of adsorption surfaces for La Sonia soil resulted in a lower zinc concentration for the extractions in deionized water and 0.01M $CaCl_2$ (Table 3.3), In other words, this soil has a higher capacity factor and a lower intensity factor compared to San Bosco soil.

Table 3.2. Soil properties of the volcanic ash-derived soils from La Sonia and San Bosco, Pococí, Costa Rica.

Soil ID	Clay	Silt	Sand	pH_{H2O}	$pH_{CaCl2\ 0.01M}$	Fe_{DC}	Al_{DC}	Fe_{AO}	Al_{AO}	OC	RSA	R-PO4
	%					mmol kg^{-1} soil				%	Hiemstra et al. (2010)	
											m^2g^{-1}	mmol kg^{-1}
La Sonia	20	30	50	5.20	4.58	423.8	466.3	238.1	1045.2	4.70	78.12	20.51
San Bosco	15	5	80	5.85	5.19	173.7	248.2	151.9	1112.9	2.87	37.6	18.45

DC=Dithionite-Citrate extract, AO= Ammonium oxalate extract, OC= Organic carbon, RSA= Reactive surface area, R-PO_4= Reversibly adsorbed phosphate.

The zinc concentration extracted in HNO_3 0.43 M for La Sonia soil was higher than that observed in San Bosco soil. This last suggests that part of the zinc adsorbed to the soil surfaces is affected by the pH and solubilizes under acid conditions. When comparing Zn concentrations obtained with the different extracts (Table 3.3), we observed two different factors controlling the zinc adsorption-solubilization process: the amount of adsorption surfaces and the pH of the solution, which regulates the intensity factor in these soils.

Table 3.3. Extractable zinc concentrations determined by different solutions for two different volcanic ash-derived soils from San Bosco and La Sonia, Pococí, Costa Rica. Soil/solution ratio= 1/10

Soil	Zn-H_2O	Zn-$CaCl_2$ 0.01M Houba et al (2000)	Zn-HNO_3 0.43M Groenenberg et al (2017)	Zn-Aqua Regia
	mmol kg^{-1} soil			
La Sonia	0.0003	0.0006	0.24	1.87
San Bosco	0.006	0.008	0.14	1.25

3.3.2 Batch adsorption experiments developed at different pH and ionic strength

As mentioned before, the addition of high KCl rates to acid and basic soils could modify the pH of the soil solution (Du et al., 2010). Consequently, changes in pH induced by the KCl additions could affect the solubility, availability, and leaching of zinc; In Figure 3.1, zinc adsorption showed a quasi-linear behavior at these low solution concentrations. In agreement with the literature (Casagrande et al., 2008, 2004; Fest et al., 2005; Kooner, 1993; Nachtegaal and Sparks, 2004; Nomaan et al., 2021; Shuman, 1986; Singh et al., 2008; Trivedi et al., 2004; Van Eynde et al., 2022b; Van Eynde, 2021), the pH strongly affected the Zn sorption pattern for both soils with reduced adsorption at low pH.

The pH effect on zinc adsorption was more evident for La Sonia than for San Bosco soil. This result was consistently observed for both the batch adsorption isotherms (Figure 3.1) and extractant solutions (Table 3.3). La Sonia soil had a higher total zinc content plus a higher content of adsorption surfaces ((hydr)oxides, clay, and organic matter) than San Bosco soil, and consequently, the changes in zinc adsorption related to pH can be more accentuated for this soil. According to modeling simulations obtained by Van Eynde et al. (2022), both –(hydr)oxides and organic matter– increase their zinc adsorption when increasing the pH. However, according to their data, at low pH, the organic matter (SOC and DOC) appears to be the principal zinc adsorption surface, while the (hydr)oxide and clay fractions have low participation at low pH, and the (hydr)oxide fraction acquires more relevance at high pH (above 5.5).

When extrapolating their results to our data, it suggests that the (hydr)oxide fraction could be more critical for zinc adsorption in San Bosco soil (pH_{H2O}= 5.85) than in La Sonia soil (pH_{H2O}=5.2), while organic matter could play a more important role for zinc adsorption in La Sonia soil. In this regard, Güngör & Bekbölet (2010) mentioned that at pH above the pKa values of the humic acid binding sites (e.g., carboxylic and phenolic groups), the metals are attracted to the negative charge of these functional groups. This negative charge results from the deprotonation of the functional groups at high solution pH, which increases the metal-organic matter complexation reactions; consequently, the zinc adsorption to the organic matter increases with the pH. Boguta and Sokołowska (2016) agree that the stronger zinc complexation to the organic matter at higher pH is related to the higher dissociation degree of the functional groups of humic acids. In addition, they suggest a minimization of steric effects related to the expansion of the humic acid structure at elevated pH.

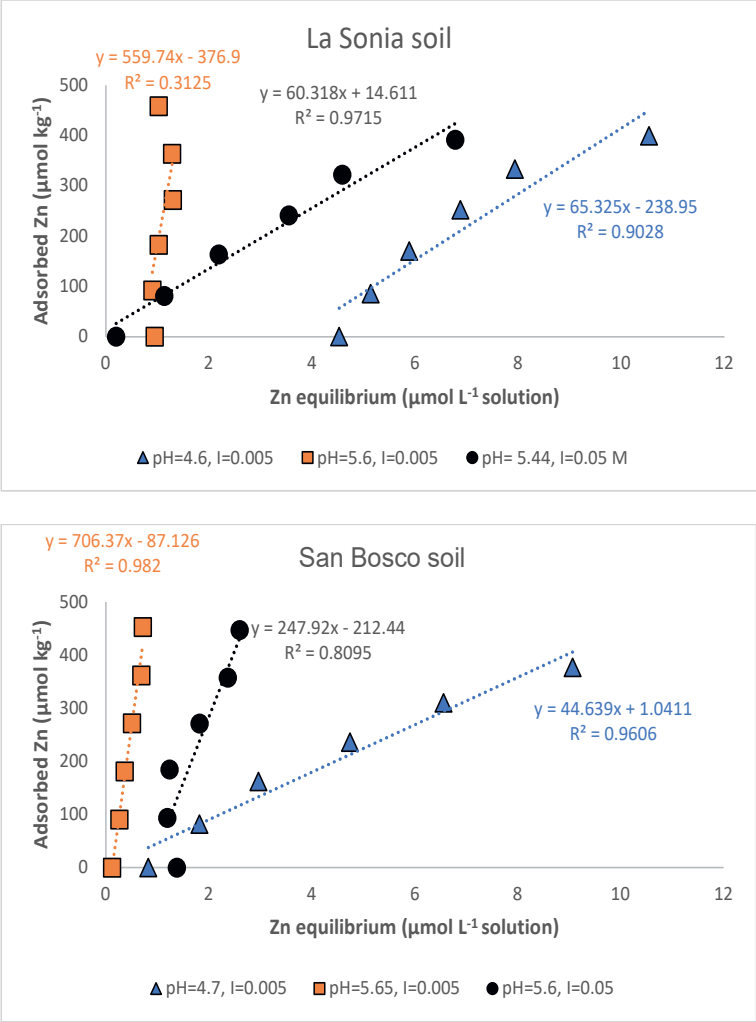

Figure 3.1. Batch adsorption experiments developed at different pH values and ionic strength (0.005 and 0.05 M KCl background solutions) for two different volcanic ash-derived soils.

On the other hand, considering that the addition of KCl to the soil system corresponds to a higher ionic strength of the soil solution, we also developed zinc batch adsorption isotherms at an increased ionic strength. This experiment showed lower zinc adsorption when increasing the ionic strength for both soils.

Regarding the ionic strength effect on zinc adsorption to pure oxide suspension systems, Kooner (1993) studied zinc adsorption for pure goethite suspension systems, while Van Eynde et al. (2022b) evaluated its effect on a pure ferrihydrite suspension system. Kooner (1993) concluded that a ten times increase of the ionic strength did not affect the zinc adsorption on pure goethite aqueous systems, while

Van Eynde (2021) found a small effect of ionic strength on the Zn adsorption edges using $NaNO_3$ 0.01, 0.1 and 1M background solutions. Additionally, Van Eynde et al. (2022b) found no differences for low pH and a slight difference (lower adsorption at higher ionic strength) for high pH values.

From our experimental data detailed in Figure 3.1, the most plausible explanation for the lower zinc adsorption noticed at high ionic strength for our volcanic soils is a mechanism related to the organic matter or potassium competition with non-specifically adsorbed zinc, as Kooner (1993) and Van Eynde et al. (2022b) found just slight differences for zinc adsorption to pure oxide suspension systems at different ionic strengths.

Regarding the potassium-zinc competition found in our experiments, direct competition between potassium and specifically adsorbed zinc at the surface of (hydr)oxides seems unlikely to occur, as there is a big difference in the reaction equilibrium constants (logK) between both nutrients with hydr(oxide) surfaces (Mendez and Hiemstra, 2020b; Van Eynde et al., 2022b). However, competition of zinc with other cations could be expected for non-specifically adsorbed zinc. For instance, Casagrande et al. (2004) observed that part of the zinc was non-specifically adsorbed for a variable charge Oxisol (Anionic Acrudox, pH= 4.8 and 5.1). This report suggests there could be a Zn fraction in soils potentially affected by direct cation exchange competition, which agrees with Shuman (1986), that evaluated zinc adsorption at different ionic strengths in two ultisols (Rhodic Paleudult and Typic Paleudult) and found that at high ionic strengths, the sodium competes with zinc due to the ionic exchange effect.

For other metal cations, the increase of complexation reactions with the companying anion could influence the higher solubility of the metal. For instance, Temminghoff et al. (1995) found an increase in cadmium complexation from 13% to 90% when the background solution's ionic strength was increased from 0.003 to 0.3 M using a $CaCl_2$ as background solution. Furthermore, Boekhold, Temminghoff, & Van Der Zee (1993) evaluated the influence of different electrolyte solutions on cadmium adsorption; they also found lower adsorption for $CaCl_2$ electrolyte systems than $Ca(NO_3)_2$ systems and lower adsorption for NaCl systems compared to $NaNO_3$. For zinc, Shuman (1986) found higher zinc adsorption for sulfate-based background solutions than chloride or nitrate-based ones, suggesting low participation of zinc chloride complexation reactions. This low complexation of zinc for chloride systems agrees with the low logK value for the production of $ZnCl^+$ complexes, as reported by U.S. EPA (1999). For our experiments, we only tested a chloride-based background solution.

On the other hand, both chemical factors that were evaluated in the adsorption isotherms (pH and ionic strength) for our volcanic soils, but mainly the ionic strength modified the DOC content (Table 3.4). The DOC content increased with the ionic strength, which was more evident for La Sonia soil. The DOC

exerts a significant complexation effect with metals like Cu and Zn, reducing the overall adsorption to the solid surfaces at low and high pH (Mesquita and Carranca, 2005). The latter could be related to the low molecular weight and low aromatization state of these dissolved organic molecules that could form soluble complexes with metals, as suggested by Fan et al. (2016).

Table 3.4. Mean dissolved organic carbon (DOC) in the solution extracts from the zinc adsorption isotherms developed at different pH and ionic strength. Data were obtained for two Andosols from San Bosco and La Sonia, Pococí, Costa Rica.

Soil ID	pH	Ionic Strength	DOC mg L^{-1}
San Bosco	4.70	0.005M	5.43 ± 0.14
San Bosco	5.59	0.005M	5.98 ± 0.15
San Bosco	5.45	0.05M	6.81 ± 0.17
La Sonia	4.65	0.005M	10.81 ± 0.35
La Sonia	5.61	0.005M	10.88 ± 0.35
La Sonia	5.44	0.05M	15.43 ± 0.56

As the DOC complexes zinc, the higher abundance of DOC at higher solution ionic strength could decrease zinc adsorption to the solid soil surfaces and increase transport of complexed zinc under highly fertilized volcanic soils conditions.

Based on the later results, two of the soil chemical parameters modified by the addition of high rates of KCl (the pH and the ionic strength) strongly influence the zinc sorption patterns. Consequently, the application of high rates of KCl to volcanic ash-derived soils, which could modify the pH and the ionic strength, increased the zinc concentration in the solution. Increasing the zinc concentration in the solution by applying high fertilizer rates can be advantageous for plant production systems developed in zinc-deficient soils (e.g., the alluvial volcanic soils from the Costa Rican Atlantic region). However, the higher zinc solubilization could also result in increased leaching and losses under the high precipitation regimes and the extreme precipitation events that characterize this Costa Rican region (see Figure S.3.1 from Supplementary Information) and other tropical and subtropical humid volcanic regions.

Finally, according to the linear adsorption isotherms and aiming to generate information for further solute transport modeling purposes, we estimated the retardation factor based on linear adsorption (*Kd*). This retardation factor decreased with increasing the ionic strength and decreasing the solution pH. For instance, the retardation factor in La Sonia soil was 498, 55, and 59 for the control treatment (high pH and low ionic strength), the increased ionic strength treatment, and the decreased pH treatment, respectively.

Meanwhile, the retardation factor based on linear adsorption resulted in 473, 167, and 31 for the control, the increased ionic strength, and the decreased pH treatment, respectively, for San Bosco soil.

3.3.3 Transport experiments developed in undisturbed volcanic soil columns:

As shown in Figure 3.2, the application of KCl modified the solution pH for La Sonia soil but did not influence the solution pH for San Bosco soil column. For instance, the KCl concentration showed an inverse relationship with the pH, decreasing the leachate pH when KCl concentration increased in the solution for La Sonia soil (Figure 3.2.a). The leachate pH returned to higher values when the KCl concentrated solution was removed from the soil column, flushing it with a more diluted $CaCl_2$ 0.001 M solution (Figure 3.2.a). This behavior demonstrates the interaction of the saline fertilizer solutions with the surface charge, in agreement with previous reports about allophanic soils (Black and Campbell, 1982).

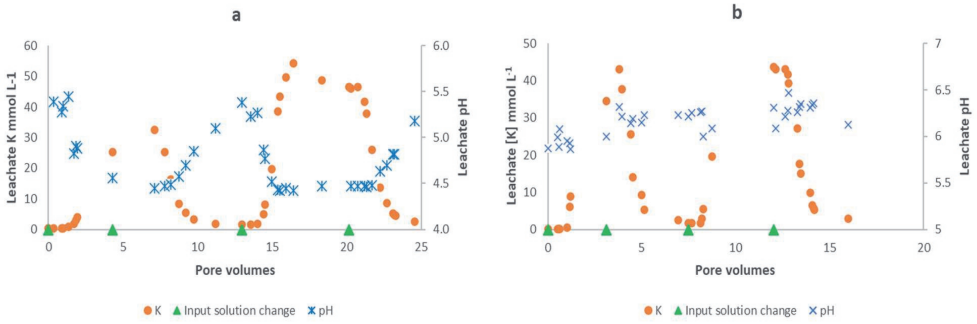

Figure 3.2. Potassium concentration breakthrough curves and their effect on the leachate pH for undisturbed Andosol soil columns from La Sonia (a), and San Bosco (b), Pococí, Costa Rica.

This decrease of the solution pH due to KCl additions (increasing ionic strength) showed a robust non-linear relationship for La Sonia soil but no clear relationship for San Bosco soil (Figure S.3.2, Supplementary Information). For La Sonia soil, the change of leachate pH was more prominent for ionic strength values below 0.01 mol L^{-1} (Figure S.3.2). This behavior implies that the enhanced zinc leaching related to pH changes in this soil could occur even for lower KCl concentrations than those evaluated in our experiments (0.064 mol L^{-1}).

For San Bosco soil, which has a higher pH and a lower content of (hydr)oxides and organic matter (Table 3.2), the changes in the solution's ionic strength did not correlate with the leachate pH (Figure S.3.2), and the variation of pH was not as accentuated as for La Sonia soil.

Our batch adsorption experiments showed that the ionic strength directly affects zinc desorption in these volcanic soils. Furthermore, as shown in Figure S.3.2 for La Sonia soil, it also affected zinc desorption indirectly, as it strongly correlates with the pH of the leachate solution. The net result of applying a high KCl rate to La Sonia soil was the increased zinc solubilization.

The zinc concentration and activity in the leachate increased as the potassium concentration also increased (Figure 3.3), with a strong correlation between potassium and zinc leachate concentrations for La Sonia soil and a moderate correlation for San Bosco soil (Figure S.3.3, Supplementary Information). Our results showed the intensification of zinc desorption and leaching induced by high KCl concentrations for our low pH volcanic soil (La Sonia). From our results, we consider this enhanced leaching of zinc is related to the effect of pH change as found by several authors (Arias et al., 2005; Casagrande et al., 2008, 2004; Nachtegaal and Sparks, 2004; Shuman, 1986; Van Eynde et al., 2022b), by the impact of the ionic strength as found by Shuman (1986), and probably by the increased DOC that could rise the zinc complexation in the dissolved fraction.

Additionally, the intensified zinc desorption could also be related to the competition of zinc with other divalent cations like Ca^{2+} and Mg^{2+} that probably are exchanged from the adsorption sites by the high potassium concentrations evaluated in our experiments. Wang et al. (1997) found a dramatic decrease in cadmium and zinc adsorption in the presence of calcium for subsurface soils, which they related to competition for binding sites between these metals and the added calcium.

For San Bosco soil, the KCl application also influenced the leachate's zinc concentrations (Figure S.3.3), showing higher zinc concentrations when potassium concentrations increased. However, the correlation between potassium and zinc concentrations in the leachate was moderate (Pearson's correlation coefficient =0.8) for this soil. This result is probably related to the low correlation between the potassium concentrations and the solution pH in this soil (Figure 3.2.b), which according to literature, pH is the principal factor that modifies the zinc solubilization patterns from pure and multi-surface soil systems (Casagrande et al., 2004; Shuman, 1986; Van Eynde et al., 2022b). However, the trends observed in K and Zn behavior for San Bosco soil (Figure 3.3) indicate that the observed zinc mobilization in this soil is probably not dominated by the pH effect (as for San Bosco soil, zinc and pH did not correlate), but still, there is concordance between potassium and zinc leachate concentrations (Figure S.3.3). This is more evident when assessing the trends of potassium and zinc concentrations in the leachate for La Sonia soil, reinforcing the combined effect of pH and ionic strength on zinc solution partition.

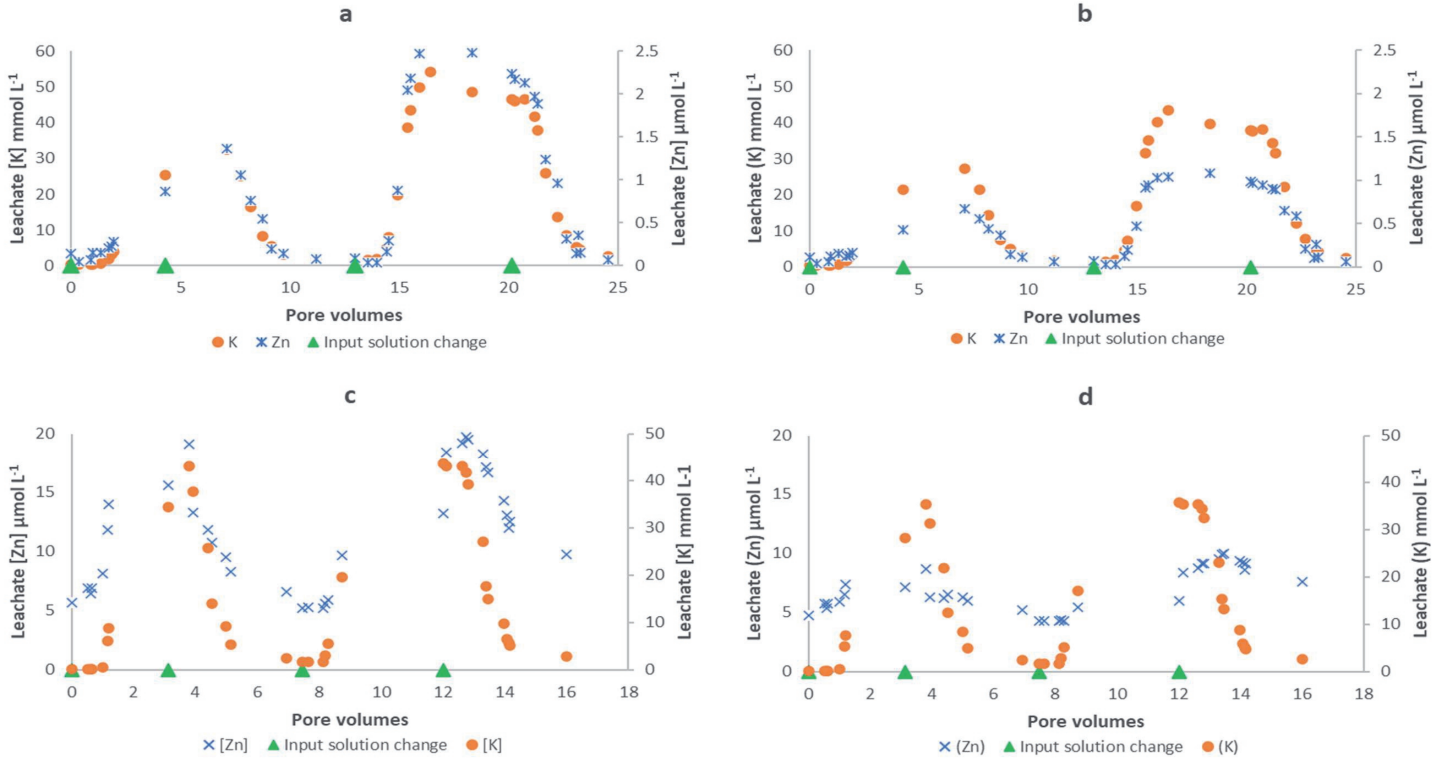

Figure 3.3. K and Zn breakthrough curves (concentrations (a, c), and activities (b, d)) determined in the leachate of undisturbed Andosol columns from La Sonia (a, b) and San Bosco (c, d), Pococí, Costa Rica. The input solution consisted of $CaCl_2$ 0.001 + KCl 0.064 M solution pulses, which were cleaned with a $CaCl_2$ 0.001 M solution. Green triangles indicate changes of the input solution between $CaCl_2$ 0.001 + KCl 0.064 M solution and $CaCl_2$ 0.001M solutions. Please note the different scales for the y-axis.

Moreover, the addition of high rates of KCl could affect the DOC content, as evidenced in Table 3.4. We suppose that the solution's monovalent cation (K^+) intensification that replaces divalent cations adsorbed to the organic matter particles could increase the deflocculation of these organic particles, promoting a higher DOC content in the liquid fraction. Therefore, the higher DOC content in the solution could modify the zinc equilibrium between the solid and suspended/soluble fraction, as the dissolved organic particles can complex more zinc. The higher zinc complexation to dissolved particles could result in higher zinc transport losses. On the other hand, a high chloride amount in the soil solution product of the addition of high rates of KCl could not have a substantial complexation effect on zinc desorption for our experiments, as the log K value suggests that $ZnCl^+$ is not as stable as other chloride-cation complexes like $CdCl^+$ (U.S. EPA, 1999).

Regarding the total amount of zinc that leached from the undisturbed soil columns, for La Sonia soil, the leached fraction for the whole experiment (total amount of 14.22 µmol Zn kg^{-1} soil) corresponded to 2370%, 5.9%, and less than 1% of the amount of zinc determined by the $CaCl_2$ 0.01 M, HNO_3 0.43 M extracts, and by the aqua regia digestion, respectively (see Table 3.3). On the other hand, for San Bosco soil column, the total amount of zinc leached was higher (112.3 µmol Zn kg^{-1} soil) than for La Sonia soil, and the leached fraction of San Bosco soil corresponded to 1403%, 80%, and 6% compared to the amounts of zinc determined by the $CaCl_2$ 0.01 M, the HNO_3 0.43 M extracts, and the aqua regia digestion, respectively.

The previous results showed that the $CaCl_2$ 0.01 M solution sub-estimates the reactive zinc fraction that can be affected by potassium chloride additions. In contrast, for the HNO_3 0.43 M solution, we cannot conclude about the performance of this extractant to determine the reactive zinc fraction, principally because we have only two different results to compare. For La Sonia soil, the leached fraction corresponded to a very low percentage of the amount determined by the HNO_3 0.43M extractant; meanwhile, for San Bosco it corresponded to 80% of the amount determined by this extractant solution. This last result provides evidence of the smaller intensity factor for La Sonia soil compared to San Bosco soil, all these in agreement with the higher clay content, higher (hydr)oxides content, and higher reactive surface area of La Sonia soil, which could promote higher zinc adsorption.

On the other hand, we observed contrasting results when comparing the outcome of the zinc batch adsorption isotherms against the column desorption and transport experiments. For instance, the adsorption experiments suggest very high values for the retardation factor, but the zinc desorption from the column transport experiment did not show a retardation factor as high as those indicated by the adsorption isotherms (Figure 3.3). The differences between the retardation factor of the adsorption isotherms and the columns desorption and transport experiments could be related to different reasons: First, the adsorption and

desorption processes do not always behave as linear functions; mostly due to hysteresis that might be observed between these two opposite processes. Second, the zinc desorption breakthrough curves shown in Figure 3.3 could obey the breakthrough of the parameters that modify the zinc solubility (e.g., pH and ionic strength) and probably not represent the breakthrough curves for the complete transport of zinc in these systems.

Correspondingly, Zn will probably experience different transport results in these columns if we keep a constant pH and ionic strength. When controlling the pH and ionic strength for zinc adsorption/desorption experiments developed in different soils, Singh et al. (2008) found that desorption experiments followed the same trend as adsorption ones; consequently, the same retardation factor could be applied to describe adsorption and desorption transport processes in their soils. In contrast, for our desorption and transport experiment in which the pH and the ionic strength varied as a function of the potassium chloride concentrations, the adsorption isotherms cannot be used to explain the results of the desorption breakthrough curves.

Again, both chemical variables (pH and ionic strength) influenced the desorption of reactive zinc from these volcanic soils, and the change in these variables could result in enhanced zinc transport, as evidenced in the column transport experiments. Then, the multi-component interactions of potassium fertilizers in volcanic soil systems should be considered to manage better the highly demanded potassium and the commonly deficient zinc nutrient to produce highly nutrient-demanding crops in tropical volcanic soils.

3.4 Conclusions:

- The applications of high KCl rates to tropical volcanic soils can modify the pH and the ionic strength of the soil solution, as demonstrated in our laboratory-scale experiments. However, field experiments are still necessary to corroborate this situation in field production plots.
- Changes in ionic strength induced by KCl additions could increase DOC amounts, as evidenced in the batch adsorption experiments.
- Both chemical factors (lower pH and higher ionic strength) modified by the KCl additions to volcanic soils promote higher zinc concentrations in solution, which might result in higher zinc losses from these soil systems. This situation could be important for humid weather conditions like the region where we collected our soil samples.

- The modeling of Zn leaching losses from volcanic soil systems should consider the changes in chemical parameters that modify zinc solubility (e.g., pH and ionic strength), as simple approaches that use constant values of adsorption coefficients like Kd to estimate retardation factors could fail in the prediction of the real reactive transport.
- Zinc deficiencies currently present in tropical volcanic soils could be exacerbated in the middle and long term due to the application of very high rates of KCl fertilizer. The rate at which deficiencies could appear seems to be a function of the soil-specific intensity and capacity factors, with higher zinc leaching losses for the soil with lower buffer capacity.

Data availability statement:

The datasets generated and analyzed during the current study are available under request. Also, the data are being deposited in the 4TU.ResearchData repository, DOI: 10.4121/20108906.

3.5 References:

Arias, F., Mata, R., Alvarado, A., Serrano, E., Laguna, J., 2010. Caracterización química y clasificación taxonómica de algunos suelos cultivados con banano en las llanuras aluviales del Caribe de Costa Rica. Agron. Costarric. 34, 177–195.

Arias, M., Pérez-Novo, C., Osorio, F., López, E., Soto, B., 2005. Adsorption and desorption of copper and zinc in the surface layer of acid soils. J. Colloid Interface Sci. 288, 21–29. https://doi.org/10.1016/j.jcis.2005.02.053

Baird, R., Eaton, A., Rice, E. (Eds.), 2017. Standard Methods, 23rd ed, Standard Methods for the Examination of Water and Wastewater. https://doi.org/10.1016/B978-0-12-382165-2.00237-3

Barrow, N.J., 1993. Mechanisms of Reaction of Zinc with Soil and Soil Components BT - Zinc in Soils and Plants: Proceedings of the International Symposium on 'Zinc in Soils and Plants' held at The University of Western Australia, 27–28 September, 1993, in: Robson, A.D. (Ed.), . Springer Netherlands, Dordrecht, pp. 15–31. https://doi.org/10.1007/978-94-011-0878-2_2

Black, A.S., Campbell, A.S., 1982. Ionic strength of soil solution and its effect on charge properties of some New Zealand soils. J. Soil Sci. 33, 249–262. https://doi.org/10.1111/j.1365-2389.1982.tb01763.x

Boekhold, A.E., Temminghoff, E.J.M., Van Der Zee, S.E.A.T.M., 1993. Influence of electrolyte composition and pH on cadmium sorption by an acid sandy soil. J. Soil Sci. 44, 85–96. https://doi.org/10.1023/A:1004909322206

Boguta, P., Sokołowska, Z., 2016. Interactions of Zn(II) Ions with Humic Acids Isolated from Various Type of Soils. Effect of pH, Zn Concentrations and Humic Acids Chemical Properties. PLoS One 11, 1–20. https://doi.org/10.1371/journal.pone.0153626

Burt, R., 2004. Soil Survey Laboratory Methods Manual. Soil Survey Investigations report No.42, Version 4.0.

Cakmak, I., Hoffland, E., 2012. Zinc for the improvement of crop production and human health. Plant Soil 361, 1–2. https://doi.org/10.1007/s11104-012-1504-0

Casagrande, J.C., Alleoni, L.R.F., De Camargo, O.A., Arnone, A.D., 2004. Effects of pH and ionic strength on zinc sorption by a variable charge soil. Commun. Soil Sci. Plant Anal. 35, 2087–2095. https://doi.org/10.1081/LCSS-200028914

Casagrande, J.C., Soares, M.R., Mouta, E.R., 2008. Zinc adsorption in highly weathered soils. Pesqui. Agropecu. Bras. 43, 131–139. https://doi.org/10.1590/S0100-204X2008000100017

Castillo, L.E., Ruepert, C., Solis, E., 2000. Pesticide residues in the aquatic environment of banana plantation: Areas in the north Atlantic zone of Costa Rica. Environ. Toxicol. Chem. 19, 1942–1950. https://doi.org/10.1002/etc.5620190802

Cattan, P., Cabidoche, Y.M., Lacas, J.G., Voltz, M., 2006. Effects of tillage and mulching on runoff under banana (Musa spp.) on a tropical Andosol. Soil Tillage Res. 86, 38–51. https://doi.org/10.1016/j.still.2005.02.002

Comte, I., Cattan, P., Charlier, J.B., Gentil, C., Mottes, C., Lesueur-Jannoyer, M., Voltz, M., 2018. Assessing the environmental impact of pesticide use in banana cropping systems. Acta Hortic. 1196, 195–202. https://doi.org/10.17660/ActaHortic.2018.1196.24

De Troyer, I., Merckx, R., Amery, F., Smolders, E., 2014. Factors Controlling the Dissolved Organic Matter Concentration in Pore Waters of Agricultural Soils. Vadose Zo. J. 13, vzj2013.09.0167. https://doi.org/10.2136/vzj2013.09.0167

Du, Z., Zhou, J., Wang, H., Chen, X., Wang, Q., 2010. Communications in Soil Science and Plant Analysis Soil pH Changes from Fertilizer Site as Affected by Application of Monocalcium Phosphate and Potassium Chloride Soil pH Changes from Fertilizer Site as Affected by Application of Monocalcium Phosphate and Potassium Chloride. Commun. Soil Sci. Plant Anal. 41, 1779–1788. https://doi.org/10.1080/00103624.2010.492064

Fallas-Corrales, R., van der Zee, S.E.A.T.M., 2020. Diagnosis and management of nutrient constraints in papaya, in: Srivastava, A.K., Chengxiao, H. (Eds.), Fruit Crops. Elsevier Inc., pp. 607–628. https://doi.org/10.1016/b978-0-12-818732-6.00042-3

Fallas, R., Bertsch, F., Barrientos, M., 2014. Curvas de absorción de nutrientes en papaya (Carica papaya L.) CV. "Pococí" en las fases de crecimiento vegetativo, floración e inicio de cosecha. Agron. Costarric. 38, 43–54.

Fan, T.T., Wang, Y.J., Li, C.B., He, J.Z., Gao, J., Zhou, D.M., Friedman, S.P., Sparks, D.L., 2016. Effect of Organic Matter on Sorption of Zn on Soil: Elucidation by Wien Effect Measurements and EXAFS Spectroscopy. Environ. Sci. Technol. 50, 2931–2937. https://doi.org/10.1021/acs.est.5b05281

Fest, E.P.M.J., Temminghoff, E.J.M., Griffioen, J., Van Riemsdijk, W.H., 2005. Proton buffering and metal leaching in sandy soils. Environ. Sci. Technol. 39, 7901–7908. https://doi.org/10.1021/es0505806

Groenenberg, J.E., Römkens, P.F.A.M., Zomeren, A. Van, Rodrigues, S.M., Comans, R.N.J., 2017. Evaluation of the Single Dilute (0.43 M) Nitric Acid Extraction to Determine Geochemically Reactive Elements in Soil. Environ. Sci. Technol. 51, 2246–2253. https://doi.org/10.1021/acs.est.6b05151

Güngör, E.B.Ö., Bekbölet, M., 2010. Zinc release by humic and fulvic acid as influenced by pH, complexation and DOC sorption. Geoderma 159, 131–138. https://doi.org/10.1016/j.geoderma.2010.07.004

Hernández-Hernández, C.N.A., Valle-Mora, J., Santiesteban-Hernández, A., Bello-Mendoza, R., 2007. Comparative ecological risks of pesticides used in plantation production of papaya: Application of the SYNOPS indicator. Sci. Total Environ. 381, 112–125. https://doi.org/10.1016/j.scitotenv.2007.03.014

Hiemstra, T., Antelo, J., Rahnemaie, R., Riemsdijk, W.H. va., 2010. Nanoparticles in natural systems I: The effective reactive surface area of the natural oxide fraction in field samples. Geochim. Cosmochim. Acta 74, 41–58. https://doi.org/10.1016/j.gca.2009.10.018

Houba, V.J.G., Temminghoff, E.J.M., Gaikhorst, G.A., van Vark, W., 2000. Soil analysis procedures using 0.01 M calcium chloride as extraction reagent. Commun. Soil Sci. Plant Anal. 31, 1299–1396. https://doi.org/10.1080/00103620009370514

Janke, C.K., Moody, P., Bell, M.J., 2020. Three-dimensional dynamics of nitrogen from banded enhanced efficiency fertilizers. Nutr. Cycl. Agroecosystems 118, 227–247. https://doi.org/10.1007/s10705-020-10095-5

Kalinichev, A.G., Iskrenova-Tchoukova, E., Ahn, W.Y., Clark, M.M., Kirkpatrick, R.J., 2011. Effects of Ca^{2+} on supramolecular aggregation of natural organic matter in aqueous solutions: A comparison of

molecular modeling approaches. Geoderma 169, 27–32. https://doi.org/10.1016/j.geoderma.2010.09.002

Kaur, G., Sharma, B.D., Seth, A., Bhardwaj, S.S., 2010. Zinc adsorption as affected by supporting electrolyte in benchmark soils of Punjab in Northwest India. Commun. Soil Sci. Plant Anal. 41, 2685–2698. https://doi.org/10.1080/00103624.2010.517883

Khan, S.A., Mulvaney, R.L., Ellsworth, T.R., 2013. The potassium paradox: Implications for soil fertility, crop production and human health. Renew. Agric. Food Syst. 29, 3–27. https://doi.org/10.1017/S1742170513000318

Kooner, Z.S., 1993. Comparative study of adsorption behavior of copper, lead, and zinc onto goethite in aqueous systems. Environ. Geol. 21, 242–250. https://doi.org/10.1007/BF00775914

Kumahor, S.K., Hron, P., Metreveli, G., Schaumann, G.E., Klitzke, S., Lang, F., Vogel, H.J., 2015. Transport of citrate-coated silver nanoparticles in unsaturated sand. Sci. Total Environ. 535, 113–121. https://doi.org/10.1016/j.jconhyd.2016.10.001

Liu, D.Y., Liu, Y.M., Zhang, W., Chen, X.P., Zou, C.Q., 2019. Zinc uptake, translocation, and remobilization in winter wheat as affected by soil application of zn fertilizer. Front. Plant Sci. 10, 1–10. https://doi.org/10.3389/fpls.2019.00426

Lumsdon, D., Evans, L., Bolton, K., 1995. The Influence of pH and Chloride on the Retention of Cadmium, Lead, Mercury, and Zinc by Soils. J. Soil Contam. 4, 137–150. https://doi.org/10.1080/15320389509383488

Megchún-García, J.V., Refugio, C.-C.M. del, Rodríguez-Lagunes, D.A., Murguía González, J., Lango Reynoso, F., Leyva-Ovalle, O.R., 2019. Impact of thiamethoxam in papaya cultivation (Carica papaya linnaeus) in rotation with watermelon (Citrullus lanatus) crops. Agric. 9, 1–11. https://doi.org/10.3390/agriculture9060129

Mendez, J.C., Bertsch, F., 2012. Guía para la interpretación de la fertilidad de los suelos de Costa Rica. Asociación Costarricense de la Ciencia del Suelo, San José, Costa Rica.

Mendez, J.C., Hiemstra, T., 2020. Surface area of ferrihydrite consistently related to primary surface charge, ion pair formation, and specific ion adsorption. Chem. Geol. 532, 119304. https://doi.org/10.1016/j.chemgeo.2019.119304

Mesquita, M.E., Carranca, C., 2005. Effect of dissolved organic matter on copper-zinc competitive adsorption by a sandy soil at different pH values. Environ. Technol. 26, 1065–1072. https://doi.org/10.1080/09593332608618493

Nachtegaal, M., Sparks, D.L., 2004. Effect of iron oxide coatings on zinc sorption mechanisms at the clay-mineral/water interface. J. Colloid Interface Sci. 276, 13–23. https://doi.org/10.1016/j.jcis.2004.03.031

Nanzyo, M., Dahlgren, R., Shoji, S., 1993. Chapter 6 Chemical Characteristics of Volcanic Ash Soils. Dev. Soil Sci. 21, 145–187. https://doi.org/10.1016/S0166-2481(08)70267-8

Ndayiragije, S., Delvaux, B., 2004. Selective sorption of potassium in a weathering sequence of volcanic ash soils from Guadeloupe, French West Indies. Catena 56, 185–198. https://doi.org/10.1016/j.catena.2003.10.010

Nomaan, S.M., Stokes, S.N., Han, J., Katz, L.E., 2021. Application of spectroscopic evidence to diffuse layer model (DLM) parameter estimation for cation adsorption onto ferrihydrite in single- and bi-solute systems. Chem. Geol. 573, 120199. https://doi.org/10.1016/j.chemgeo.2021.120199

Qaswar, M., Dongchu, L., Jing, H., Tianfu, H., Ahmed, W., Abbas, M., Lu, Z., Jiangxue, D., Khan, Z.H., Ullah, S., Huimin, Z., Boren, W., 2020. Interaction of liming and long-term fertilization increased crop yield and phosphorus use efficiency (PUE) through mediating exchangeable cations in acidic soil under wheat–maize cropping system. Sci. Reports 2020 101 10, 1–12. https://doi.org/10.1038/s41598-020-76892-8

Rallos, R., Asio, V., Villamayor, F., 2017. Soil-Landscape Relationship in the Northern Volcanic Mountain of Leyte, Philippines. Ann. Trop. Res. 104, 87–104. https://doi.org/10.32945/atr3916.2017

Shuman, L.M., 1986. Effect of Ionic Strength and Anions on Zinc Adsorption by Two Soils. Soil Sci. Soc. Am. J. 50, 1438–1442. https://doi.org/10.2136/sssaj1986.03615995005000060012x

Sillanpää, M., 1982. Micronutrients and the nutrient status of soils: a global study. FAO soils bulletin 48. FAO, Rome, Italy.

Singh, D., McLaren, R.G., Cameron, K.C., 2008. Effect of pH on zinc sorption-desorption by soils. Commun. Soil Sci. Plant Anal. 39, 2971–2984. https://doi.org/10.1080/00103620802432873

Skyllberg, U., Magnusson, T., 1995. Cations adsorbed to soil organic matter - A regulatory factor for the release of organic carbon and hydrogen ions from soils to waters. Water, Air, Soil Pollut. 85, 1095–1100. https://doi.org/10.1007/BF00477127

Temminghoff, E.J.M., Van Der Zee, S.E.A.T.M., De Haan, F.A.M., 1995. Speciation and calcium competition effects on cadmium sorption by sandy soil at various pHs. Eur. J. Soil Sci. 46, 649–655.

Tkaczyk, P., Mocek-Płóciniak, A., Skowró Nska, M., Bednarek, W., Ku´smierzku´smierz, S., Zbieta Zawierucha, E., 2020. The Mineral Fertilizer-Dependent Chemical Parameters of Soil Acidification under Field Conditions. Sustainability 12, 2–11. https://doi.org/10.3390/su12177165

Trivedi, P., Dyer, J.A., Sparks, D.L., Pandya, K., 2004. Mechanistic and thermodynamic interpretations of zinc sorption onto ferrihydrite. J. Colloid Interface Sci. 270, 77–85. https://doi.org/10.1016/S0021-9797(03)00586-1

Turner, D.W., Barkus, B., 1983. The uptake and distribution of mineral nutrients in the banana in response to supply of K, Mg and Mn. Fertil. Res. 4, 89–99. https://doi.org/10.1007/BF01049669

U.S. EPA, 1999. MINTEQA2/PRODEFA2, A Geochemical Assessment Model for Environmental Systems: User Manual Supplement for Version 4.0.

Van Eynde, E., 2021. Environmental availability of micronutrients in tropical soils. Wageningen University and Research.

Van Eynde, E., Groenenberg, B.J., Hoffland, E., Comans, R.N.J., 2022a. Solid-solution partitioning of micronutrients Zn, Cu and B in tropical soils: mechanistic and empirical models. Geoderma 414, 115773. https://doi.org/10.1016/j.geoderma.2022.115773

Van Eynde, E., Hiemstra, T., Comans, R.N.J., 2022b. Interaction of Zn with ferrihydrite and its cooperative binding in the presence of PO4. Geochim. Cosmochim. Acta 320, 223–237. https://doi.org/10.1016/j.gca.2022.01.010

Wang, W.Z., Brusseau, M.L., Artiola, J.F., 1997. The use of calcium to facilitate desorption and removal of cadmium and nickel in subsurface soils. J. Contam. Hydrol. 25, 325–336. https://doi.org/10.1016/S0169-7722(96)00046-0

Xu, F., Yao, Y., Alvarez, P.J.J., Li, Q., Fu, H., Yin, D., Zhu, D., Qu, X., 2019. Specific ion effects on the

aggregation behavior of aquatic natural organic matter. J. Colloid Interface Sci. 556, 734–742. https://doi.org/10.1016/j.jcis.2019.09.001

Zhao, M., Dai, Y., Zhang, M., Feng, C., Qin, B., Zhang, W., Zhao, N., Li, Y., Ni, Z., Xu, Z., Tsang, D.C.W., Qiu, R., 2020. Mechanisms of Pb and/or Zn adsorption by different biochars: Biochar characteristics, stability, and binding energies. Sci. Total Environ. 717, 136894. https://doi.org/10.1016/j.scitotenv.2020.136894

3.6 Supplementary information:

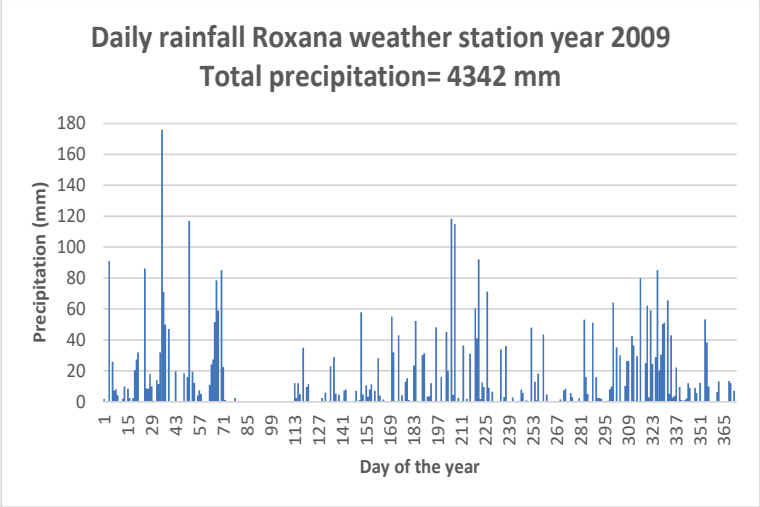

Figure S.3.1. Daily rainfall data for a close weather station from the sampled field plots. Example of data for the year 2009.

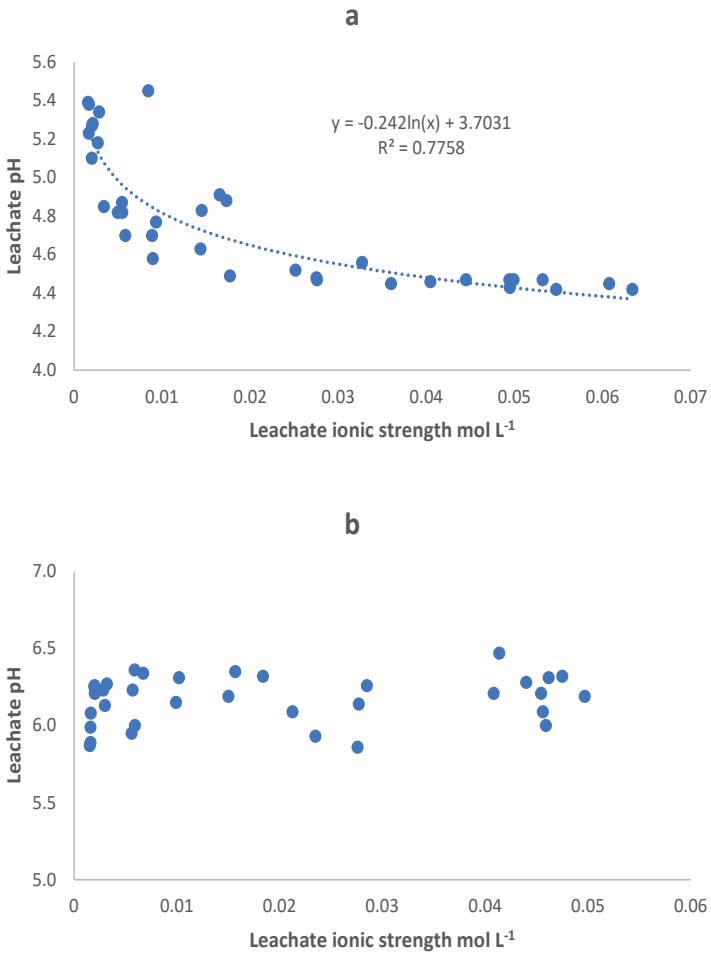

Figure S.3.2. Leachate pH and leachate molar ionic strength relationship for undisturbed soil columns from La Sonia (a) and San Bosco (b), Pococí, Costa Rica submitted to solute transport experiments with the application of potassium chloride at high concentrations.

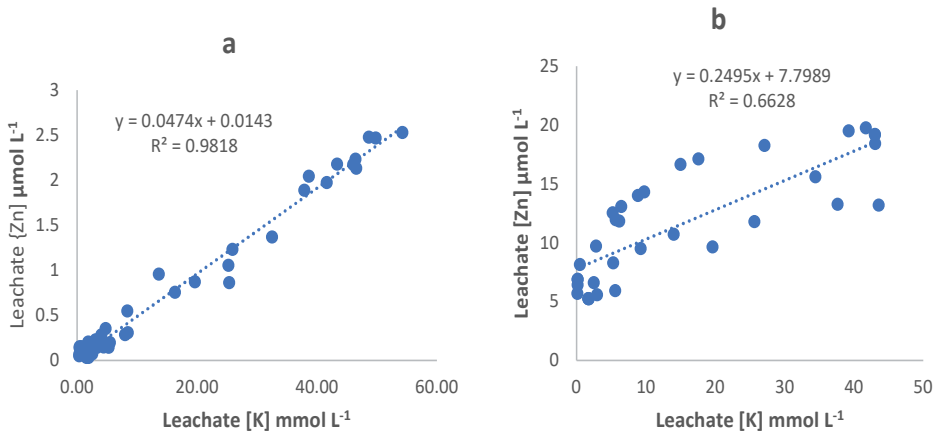

Figure S.3.3. The relationship between K and Zn concentrations for the potassium transport experiments developed in undisturbed soil columns from La Sonia (a) and San Bosco (b), Pococí, Costa Rica. Note the differences in the scale of the Y-axis.

Chapter 4

The effect of flow rate and solution chemistry on apparent solute transport parameters in unsaturated soil column experiments

Róger A. Fallas-Corrales, Johannes C.L. Meeussen, Sjoerd E.A.T.M. van der Zee, Harm P.A. Gooren, Manuel E. Camacho

Submitted.

Abstract

Prediction of solute transport rates in soils requires a number of estimated transport parameters, such as; porosity, hydraulic conductivity, dispersivity, mass transfer coefficient between stagnant and mobile pore water among others as model inputs. Such parameters can be estimated from undisturbed column experiments and are generally assumed to be constants. In the present work we evaluate whether this assumption is correct by performing a series of NaCl tracer transport experiments using undisturbed volcanic soil cores under unsaturated conditions and monitoring the effect of flux density and solute concentrations on transport parameters. Our results indicate that these parameters depend on experimental conditions and thus they should not be considered constant. To investigate the underlying processes, we evaluated the effect of hysteresis between loading (increasing concentrations) and unloading (decreasing concentrations) of the soil cores and assessed whether the observed effects could be explained merely by physical processes or that a combination of physical and chemical phenomena is likely. The observation that breakthrough curve hysteresis was affected by solute concentration levels indicates that a chemical factor is likely to contribute to this behavior. This work demonstrates that hydrodynamic parameters as determined from experiments on undisturbed unsaturated soil cores depend on flow rate and concentration of the applied solutes. It is important to be aware of these effects and of the range in fitted parameter values when modelling and predicting nutrient transport in soil systems.

Keywords

Multi-step Flux Transport, Ionic strength, hysteresis, Breakthrough curves, unsaturated soil, volcanic soils.

4.1 Introduction

Avoiding excessive leaching of pesticides, nutrients, and heavy metals from highly permeable soils that have been submitted to intensive agriculture has become a priority in agriculture and environmental sciences. Therefore, proper management and understanding of solute transport processes within these systems is very important.

In this regard, modeling represents a valuable tool for predicting solute movement and for proposing management practices to reduce leaching. Typically, modeling solute transport in soil systems uses the Convection-Dispersion Equation (CDE) for single porosity systems, or the Mobile-Immobile dual-porosity model (MIM) for two-phase flow non-equilibrium systems (Šimůnek and van Genuchten, 2008; van Genuchten and Wierenga, 1976). For one-phase flow systems, the required model parameters include the soil water characteristics, water flow velocity, dispersion coefficient, and retardation factor, while more

complex non-equilibrium flow systems would require additional parameters (Arora et al., 2012; Šimůnek and van Genuchten, 2008; van Genuchten and Wierenga, 1976).

In theory these parameters are expected to be constant. However, recent findings about the most commonly used soil solute transport models (e.g., CDE MIM) have shown: 1) a parameter dependence on saturation and flow rates (Chen et al., 2021; Hasan et al., 2020; Kumahor et al., 2015a), and 2) variation of parameter values with time and length with inconsistencies between measured and optimized parameter values (Hasan et al., 2019; Karadimitriou et al., 2017, 2016). These interactions between model parameters could be even more complex, in case chemical interactions affect the hydrodynamic parameter values (Caron et al., 2015; Muniruzzaman and Rolle, 2021, 2019; Rolle et al., 2013b, 2013a).

Among soil chemical features with the potential to affect hydrodynamic parameters of solute transport models, the ionic strength (IS) appears to be particularly important. The reason is that ionic strength closely relates to charge interaction processes: 1) modifying the charge indirectly in variable charge soils due to the variation of the solution concentration (changing soil pH), and 2) ionic strength is directly related to the diffusion process, which is commonly included in the definition of the effective hydrodynamic dispersion coefficient (Radcliffe and Simunek, 2010). This variable charge behavior can occur in volcanic ash-derived soils, where the nanocrystalline allophane and ferrihydrite are the main soil colloids, in addition to the soil organic matter that plays an important role in the variable charge behavior (Nanzyo et al., 1993a).

On the other hand, some reports have shown hysteresis within the breakthrough curve for experiments developed at the same hydrodynamic conditions but at loading or unloading the solute (Chen et al., 2021; Erfani et al., 2021), providing different values of the hydrodynamic model parameters for loading than for unloading the solute. This hysteretic behavior is affected by differences between the input and resident solute concentration during input and discharging (Chen et al., 2021).

Based on recent findings about the effect of chemical interactions on hydrodynamic solute transport parameters (Muniruzzaman and Rolle, 2021, 2019; Rolle et al., 2013b), and the relationship of the diffusion process with the concentration gradient, the innovative physical explanation proposed by Chen et al. (2021) to explain the hysteretic breakthrough curve behavior may still be lacking a more detailed consideration of the chemistry-related aspects. So, we hypothesize that hysteretic breakthrough curves are also solution concentration-dependent, and therefore the transport model parameters are also concentration-dependent.

The objectives of the present paper are: i) to determine the effect of the solution concentration on transport hysteresis for loading and unloading breakthrough curves developed in undisturbed volcanic soil cores, ii) to determine the effect of solution concentration on the values of hydrodynamic parameters of

solute transport models, and iii) to determine the effect of different water fluxes on parameter values for solute transport models applied to undisturbed volcanic soil columns.

4.2 Materials and methods

4.2.1 Soil sampling and characterization

Undisturbed volcanic soil core samples were collected using sharp-edged PVC cylinders from two different locations: 1) San Bosco (10.279290, -83.802527), and 2) La Sonia (10.275865, -83.793791) in Pococí, Costa Rica. The elevation for both locations was 110 meters above sea level. According to the georeferenced coordinates, these soils were classified as Aluandic Dystric Andosol (Fluvic) (World Reference Base soil classification system). However, both soils differed significantly in clay, organic matter content, and reactive surface area (Table S.4.1).

The samples taken from La Sonia used for both breakthrough curve experiments (density flux and solution concentrations) were collected from a no-tillage area in a papaya (*Carica papaya* L.) plantation field. Meanwhile, for San Bosco, the samples used to evaluate the effect of the flux density were collected from San Bosco plot in a recently plowed soil (approximately one month after plowing). The sample used to evaluate the effect of the solution concentration on hysteresis and transport parameters was collected in the same plot with a time-lapse of more than one year after the first sampling; during this period, San Bosco soil was not tilled.

Organic carbon content was determined by a dry combustion analyzer (Elementar Vario Macro cube), assuming the lack of carbonates in the samples, and the particle size analysis was determined by the hydrometer method (Gee and Or, 2002) using disturbed samples obtained from these field plots.

The undisturbed soil cores were used in breakthrough curve solute transport experiments, designed to cover presented different approaches. These experiments are described in detail as follows.

4.2.2 Implementation of the Multi-Step Flux Transport device

We conducted all the breakthrough curve solute (tracer) transport experiments in a Multi-Step Flux Transport device (Diamantopoulos et al., 2015; Kumahor et al., 2015a; Weller et al., 2011) at different flow rates and later at constant flow rate and different ionic strengths. The experiments were developed under unsaturated conditions.

A Multi-Step Flux Transport (MSFT) device was built as specified by Kumahor et al. (2015a), but with modifications in the input solution system. The input solution was applied using a Gilson Minipuls 3 peristaltic pump (Gilson, France) connected to a set of five needles inserted in a thin sponge, which was placed at the upper boundary of our column. This modification to the MSFT device allowed a quasi-steady

state and a homogeneous application of the tracer solution. The MSFT device recorded data to a CR1000 datalogger (Campbell Scientific, UK), and the weight balances of the system registered data directly to a PC.

At the lower boundary of the column, a porous suction plate was set up, with a non-adsorbing nylon membrane of 0,45 µm porous diameter (ecoTech Umwelt-Meßsysteme GmbH, Germany). This porous plate was connected to a vacuum system controlled by the Campbell Scientific CR1000 datalogger. The column's lower boundary pressure was regulated according to the pressure head registered by the mini-tensiometers installed in the column. The suction in the lower boundary was automatically adjusted to produce gravitational flow in the column during the development of the experiments.

With this approach, some model parameters were controlled, and others were directly measured; for instance, soil water content was quasi-constant during the development of the breakthrough curve experiments, and the corresponding matric potentials, the volumetric water contents, and fluxes are measured directly at detailed timestep.

Further details and diagrams about the control and construction of the Multi-step Flux Transport device are available in the literature (Diamantopoulos et al., 2015; Kumahor et al., 2015a, 2015b; Weller et al., 2011), and summarized in Figure 4.1.

The own-made electrical conductivity sensors (two-electrode version) registered the tracer movement within the column (RawEC). These two-electrode sensors were based on the design of the four-electrode conductivity sensor implemented by Inoue et al. (2000). We placed the RawEC sensors at 0.5 cm from the bottom of the columns. For San Bosco soil experiments, we initially calibrated the results of the RawEC (mV V^{-1}) measurements against EC measurements (mS cm^{-1}). On the other hand, electronic mini-tensiometers measured the pressure heads in the columns. These mini-tensiometers were built using Deltran® DPT-100 disposable pressure transducers (Utah Medical, Utah, USA) and a porous ceramic tip (Rhizo Instruments, The Netherlands) connected to the pressure transducer.

We measured the lab room temperature by the wiring panel of the CR1000 datalogger and by a thermocouple sensor, we kept the lab room temperature between 21 and 23,5 °C to minimize the effects of the temperature on the recordings. To regulate the room temperature, we used: 1) an air conditioning system also controlled by the CR1000 datalogger, and 2) applied special insulation in the room windows to reduce the effect of solar radiation on the room temperature.

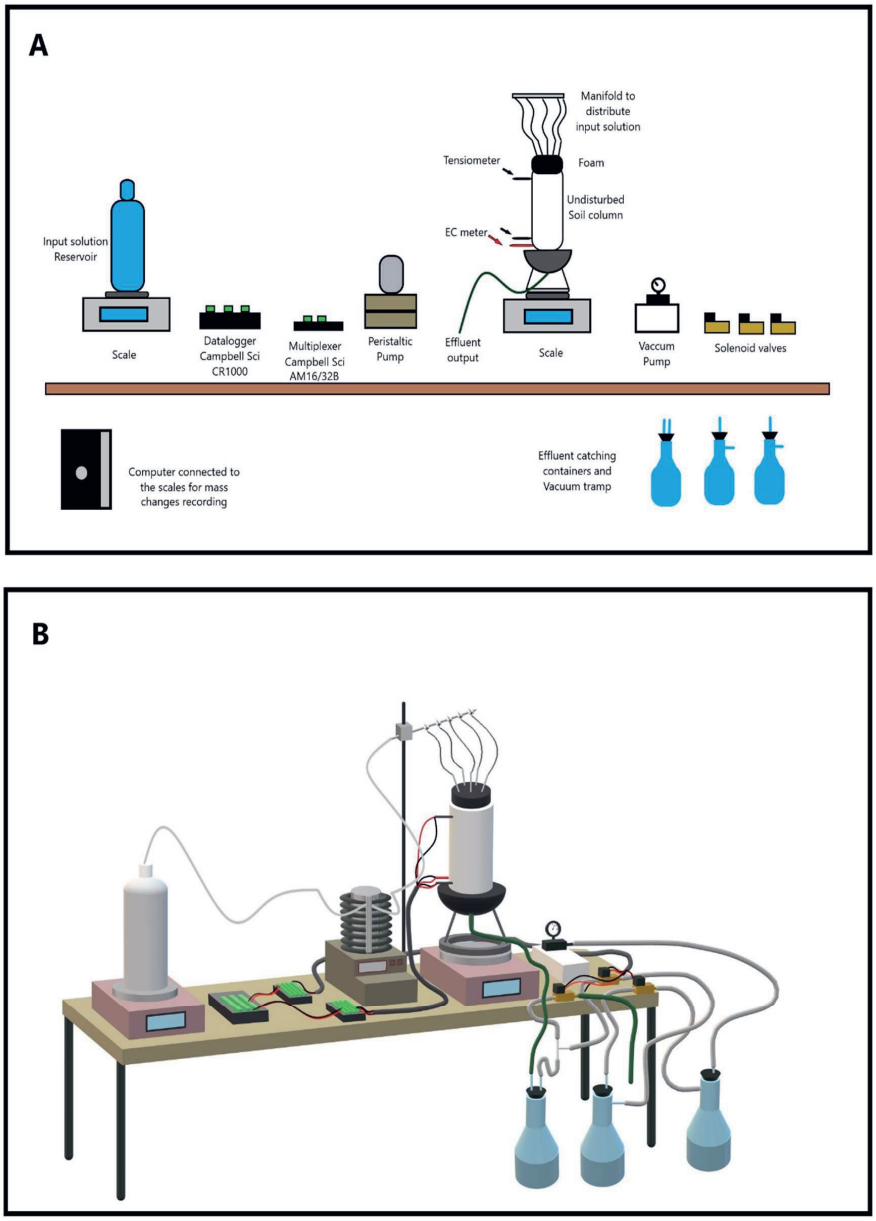

Figure 4.1. Multi-Step Flux Transport (MSFT) setup implemented to conduct tracer transport experiments in undisturbed volcanic soil columns. A) Detailed information about MSFT device components. B) General diagram of the MSFT device. The weight balances sent data directly to a PC.

Additionally, we corrected the breakthrough curves noise produced by temperature, estimating the moving average for each variable considering data from 3 hours of measurements in the calculation of the moving average. This correction was performed using the *rollapply()* function from the zoo package (Zeileis and Grothendieck, 2005) in the R software (R Core Team, 2021).

4.2.3 Tracer transport experiments

4.2.3.1 Tracer transport experiments developed at different flow rates

Table 4.1 describes the sequence of breakthrough curves experiments (sequential step inputs) performed for both undisturbed soil columns at different fluxes.

Table 4.1. Description of the set of tracer transport experiments developed at different fluxes of the input solution for two undisturbed volcanic ash-derived soils from La Sonia and San Bosco, Pococí, Costa Rica.

ID	Mean flow rate cm h^{-1}	Soil	Experiment	Solution applied	Applied pore volumes
A	0.035	La Sonia	Unloading	Tap water	1.9
B	0.059	La Sonia	Loading	NaCl 0.01M	2.0
C	0.097	La Sonia	Unloading	Tap water	3.7
D	0.187	La Sonia	Loading	NaCl 0.01M	3.1
E	0.279	La Sonia	Unloading	Tap water	3.9
A	0.038	San Bosco	Loading	NaCl 0.01M	3.0
B	0.066	San Bosco	Unloading	Tap water	3.0
C	0.107	San Bosco	Loading	NaCl 0.01M	4.1
D	0.209	San Bosco	Unloading	Tap water	3.7
E	0.313	San Bosco	Loading	NaCl 0.01M	4.4

These tracer experiments consisted of subsequent breakthrough curve sub-experiments performed on the same undisturbed soil columns. The breakthrough curves for La Sonia soil were conducted on an undisturbed soil column of 16.9 cm length and 8.3 cm diameter. For this soil, the experiments started with a NaCl 0.01 M saturated column, which previously received four pore volumes of the NaCl 0.01 M solution.

On the other hand, we performed the breakthrough curve tracer experiments for San Bosco soil in an 11 cm length and 8.4 cm diameter soil core. For this soil, the experiments started with a tap water-saturated column. Unfortunately, the sub-experiments that applied the lower fluxes for La Sonia soil were interrupted because of difficulties accessing the laboratory during 2020 due to the Covid-19 restrictions.

Between each sub-experiment, when the flux of the input solution was increased, we allowed the system to equilibrate the pressure for at least 3 hours before applying the new input solution. We started each new sub-experiment with the column equilibrated to the concentration of the previously applied solution, then we did not apply additional pore volumes to equilibrate the soil column chemically.

4.2.3.2 Tracer transport experiments developed at different ionic strengths and constant flow rates

Using another two columns collected at the same locations (La Sonia and San Bosco), we performed another set of tracer transport sub-experiments keeping a constant flux density but varying sequentially the input concentration solutions (by step inputs). The soil columns for both soils consisted of a soil core of 11.9 cm length and 8.3 cm inner diameter.

For this set of experiments, we started with freshly sampled soil columns, then we saturated the columns with just tap water, and subsequently, we applied a NaCl 0.012 M solution until obtaining a complete breakthrough curve as a pre-treatment. After that, we started our set of experiments by sequentially reducing the input solution concentration (NaCl) by step inputs until the breakthrough curve arrived completely for each sub-experiment. Finally, we successively increased the concentration of each breakthrough curve sub-experiment by step inputs of NaCl application. We developed these sub-experiments at a constant flux of 0.208 and 0.203 cm h^{-1} for La Sonia and San Bosco soils, respectively. The experiments consisted of the sequential breakthrough curve sub-experiments detailed in Table 4.2. There was a problem with the leachate evacuation system in the Multi-Step Flux Transport device for La Sonia soil for the first sub-experiment (A). Therefore, we excluded this data from the analysis of results.

Table 4.2. Breakthrough curve experiments developed at different concentrations and constant flux density of the input solution for two volcanic ash-derived soils from Pococí, Costa Rica.

ID	Kind of experiment	Soil	Initial resident solution	Input solution	Applied pore volumes
A	Unloading	La Sonia	0.012 M NaCl	0.008 M NaCl	5.9*
		San Bosco			6.0
B		La Sonia	0.008 M NaCl	0.004 M NaCl	4.17
		San Bosco			4.3
C		La Sonia	0.004 M NaCl	0.001 M NaCl	3.7*
		San Bosco			3.9
D		La Sonia	0.001M NaCl	Deionized water	17.3
		San Bosco			15.7
E	Loading	La Sonia	Deionized Water	0.001 M NaCl	6.7
		San Bosco			5.7
F		La Sonia	0.001 M NaCl	0.004 M NaCl	6.1
		San Bosco			7.0
G		La Sonia	0.004 M NaCl	0.008 M NaCl	4.2
		San Bosco			4.9
H		La Sonia	0.008 M NaCl	0.012 M NaCl	4.5
		San Bosco			4.0

*Incomplete or missing data

4.2.4 Soil Water Characteristics

We determined the soil water characteristics using the same soil columns employed during the tracer transport experiments. After finishing the tracer transport experiments, we developed a Simplified Evaporation Method experiment on these columns according to Peters and Durner (2008). From this experiment, we obtained the soil water characteristics for the soil columns with these evaporation experiments and fitted the van Genuchten-Mualem parameters for further modeling purposes. The optimization of the van Genuchten-Mualem parameters (θ_s, θ_r, α, and n) assumed $m = 1 - \frac{1}{n}$. This

procedure was developed in the SoilHyp package version 0.1.4 in the R software (Dettmann and Andrews, 2018).

4.2.5 Parameterization of the solute transport models

From the breakthrough curve experiments developed in the Multi-Step Flux transport device, we directly obtained the soil bulk density, the mean soil water content (θ), the flux density of the input solution, the average pore water velocity (v=q/θ), and the quantity of water that corresponded to one pore volume (θ * soil core's volume) for each sub-experiment. Also, the soil water characteristics (unsaturated hydraulic conductivity and pF curve) were determined directly from the Simplified Evaporation Method experiments (Peters and Durner, 2008) as previously indicated.

The breakthrough curve data was optimized to the CDE and to the MIM, considering the parameter values directly measured from the column experiments. We fitted the hydrodynamic dispersion coefficient (D) and the retardation factor (R) in the CXTFIT/STANMOD software (Toride et al., 1995).

While assessing data from San Bosco soil (experiments developed at different fluxes), we observed an early arrival of the breakthrough curve (earlier arrival than one pore volume). This situation could suggest the presence of preferential flow; then, we fitted the Mobile-Immobile model to the different breakthrough curve datasets obtained experimentally with this soil column.

Due to reported inconsistencies in the determination of the Mobile-Immobile β parameter (Hasan et al., 2019; Karadimitriou et al., 2017, 2016), we did not fit this parameter to breakthrough curve data. Instead, we assumed that the mobile water fraction corresponded to the water content between the mean volumetric water content of the experiment and the residual water content (θ-θ_r), which was previously estimated from soil water characteristics using the van Genuchten-Mualem model (van Genuchten, 1980). Besides the hydrodynamic dispersion coefficient and the retardation factor, for the non-equilibrium experiments, we also fitted the mass transfer coefficient between the mobile and immobile regions (α_{MI} parameter).

Using the respective average soil pore water velocity and assuming n=1 (a linear relationship) in Equation 4.1 and Equation 4.2, we estimated the dispersivity for the different sub-experiments from the optimized effective dispersion coefficient.

$$D = \lambda * v^n \qquad \text{(Equation 4.1)}$$

Where D corresponds to the hydrodynamic dispersion coefficient, λ is the longitudinal dispersivity (L), v corresponds to the average pore water velocity (L T^{-1}), and n is an empirical constant. This equation

is valid for saturated conditions, even though it has also been used under unsaturated conditions considering the parameter's dependence on the soil moisture (Equation 4.2)

$$D(\theta, v) = \lambda(\theta) * v^n \quad \text{(Equation 4.2)}$$

Where, θ corresponds to the volumetric water content.

4.3 Results and Discussion

4.3.1 The effect of solution concentration and hysteresis on apparent solute transport parameters

4.3.1.1 La Sonia soil

Results obtained from the tracer transport experiments conducted at different ionic strengths and constant flow rates using La Sonia soil are presented in Figure 4.2. There were some technical problems during these experiments, which prevented us from collecting a complete set of experimental data. For instance, we lost the experiment reducing concentration from NaCl 0.012 to 0.008 M for La Sonia soil because of a failure in the Multi-step Flux Transport device (Figure 4.2.A), and the unloading sub-experiment cleaning from NaCl 0.004 to 0.001M was interrupted before completing the breakthrough curve (Figure 4.2.C). Therefore, these two datasets were excluded from the data analysis and parameter optimization process.

For La Sonia soil, the breakthrough of the solute was measured by the changes in the raw electric conductivity, however the calibration of the sensor against electric conductivity (mS cm^{-1}) was not carried out.

While comparing among the two remaining unloading experiments (Figures 4.2.B and 4.2.D), the mean arrival of the breakthrough curve was delayed for the lower concentration experiment (Figure 4.2.D) and required around fifteen pore volumes to get stable. This in comparison with less than five pore volumes in case of 0.004 M NaCl. This behavior demonstrates a significant effect of solution concentration on breakthrough curves and thus on transport rates.

When assessing the loading sub-experiments (Figures 4.2.E to 4.2H), the breakthrough was also delayed with the reduction of the tracer solution concentration. This behavior suggests a potential influence of surface charge-related processes on solute transport rates in these volcanic ash-derived soils.

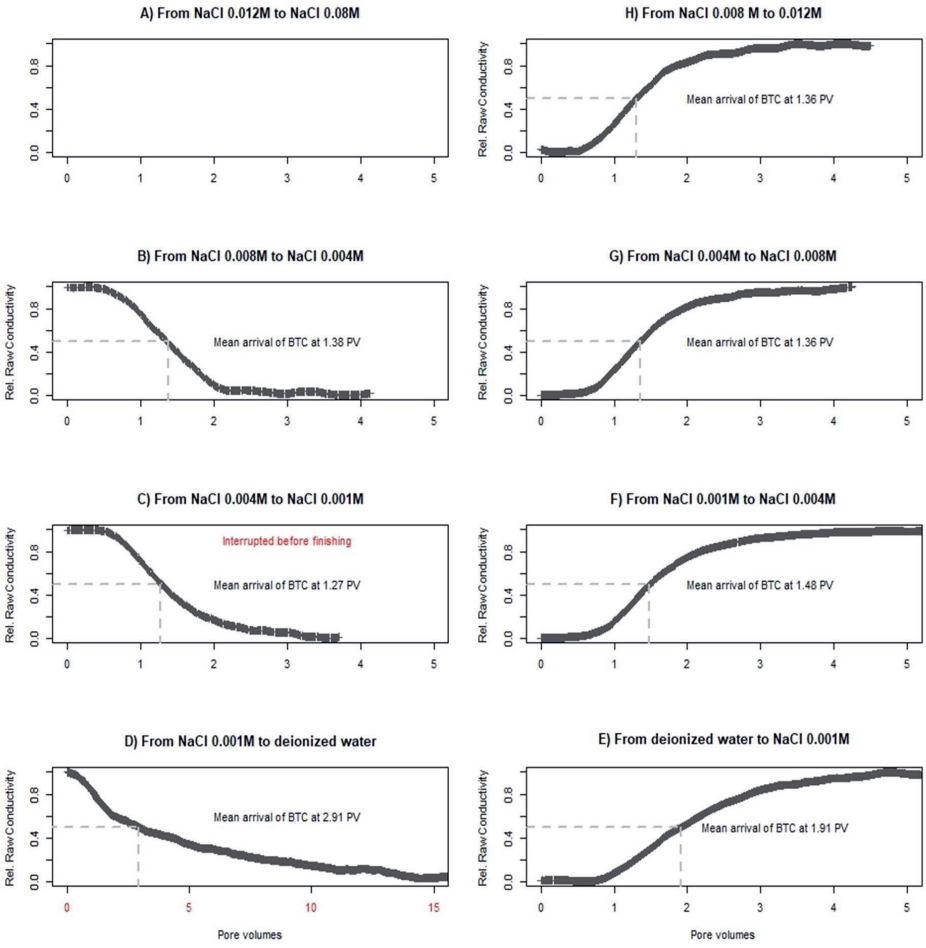

Figure 4.2. NaCl tracer breakthrough curve experiments developed at different ionic strength by step inputs in an undisturbed volcanic soil column from La Sonia, Pococí, Costa Rica. The breakthrough curves are expressed in terms of relative raw conductivity.

In general, Andosols are recognized to contain variable charge minerals and, in some cases, high contents of variable charge organic matter and allophane minerals (Auxtero et al., 2004; Nanzyo et al., 1993a; Sansoulet et al., 2007). For our experiments, the increase of salt concentration promotes the H^+ desorption from the oxide surface and from the functional groups of the organic matter. However, most of the negative charge generated by this salt induced proton desorption is neutralized by the higher positive charge present in the system, as a result of the higher amount of Na^+. Therefore, even our soils have variable

charge behavior (Figure S.4.1), this process is not likely to cause an important chemical retardation of the NaCl solution.

An additional charge-related process that we considered is modifying the solute transport model parameters for these experiments is the Donnan volume expansion-contraction according to the ionic strength variation, which is expected to present larger volumes at lower ionic strengths. For instance, for the estimation of the Donnan volume in the application of the NICA-Donnan model (Benedetti et al., 1996; Milne et al., 2003), the Donnan-volume change can be estimated empirically using the solution's ionic strength. The changes in the Donnan volume could affect the adsorption process and the diffusion process making less accessible the small pores.

Our breakthrough curve experiments (both loading and unloading conditions) also presented hysteresis, which magnitude varied as a function of the solution concentration of each experiment. As shown in Figure 4.2, at lower concentrations, the charge-related processes played a more critical role in the arrival position of the breakthrough curve and produced a more pronounced hysteresis effect. This result could also be related to the lower diffusive flux that could be expected at lower concentrations according to Fick's first law ($J = -D\frac{\partial C}{\partial x}$).

The direction in which diffusion and advection occur during the loading or unloading conditions was proposed by Chen et al. (2021) to explain this retarded arrival of the breakthrough curves for cleaning experiments. We agree with this explanation about the physical mechanisms that drive the hysteresis process, which is based on the differences in the concentration field generated for the loading and unloading conditions. However, our data suggest that other chemical-related processes produced by different input solution concentrations could also be responsible for the hysteresis observed between loading and unloading breakthrough curves.

Therefore, the interaction between charge-related and physical processes produces different solute transport model parameters, which are also concentration-dependent, and not constant values as typically implemented. Table 4.3 shows the results of the parameter optimization for these experiments applying the CDE. For the unloading experiments, the observed values of the R, D, and λ increased considerably for the lower concentration evaluated (Table 4.3), with a major effect on the retardation factor. On the other hand, for loading experiments, these parameters obtained similar values for high concentration experiments and increased considerably for the lowest concentration experiment.

In this regard, Katou et al. (1996) and Kolahchi & Jalali (2006) while developing adsorption isotherms and breakthrough curve experiments showed that the adsorption coefficient increases as the

concentration in solution decreases, and they observed that retardation factor depends on the concentration and composition of the invading solution.

As shown in Table 4.3, the dispersion coefficient (D) was also modified by the different concentrations applied, then the concentrations impacted not only to the adsorption process but also influenced dispersion-diffusion related processes. The increase of the effective dispersion coefficient and retardation factor was more notorious for the unloading sub-experiments. These results have important implications for the parameterization of solute transport models when using tracer solutions, as the parameter results could depend on the solution concentration and how the experiment is conducted (loading or unloading). Furthermore, these differences observed for parameter values have important implications for modeling nutrient transport in soils systems. The fertilizer movement in soils could experience gradients of concentrations that, in some cases, would achieve similar ionic strength compared to the conditions applied in this set of experiments. For instance, potassium chloride is applied in agricultural soils at high concentrations, at different frequencies, and under variable environmental conditions (Fratoni et al., 2017; Mohr and Tomasiewicz, 2012), and according to Kolahchi and Jalali (2006), the variation of the potassium concentration could affect its adsorption coefficient.

Our results about the concentration-dependence of solute transport parameters are also supported by the observations of Chen et al. (2021), who using synchrotron x-ray imaging (sXRCT) in an experiment cleaning a 3 M KI solution while applying deionized water observed that the reduction of concentration from 3M to 1 M lasted 150 seconds, meanwhile the reduction of the concentration from 1 M to 0 M required 396 seconds in their experiments. Chen et al. (2021) mentioned that this tailing (increased time to achieve the lower concentration from 1 M to 0M) is characteristic of non-Fickian transport with stagnant and mobile regions. However, for their experiment they were not able to relate this tailing to the presence of stagnant regions as the *s*XRCT images did not evidence the presence of stagnant regions in their repacked porous sand system.

The results of different parameter values obtained at different concentrations from our experiments also agree with other findings reported in the literature (Muniruzzaman and Rolle, 2021; Rolle et al., 2013a; Sansoulet et al., 2007) and challenge the application of simple modeling approaches to determine the movement of saline fertilizer solutions.

For instance, it is not recommended to model the potassium chloride transport in this soil with a constant value for the retardation factor obtained by linear adsorption isotherms. Additionally, the observed hysteresis questions the implementation of constant parameters for modeling the movement of saline fertilizer solutions in soils.

Table 4.3. Measured and optimized solute transport parameters for NaCl tracer breakthrough curve experiments developed at different ionic strengths in an undisturbed volcanic soil column from La Sonia, Pococí, Costa Rica.

Sub-experiment	Measured parameters			CDE optimized parameters			Optimized vs fitted	
	θ_m	v	λ	D	R	Peclet number†	MSE	r^2
	$cm^3\ cm^{-3}$	$cm\ h^{-1}$	cm	$cm^2\ h^{-1}$				
Unloading (NaCl 0.012 to 0.008 M)	NA	NA	NA	NA	NA	NA	NA	NA
Unloading (NaCl 0.008 to 0.004 M)	0.644	0.323	0.82	0.267	1.51	14.6	0,0004	0.997
Unloading (NaCl 0.004 to 0.001 M)	NA	NA	NA	NA	NA	NA	NA	NA
Unloading (NaCl 0.001 to deionized water)	0.649	0.322	10.53	3.42	5.59	1.13	0,0002	0.998
Loading (deionized water to NaCl 0.001M)	0.648	0.321	1.32	0.425	2.22	9.0	0,0001	0.999
Loading (NaCl 0.001 M to NaCl 0.004 M)	0.648	0.320	1.23	0.382	1.74	9.7	0,0001	0.999
Loading (NaCl 0.004 M to NaCl 0.008 M)	0.640	0.320	1210	0.392	1.56	9.8	0,0002	0.999
Loading (NaCl 0.008 M to NaCl 0.012 M)	0.640	0.320	1210	0.390	1.50	9.9	0,0001	0.999

Where, θ_m corresponds to the mean volumetric soil water content for each experiment, v corresponds to the mean pore water velocity ($cm\ h^{-1}$), λ corresponds to dispersivity, D corresponds to the hydrodynamic dispersion coefficient, R corresponds to retardation factor, MSE corresponds to the Mean Square Error, NA= data not available.

Peclet number: v*L/D

4.3.1.2 San Bosco soil

While assessing the experiments performed for San Bosco soil, the tracer solution concentration also affected the position (pore volumes) of the arrival of the breakthrough curves (Figure 4.3). At low ionic strengths (low tracer concentrations), the charge-related processes became more critical, showing a substantial delay in the arrival of the breakthrough curves. (Figure 4.3).

The loading and unloading sub-experiment for the concentrations between 0.004 and 0.001M NaCl showed a distinctive earlier arrival of the breakthrough curves (Figure 4.3.C and 4.3.F). With our current set of data, we do not have an explanation to this behavior presented in this soil. As well, we observed a substantial delay for the arrival of the breakthrough curve and a strong tailing in the unloading sub-experiment from NaCl 0.001M to deionized water (Figure 4.3.D).

Results obtained in the experiments conducted for San Bosco soil (both loading or unloading) showed hysteresis for the breakthrough curves of the tracer solution, and the magnitude of the hysteresis was also concentration-dependent (Figure 4.3). This concentration dependence of the hysteresis was consistently observed for both soil columns and suggests that hysteresis depends not only on the direction of the advective and dispersive fluxes but also on the concentration of the input solution and its charge-related processes. This effect of charge-related processes on hysteresis and the time of arrival of the breakthrough curves show that solute transport model parameters also depend on the solute concentration and are not fixed parameters as commonly implemented.

The following section presents our model parameter optimization for breakthrough curves developed at constant flux and different solution concentrations for San Bosco soil.

Table 4.4 summarizes the directly measured and optimized model parameters for this set of experiments while applying the CDE. The hydrodynamic parameters showed very close values for the unloading experiments of San Bosco soil developed at higher concentrations (higher than 0.004M). On the other hand, the experiments developed for tracer concentrations between 0.004 and 0.001M NaCl (loading and unloading) presented distinctive lower values for the hydrodynamic parameters.

For the lower concentration experiment, both conditions (loading and unloading the solute) showed considerably larger values for the hydrodynamic solute transport parameters (Table 4.4). As mentioned before for La Sonia soil, this result could be related to the expansion of the Donnan volume at low solution concentrations which promotes a higher adsorption in the Donnan layer, plus the lower rate of the diffusive flux that is expected according to Fick's law.

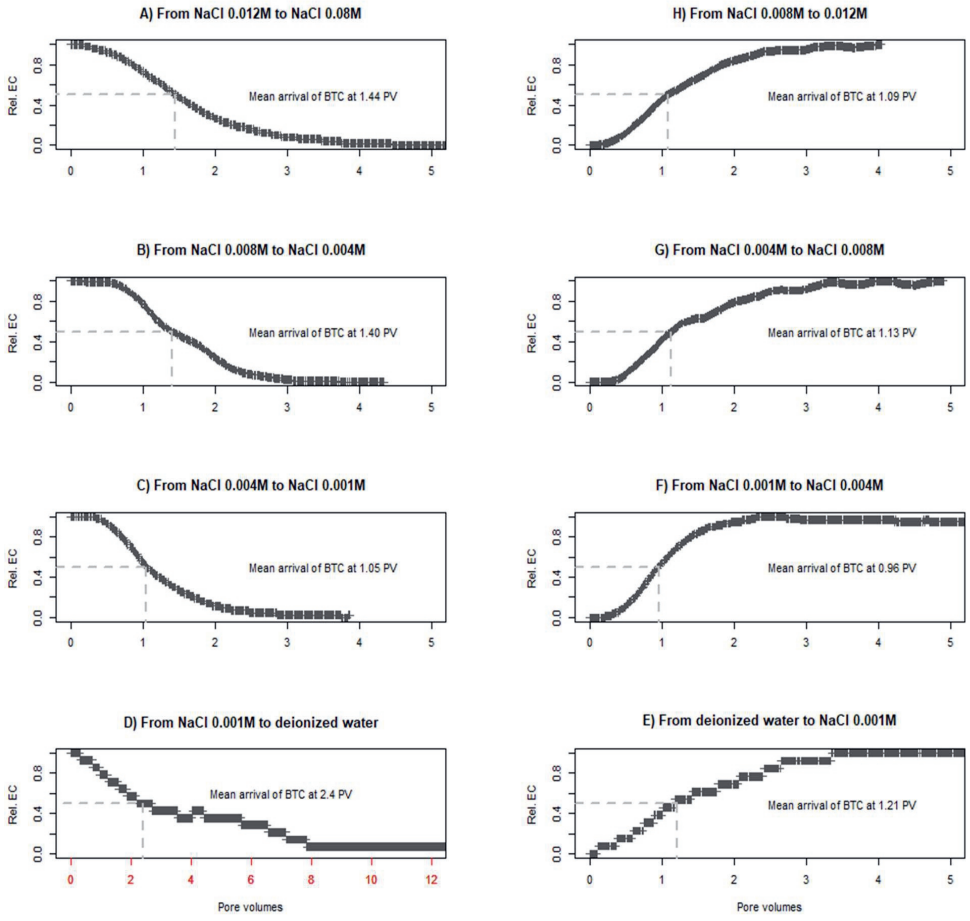

Figure 4.3. NaCl tracer breakthrough curve experiments developed at different ionic strength by step inputs in an undisturbed volcanic soil column from San Bosco, Pococí, Costa Rica. The breakthrough curves are expressed in terms of relative conductivity.

Following Fick's first law ($J = -D\frac{\partial C}{\partial x}$), the concentrations difference (delta concentration) evaluated in our experiments (numerator in right hand side of Fick's first law) decreases for the low ionic strength solutions evaluated, while the distance for diffusion (denominator in right hand side of Fick's law) increases due to the rise of the Donnan volume. So, if we assume a constant diffusion coefficient (as typically assumed), the net expected result is a lower diffusive flux at low salt concentrations and

consequently, a larger tailing and more pore volumes required to achieve a new equilibrium concentration (more time or more pore volumes required to complete the arrival of the breakthrough curve).

For the higher salt fluxes evaluated in our experiments, and assuming a constant effective diffusion coefficient (D), the expected result is an increase of the concentrations difference and a decrease in the distance for diffusion with a net higher diffusive flux. This expected behavior agrees with the observed results about the breakthrough curve delay at low ionic strength (Figures 4.2 and 4.3).

Additionally, our optimized parameter results for a constant flow rate and different concentrations suggest that the assumption of a constant dispersion coefficient is not valid for all the concentrations evaluated, which agrees with the results recently obtained by Chen et al. (2021).

Table 4.4. Measured and optimized solute transport parameters for NaCl tracer breakthrough curve experiments developed at different ionic strengths in an undisturbed volcanic soil column from San Bosco, Pococí, Costa Rica. Mean flux 0.203 cm h^{-1}. The Convection-Dispersion Equation (CDE) model was implemented.

Sub-experiment	Measured parameters			CDE optimized parameters			Optimized vs fitted	
	θ_m	v	λ	D	R	Peclet number†	MSE	r^2
	$cm^3\ cm^{-3}$	$cm\ h^{-1}$	cm	$cm^2\ h^{-1}$				
Unloading NaCl 0.012 to 0.008 M)	0.555	0.364	1.95	0.71	1.72	6.10	2.6E-4	0.99
Unloading (NaCl 0.008 to 0.004 M)	0.558	0.363	2.01	0.73	1.73	5.92	3.2E-4	0.99
Unloading (NaCl 0.004 to 0.001 M)	0.567	0.358	1.76	0.63	1.29	6.76	7.8E-5	0.99
Unloading (NaCl 0.001 to deionized water)	0.574	0.353	8.24	2.91	4.66	1.44	2.3E-3	0.97
Loading (deionized water to NaCl 0.001M)	0.574	0.353	3.31	1.17	1.58	3.59	1.7E-3	0.98
Loading (NaCl 0.001 M to NaCl 0.004 M)	0.570	0.356	1.46	0.52	1.09	8.14	0,00	0.99
Loading (NaCl 0.004 M to NaCl 0.008 M)	0.568	0.357	2.66	0.95	1.5	4.47	3.2E-4	0.99
Loading (NaCl 0.008 M to NaCl 0.012 M)	0.566	0.358	2.49	0.89	1.37	4.79	2.8E-4	0.99

Where, θ_m corresponds to the mean volumetric soil water content for each experiment, v corresponds to the mean pore water velocity ($cm\ h^{-1}$), λ corresponds to dispersivity (D/v), D corresponds to the hydrodynamic dispersion coefficient, R corresponds to retardation factor, MSE corresponds to the Mean Square Error.

Peclet number: v*L/D

4.3.2 Effect of flow rate on solute transport parameters

4.3.2.1 La Sonia soil

Figure 4.4 shows the tracer breakthrough curves developed at different fluxes on an undisturbed volcanic soil column from La Sonia, Pococí, Costa Rica, for applying NaCl 0.01M (loading experiment) and cleaning with water (unloading experiment). For La Sonia soil experiments, the data of this section was also analyzed by using the raw electric conductivity (mV V^{-1}) instead of the electric conductivity (mS cm^{-1}).

While comparing the loading experiments developed at flux rates of 0.097 and 0.279 cm h^{-1} against the unloading experiment developed at 0.187 cm h^{-1} (a flux rate in between), hysteresis was observed between loading (increasing concentration) and unloading (reducing concentration) conditions (Figure 4.4). This delayed time to complete breakthrough curves when the solute concentration is decreasing for non-reactive tracers was also reported in the literature (Chen et al., 2021; Erfani et al., 2021; Huang et al., 1995) and was consistently observed for our experiments developed at different concentrations of the input solution.

As discussed in the previous section, this hysteresis effect is not only related to the physical direction of the advective and dispersive fluxes, as proposed by Chen et al. (2021). Instead, it could be triggered by a combination of physical and chemical factors that change the adsorption and dispersion pattern of the solute.

Hysteresis affects different solute transport model parameters. For instance, from our experiments, the dispersivity (λ) increased according to the applied flux for this soil (compare the unloading sub-experiments of Table 4.5), which was contrary to the results obtained by Kumahor et al. (2015a) where dispersivity increased with the reduction of the applied flux in quartz sand repacked column.

The differences between our data and the results obtained by Kumahor et al. (2015a) could be related to the differences in water saturation between the experiments. For our experiments, saturation experienced slight changes at different fluxes, while the pore water velocity suffered a more substantial change according to the applied fluxes (Table 4.5). The results of Hasan et al. (2020) show the important dependence of dispersivity on saturation.

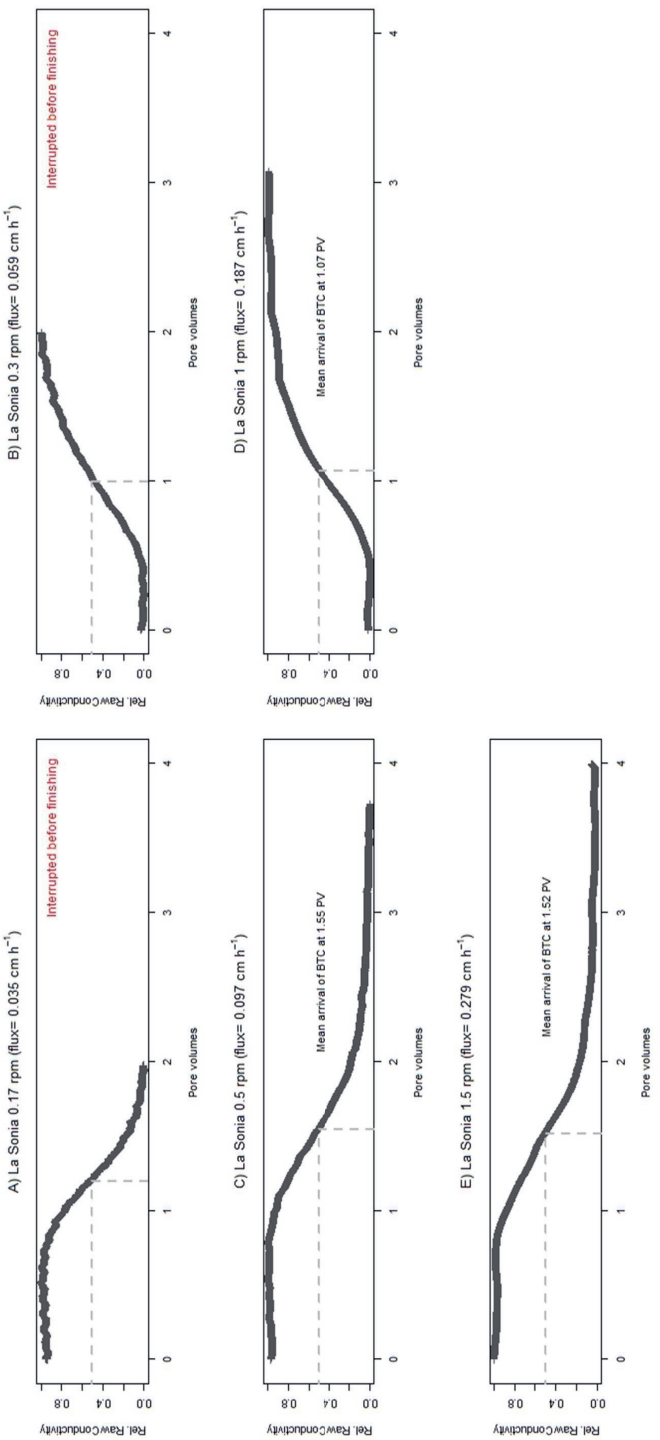

Figure 4.4. Unloading (left panels) and loading (right panels) tracer (NaCl 0.01M) breakthrough curve experiments developed at different fluxes for an undisturbed volcanic soil column from La Sonia, Pococí, Costa Rica.

Table 4.5. Measured and optimized solute transport parameters for NaCl 0.01 M tracer breakthrough curve experiments developed at different fluxes in a single-phase flow undisturbed volcanic soil column from La Sonia, Pococí, Costa Rica.

Sub-experiment	Flux	Measured parameters			CDE optimized parameters		Peclet number†	Optimized vs fitted	
		θ_m	v	λ	D	R		MSE	r^2
	cm h^{-1}	cm^3 cm^{-3}	cm h^{-1}	cm	cm^2 h^{-1}				
Unloading	0.035	NA	NA	NA	NA	NA	NA	NA	NA
Loading	0.059	0.50	0.12	1.17	0.14	1.15	14.5	0.0003	0.99
Unloading	0.097	0.51	0.19	0.68	0.13	1.72	24. 8	0.0002	0.99
Loading	0.187	0.52	0.36	1.28	0.46	1.24	10.2	0.0001	0.99
Unloading	0.279	0.51	0.54	0.85	0.46	1.66	19.9	0.0002	0.99

Where, θ_m corresponds to the mean volumetric soil water content for each experiment, v corresponds to the mean pore water velocity (cm h^{-1}), λ corresponds to dispersivity (D/v), D corresponds to the hydrodynamic dispersion coefficient, R corresponds to retardation factor, MSE corresponds to the Mean Square Error, NA= data not available.

Peclet number: v*L/D

Despite the fact that our assessed fluxes were below 0.5 cm h^{-1} (the lowest flux applied by Kumahor et al. (2015a)), our volumetric water contents were higher than those obtained by Kumahor et al. (2015a). The observed volumetric water contents for our set of experiments are probably still far from the critical volumetric water content in which the dispersivity suddenly increases with the reduction of water contents and fluxes. For instance, for the experiments developed for La Sonia soil, the mean volumetric water content was higher than 0.50 cm^3 cm^{-3}, while Kumahor et al. (2015a) observed a sudden increase in the dispersivity at volumetric water contents around 0.2 cm^3 cm^{-3}.

4.3.2.2 San Bosco soil

Different from results obtained in La Sonia soil experiments, it was observed an early arrival of the loading breakthrough curves developed at different fluxes in San Bosco soil (Figure 4.5), suggesting a two-phase flow condition (physical non-equilibrium). However, the breakthrough curves for this soil did not show the tailing that typically characterizes preferential flow conditions.

Due to the absence of tailing in the breakthrough curve results, it was possible to fit the tracer transport results to the CDE, but the retardation factor showed a non-realistic result (R lower than 1). Consequently, we fitted the data of this set of experiments to the MIM, but with special considerations for the fitting procedure. Those considerations for implementing the MIM model consisted in the direct determination of the β parameter and, consequently, the direct estimation of the pore water velocity of the mobile phase, optimizing only three parameters from the breakthrough curve data. The optimized parameters were the retardation factor (R), the dispersion coefficient (D), and the mass transfer coefficient (α_{MI} parameter).

In this regard, Karadimitriou et al. (2016), Hasan, Joekar-Niasar, Karadimitriou, & Sahimi (2019), and Karadimitriou, Joekar-Niasar, & Brizuela (2017) found substantial inconsistencies in the usage of the Mobile-Immobile Model (MIM) fitted data to model breakthrough curve results. For example, their results showed that the optimized β parameter does not correlate with measured values. Additionally, the mass transfer coefficient (α_{MI}) fitted with the MIM is not realistic, as according to the measured data, it changes with the time (Haggerty et al., 2004; Karadimitriou et al., 2016), and according to Khan & Jury (1990), and Masciopinto & Passarella (2018), it also varies with length. The conventional MIM optimization result is a constant parameter that contrasts with the measured data reported in the literature.

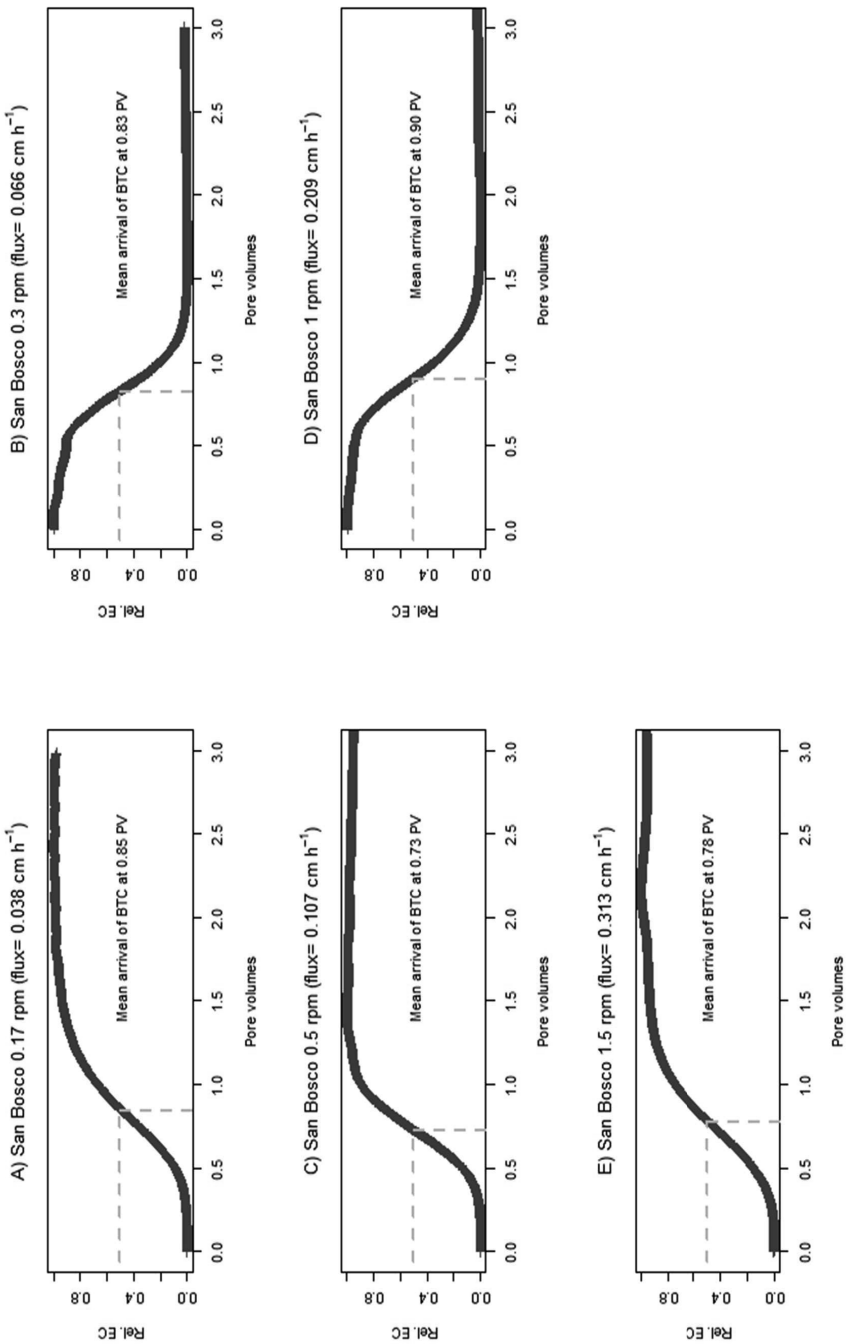

Figure 4.5. Loading (A, C, and E panels) and unloading (B, and D panels) tracer breakthrough curves (NaCl 0.01M) for an undisturbed volcanic soil from San Bosco, Pococí, Costa Rica. Experiments developed on the same soil column at different flow rates.

Therefore, while implementing the MIM model is necessary to quantify directly the value for the β parameter, and then, the direct determination of the pore water velocity in the mobile water phase.

While quantifying the β parameter, we assumed that the immobile water phase corresponded to the residual volumetric soil moisture (θ_r) obtained by the optimization of the van Genuchten-Mualem parameters from a Simplified Evaporation Method data. For San Bosco soil, this residual volumetric water content (θ_r) corresponded to 0.26 cm^3 cm^{-3} according to optimized parameters (Table S.4.1). Therefore, the calculation of the β parameter also considered the mean volumetric water content (θ_m) for each sub-experiment, according to Equation 4.3:

$$\beta = \frac{(\theta_m - \theta_r)}{\theta_m} \qquad \text{(Equation 4.3)}$$

From our optimized MIM results obtained for San Bosco soil, we found that the dispersion coefficient increased as the flow rate also increased, in agreement with the results obtained by Chen et al., (2021), but with a notable difference between loading and unloading breakthrough curves.

Despite the fact that for this soil no loading and unloading data were obtained for each applied flux, which prevents a direct comparison between the hydrodynamic dispersion coefficients for the contamination and cleaning conditions, our optimized dispersion coefficients did not appear to be larger for the unloading (cleaning) condition. The latter is in contrast with the results obtained by Chen et al. (2021), who measured directly this parameter and observed larger dispersion coefficients for the unloading condition.

The differences in the patterns of the hydrodynamic dispersion coefficient compared to those found in the literature could be caused by the following factors:

First, our experiments were developed under unsaturated conditions, while Chen et al. (2021) evaluated their experiments under saturated conditions. Second, our experiments were developed in an undisturbed soil sample system, which could be more heterogeneous than the repacked sand grain system implemented by Chen et al. (2021). Third, the pore water velocities and the Peclet number for our experiments suggest completely different transport conditions than the ones evaluated by Chen et al. (2021). Our Peclet numbers are in the intermediate range suggested by Chen et al. (2021), where it is expected that advective forces generate a heterogeneous concentration field.

However, a similar Peclet number (i.e., 10^0) could have different behavior for saturated than for unsaturated conditions. According to our data (Tables 4.5 and 4.6), applying a lower flux implies a lower pore water velocity for both soils. Therefore, if we compare hypothetical results at the same Peclet number

for saturated (higher flux) against unsaturated (lower flux) conditions, and applying the formula for the definition of the Peclet number ($Pe = \frac{v*z}{D}$), it could be expected a lower dispersion coefficient because of the lower pore water velocity at unsaturated conditions. Our pore velocities (10^{-6} to 10^{-7} m s^{-1}) are below those evaluated by (Chen et al., 2021), and our Peclet numbers are in the range of the lower Peclet number they found (10^{0}).

Additionally, according to Chen's et al. interpretation of their extrapolated data, at very low and very high Peclet numbers and pore velocities, it is no longer expected a higher D for the unloading condition.

On the other hand, the optimized retardation factor for the loading condition showed a non-monotonic behavior, with a larger value for the lower flow rate applied (Table 4.6). In addition, the dispersivity (λ=D/V_{MIM}) also showed a non-monotonic behavior for this set of experiments. Therefore, these parameters appear to be non-constant as typically implemented for modeling nutrient transport in soil systems.

Finally, consistent with the lack of tailing observed from the breakthrough curves, the optimized mass transfer coefficient between the mobile and immobile water phases showed very low values (Table 4.6).

Table 4.6. Measured and optimized solute transport parameters for NaCl 0.01 M tracer breakthrough curve experiments developed at different fluxes in a two-phase flow undisturbed volcanic soil column from San Bosco, Pococí, Costa Rica.

Sub-experiment	Flux	Measured parameters		CDE optimized parameters					Peclet number†	Optimized vs fitted	
		θ_m	V_{MIM}	λ	D	β_{MIM}	α_{MIM}	R		MSE	r^2
	cm h^{-1}	cm^3 cm^{-3}	cm h^{-1}	cm	cm^2 h^{-1}						
Loading	0.038	0.54	0.13	0.85	0.11	0.522	0,00	1.83	13	0,0006	0.99
Unloading	0.066	0.56	0.22	0.36	0.08	0.535	0,00	1.65	30.3	0,0007	0.99
Loading	0.107	0.58	0.33	0.45	0.15	0.551	0.011	1.41	24.3	0,0002	0.99
Unloading	0.209	0.60	0.61	0.38	0.23	0.567	0,00	1.73	29.3	0,0003	0.99
Loading	0.313	0.60	0.91	0.9v	0.83	0.569	0.015	1.53	12.1	0,0001	0.99

Where, θ_m corresponds to the mean volumetric soil water content for each experiment, v corresponds to the mean pore water velocity (cm h^{-1}), λ corresponds to dispersivity (D/v), D corresponds to the effective hydrodynamic dispersion coefficient, β_{MIM} corresponds to the saturation of the mobile soil water fraction in relation to the total saturation, α_{MIM} corresponds to the mass transfer coefficient between the mobile and immobile water fractions, R corresponds to retardation factor, MSE corresponds to the Mean Square Error.
Peclet number: v*L/D

4.4 Conclusions

In the present work we demonstrate that the hysteretic behavior of loading and unloading breakthrough curves depends not only on the direction of the advective and convective fluxes but also on the solution concentration due to charge-related processes like expansion-contraction of the Donnan volume and differences in the diffusive flux rate.

The observed hysteresis between loading and unloading breakthrough curves appears to depend on the concentration of the input solution, which modifies the diffusive fluxes. The lowest diffusive fluxes, plus the larger Donnan volumes presented at low solution concentrations increased the solute resident time within the system.

Solute transport model parameters are not fixed values as typically implemented for modeling nutrient transport in soil systems. Instead, they vary as a function of the flow rate and the solution concentration, which has important consequences for modeling the fate of nutrients in soil systems.

Acknowledgments:

We are very grateful to the Agronomy Research Center of the University of Costa Rica and its staff for allowing the development of the experiments in its laboratories.

Funding:

R.F.-C. acknowledges support and funding of this work by the Ministry of Science and Technology of Costa Rica (MICITT), under the PINN-MICITT contract number: 2-1-4-17-1-014.

R.F.-C. also gratefully acknowledges the University of Costa Rica for its partial complementary funding, contract number OAICE-53-2018.

Funding sources had no role in study design, in the collection, analysis, and interpretation of data, in the writing of the report, nor in the decision to submit the article for publication.

4.5 References:

Arora, B., Mohanty, B.P., McGuire, J.T., 2012. Uncertainty in dual permeability model parameters for structured soils. Water Resour. Res. 48, 1–17. https://doi.org/10.1029/2011WR010500

Auxtero, E., Madeira, M., Sousa, E., 2004. Variable charge characteristics of selected Andisols from the Azores, Portugal. Catena 56, 111–125. https://doi.org/10.1016/j.catena.2003.10.006

Benedetti, M.F., Van Riemsdijk, W.H., Koopal, L.K., 1996. Humic substances considered as a heterogeneous Donnan gel phase. Environ. Sci. Technol. 30, 1805–1813. https://doi.org/10.1021/es950012y

Caron, J., Létourneau, G., Fortin, J., 2015. Electrical Conductivity Breakthrough Experiment and Immobile Water Estimation in Organic Substrates: Is R = 1 a Realistic Assumption? Vadose Zo. J. 14. https://doi.org/10.2136/vzj2015.01.0014

Chen, Y., Steeb, H., Erfani, H., Karadimitriou, N.K., Walczak, M.S., Ruf, M., Lee, D., An, S., Hasan, S., Connolley, T., Vo, N.T., Niasar, V., 2021. Nonuniqueness of hydrodynamic dispersion revealed using fast 4D synchrotron x-ray imaging. Sci. Adv. 7, 1–7. https://doi.org/10.1126/sciadv.abj0960

Dettmann, U., Andrews, F., 2018. SoilHyP: Soil Hydraulic Properties.

Diamantopoulos, E., Durner, W., Iden, S.C., Weller, U., Vogel, H.J., 2015. Modeling dynamic non-equilibrium water flow observations under various boundary conditions. J. Hydrol. 529, 1851–1858. https://doi.org/10.1016/j.jhydrol.2015.07.032

Erfani, H., Karadimitriou, N.K., Nissan, A., Walczak, M.S., An, S., Berkowitz, B., Niasar, V., 2021. Process-Dependent Solute Transport in Porous Media. Transp. Porous Media 140, 421–435. https://doi.org/10.1007/s11242-021-01655-6

Fratoni, M.M.J., Moreira, A., Moraes, L.A.C., Almeida, L.H.C., Pereira, J.C.R., 2017. Effect of Nitrogen and Potassium Fertilization on Banana Plants Cultivated in the Humid Tropical Amazon. Commun. Soil Sci. Plant Anal. 48, 1511–1519. https://doi.org/10.1080/00103624.2017.1373791

Gee, G.W., Or, D., 2002. 2.4 Particle-Size Analysis. Methods Soil Anal., SSSA Book Series. https://doi.org/https://doi.org/10.2136/sssabookser5.4.c12

Haggerty, R., Harvey, C.F., Von Schwerin, C.F., Meigs, L.C., 2004. What controls the apparent timescale of solute mass transfer in aquifers and soils? A comparison of experimental results. Water Resour. Res. 40. https://doi.org/10.1029/2002WR001716

Hasan, S., Joekar-Niasar, V., Karadimitriou, N.K., Sahimi, M., 2019. Saturation Dependence of Non-Fickian Transport in Porous Media. Water Resour. Res. https://doi.org/10.1029/2018WR023554

Hasan, S., Niasar, V., Karadimitriou, N.K., Godinho, J.R.A., Vo, N.T., An, S., Rabbani, A., Steeb, H., 2020. Direct characterization of solute transport in unsaturated porous media using fast X-ray synchrotron microtomography. Proc. Natl. Acad. Sci. U. S. A. 117, 23443–23449. https://doi.org/10.1073/pnas.2011716117

Huang, K., Toride, N., Van Genuchten, M.T., 1995. Experimental investigation of solute transport in large, homogeneous and heterogeneous, saturated soil columns. Transp. Porous Media 18, 283–302. https://doi.org/10.1007/BF00616936

Inoue, M., Šimůnek, J., Shiozawa, S., Hopmans, J.W., 2000. Simultaneous estimation of soil hydraulic

and solute transport parameters from transient infiltration experiments. Adv. Water Resour. 23, 677–688. https://doi.org/10.1016/S0309-1708(00)00011-7

Karadimitriou, N.K., Joekar-Niasar, V., Babaei, M., Shore, C.A., 2016. Critical Role of the Immobile Zone in Non-Fickian Two-Phase Transport: A New Paradigm. Environ. Sci. Technol. 50, 4384–4392. https://doi.org/10.1021/acs.est.5b05947

Karadimitriou, N.K., Joekar-Niasar, V., Brizuela, O.G., 2017. Hydro-dynamic Solute Transport under Two-Phase Flow Conditions. Sci. Rep. 7, 1–7. https://doi.org/10.1038/s41598-017-06748-1

Katou, H., Clothier, B.E., Green, S.R., 1996. Anion Transport Involving Competitive Adsorption during Transient Water Flow in an Andisol. Soil Sci. Soc. Am. J. 60, 1368–1375. https://doi.org/10.2136/sssaj1996.03615995006000050011x

Khan, A.U.H., Jury, W.A., 1990. A laboratory study of the dispersion scale effect in column outflow experiments. J. Contam. Hydrol. 5, 119–131. https://doi.org/10.1016/0169-7722(90)90001-W

Kolahchi, Z., Jalali, M., 2006. Simulating leaching of potassium in a sandy soil using simple and complex models. Agric. Water Manag. 85, 85–94. https://doi.org/10.1016/j.agwat.2006.03.011

Kumahor, S.K., de Rooij, G.H., Schlüter, S., Vogel, H.-J., 2015a. Water Flow and Solute Transport in Unsaturated Sand—A Comprehensive Experimental Approach. Vadose Zo. J. 14, 0. https://doi.org/10.2136/vzj2014.08.0105

Kumahor, S.K., Hron, P., Metreveli, G., Schaumann, G.E., Klitzke, S., Lang, F., Vogel, H.J., 2015b. Transport of citrate-coated silver nanoparticles in unsaturated sand. Sci. Total Environ. 535, 113–121. https://doi.org/10.1016/j.jconhyd.2016.10.001

Masciopinto, C., Passarella, G., 2018. Mass-transfer impact on solute mobility in porous media: A new mobile-immobile model. J. Contam. Hydrol. 215, 21–28. https://doi.org/10.1016/j.jconhyd.2018.06.004

Milne, C.J., Kinniburgh, D.G., Van Riemsdijk, W.H., Tipping, E., 2003. Generic NICA - Donnan model parameters for metal-ion binding by humic substances. Environ. Sci. Technol. 37, 958–971. https://doi.org/10.1021/es0258879

Mohr, R.M., Tomasiewicz, D.J., 2012. Effect of rate and timing of potassium chloride application on the yield and quality of potato (Solanum Tuberosum L. 'Russet Burbank'). Can. J. Plant Sci. 92, 783–794. https://doi.org/10.4141/cjps2011-195

Muniruzzaman, M., Rolle, M., 2021. Impact of diffuse layer processes on contaminant forward and back diffusion in heterogeneous sandy-clayey domains. J. Contam. Hydrol. 237, 103754. https://doi.org/10.1016/j.jconhyd.2020.103754

Muniruzzaman, M., Rolle, M., 2019. Multicomponent Ionic Transport Modeling in Physically and Electrostatically Heterogeneous Porous Media With PhreeqcRM Coupling for Geochemical Reactions. Water Resour. Res. 55, 121–143. https://doi.org/10.1029/2019WR026373

Nanzyo, M., Dahlgren, R., Shoji, S., 1993. Chapter 6 Chemical Characteristics of Volcanic Ash Soils. Dev. Soil Sci. 21, 145–187. https://doi.org/10.1016/S0166-2481(08)70267-8

Peters, A., Durner, W., 2008. Simplified evaporation method for determining soil hydraulic properties. J. Hydrol. 356, 147–162. https://doi.org/10.1016/j.jhydrol.2008.04.016

R Core Team, 2021. R: A language and environment for statistical computing.

Radcliffe, D.E., Simunek, J., 2010. Soil Physics with HYDRUS: Modeling and Applications, 1st ed. CRC

Press. https://doi.org/10.1201/9781315275666

Rolle, M., Chiogna, G., Hochstetler, D.L., Kitanidis, P.K., 2013a. On the importance of diffusion and compound-specific mixing for groundwater transport: An investigation from pore to field scale. J. Contam. Hydrol. 153, 51–68. https://doi.org/10.1016/j.jconhyd.2013.07.006

Rolle, M., Muniruzzaman, M., Haberer, C.M., Grathwohl, P., 2013b. Coulombic effects in advection-dominated transport of electrolytes in porous media: Multicomponent ionic dispersion. Geochim. Cosmochim. Acta 120, 195–205. https://doi.org/10.1016/j.gca.2013.06.031

Sansoulet, J., Cabidoche, Y.M., Cattan, P., 2007. Adsorption and transport of nitrate and potassium in an Andosol under banana (Guadeloupe, French West Indies). Eur. J. Soil Sci. 58, 478–489. https://doi.org/10.1111/j.1365-2389.2007.00904.x

Šimůnek, J., van Genuchten, M.T., 2008. Modeling Nonequilibrium Flow and Transport Processes Using HYDRUS. Vadose Zo. J. 7, 782–797. https://doi.org/10.2136/vzj2007.0074

Toride, N., Leij, F.J., van Genuchten, M.T.., 1995. The CXTFIT code for estimating transport parameters from laboratory or field tracer experiments. Version 2.0, Research Report No. 137.

van Genuchten, M.T., 1980. A Closed-form Equation for Predicting the Hydraulic Conductivity of Unsaturated Soils. Soil Sci. Soc. Am. J. 44, 892–898. https://doi.org/https://doi.org/10.2136/sssaj1980.03615995004400050002x

van Genuchten, M.T., Wierenga, P.J., 1976. Mass Transfer Studies in Sorbing Porous Media I. Analytical Solutions. Soil Sci. Soc. Am. J. 40, 473–480. https://doi.org/10.2136/sssaj1976.03615995004000040011x

Weller, U., Ippisch, O., Köhne, M., Vogel, H.-J., 2011. Direct Measurement of Unsaturated Conductivity including Hydraulic Nonequilibrium and Hysteresis. Vadose Zo. J. 10, 654. https://doi.org/10.2136/vzj2010.0074

Zeileis, A., Grothendieck, G., 2005. Zoo: S3 infrastructure for regular and irregular time series. J. Stat. Softw. 14, 1–27. https://doi.org/10.18637/jss.v014.i06

4.6 Supplementary material

Table S.4.1. Soil physical properties and Van Genuchten-Mualem model parameters for soil samples from La Sonia and San Bosco, Pococí, Costa Rica.

Soil	Clay	Silt	Sand	Textural classification	Bulk density	Particle density	OC	Total porosity	van Genuchten-Mualem (vG-M) parameters			
	%				g cm^{-3}	g cm^{-3}	(%)	(cm^3 cm^{-3})	θ_s	θ_r	α	n
La Sonia	20	30	50	Loam	0.78	2.3	4.70	0.66	0.66	0.4	0.026	1.30
San Bosco	15	5	80	Sandy Loam	0.97	2.3	4.17	0.58	0.58	0.26	0.0216	1,40

Table S.4.2. Measured and optimized unrealistic solute transport parameters (retardation lower than 1) for NaCl 0.01 M tracer breakthrough curve experiments developed at different fluxes in a volcanic soil column from San Bosco, Pococí, Costa Rica.

Sub-experiment	Flux	Measured parameters			CDE optimized parameters		Peclet number†	Optimized vs fitted	
		θ_m	v	λ	D	R		MSE	r^2
	cm h^{-1}	cm^3 cm^{-3}	cm h^{-1}	cm	cm^2 h^{-1}				
Loading	0.038	0.54	0.07	NA	0.056	0.95	NA	0.00005	0.99
Unloading	0.066	0.56	0.117	NA	0.04	0.88	NA	0.0007	0.99
Loading	0.107	0.58	0.1841	NA	0.088	0.79	NA	0.0003	0.99
Unloading	0.209	0.60	0.348	NA	0.13	0.97	NA	0.0003	0.99
Loading	0.313	0.60	0.5085	NA	0.51	0.89	NA	0.0002	0.99

Where, θ_m corresponds to the mean volumetric soil water content for each experiment, v corresponds to the mean pore water velocity (cm h^{-1}), λ corresponds to dispersivity (D/v), D corresponds to the hydrodynamic dispersion coefficient, R corresponds to retardation factor.

Peclet number: v*L/D

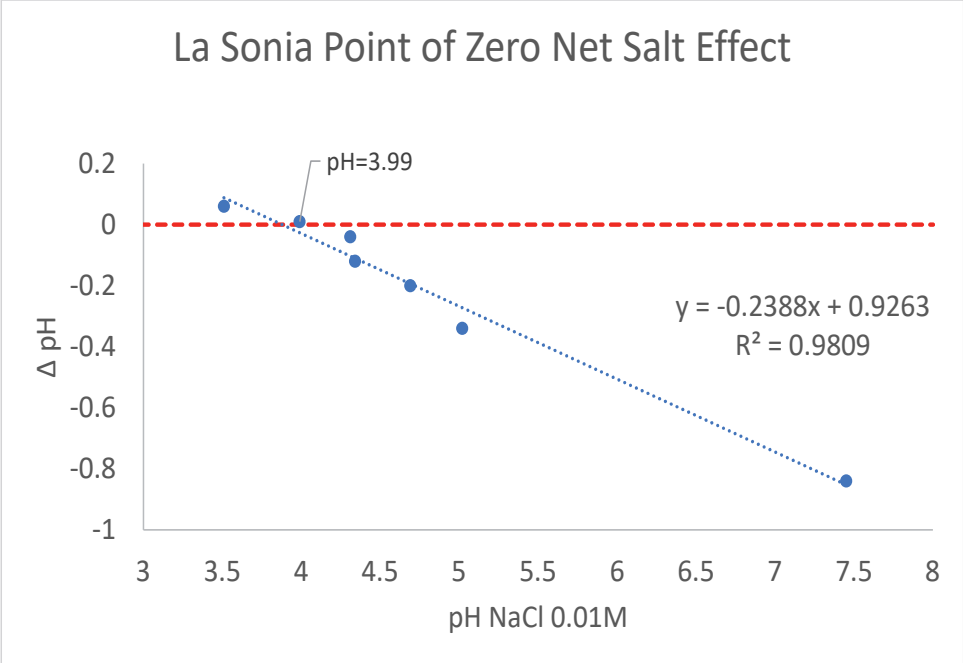

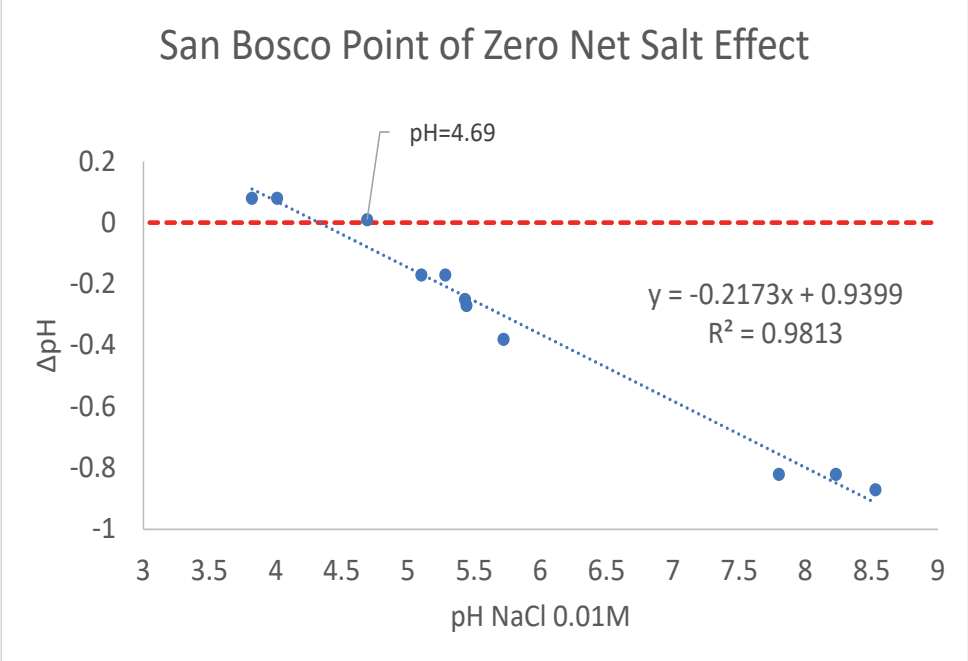

Figure S.4.1. Results of the determination of the Point of Zero Net Salt Effect for La Sonia and San Bosco soil. The pH was determined in 0.1 and 0.01 M NaCl background solution.

Chapter 5

General discussion and synthesis

5.1 Main findings

Applying mineral fertilizers to agricultural production systems has implicit agronomical and environmental consequences that depend on complex interactions between nutrients, adsorption surfaces, and the composition of the soil solution. These interactions affect nutrient availability and mobility through the soil and consequently affect fertilizer use efficiency.

To evaluate the effect of potentially important chemical interactions, in Chapter 2, we assessed whether the competitive interaction between P (phosphate) and B (boric acid) is a significantly affect the boron availability and leaching from acid volcanic ash soils. We tested this P-B interaction for a volcanic ash soil system from a region where phosphate is typically applied at very high rates, and boron deficiency is a common constraint. We consider adsorption a critical process that conditions the boron movement and availability in these systems. Also, in Chapter 3, we tested other potentially important chemical interactions that could occur in highly fertilized volcanic soils when high potassium chloride rates are applied to the system. And finally, in Chapter 4 we tested the possible effects of the variations of the flow rate and the variation in solution salt concentration on the model parameters typically used to simulate solute transport in porous soil systems

Chapter 2 evaluated the causes of boron deficiency in an acid volcanic ash-derived soil. According to the objectives proposed in this chapter, we defined by modeling the principal boron adsorption surface. For our Andosol, there were no significant differences in boron adsorption for different background solutions (NaCl 0.01 M and $CaCl_2$ 0.01 M), which suggest that for this soil under the conditions of the experiments, the boron adsorption is dominated by the oxide fraction (Table S.2.4, from Chapter 2), and as modeling suggest predominantly as an outer-sphere process. Also, we found that boron adsorption was not notably affected by phosphate applications when boron was present at low solution concentrations, and phosphate slightly modified the boron adsorption only when boron was present in solution at concentrations higher than 50 μmol L^{-1}. Since boron concentrations are typically very low for these volcanic soils, we expect that phosphate applications do not increase the desorption of the native boron fractions in these soils. Therefore, the boron availability will not increase because of the phosphate fertilizer addition.

Regarding the modeling results, the CD-MUSIC-NICA-Donnan model simulated the results obtained in the adsorption experiments well. It is important to note that this approach was based on theoretical mechanisms, using state-of-the-art model parameters obtained for ferrihydrite and humic acid systems (Goli et al., 2019; Mendez and Hiemstra, 2020c; Van Eynde et al., 2020a). Probably, the successful application of the model to our P-B dataset depends to a great extent on the direct experimental determination of the reactive surface area of the soil and on the availability of the necessary parameters for its implementation with a nanocrystalline particle that represented very well the alumino-silicate and

(hydr)oxide fraction of this soil. Despite the low micromolar boron concentrations, experimental data and model results had a very good agreement. The model can also simulate the impact of different management practices on boron adsorption. For example, adding or increasing the organic matter content in the evaluated Andosol will probably have a small imperceptible effect on increasing the boron retention in this acid volcanic soil. The latter is because boron adsorption at low solution pH occurs principally at the (hydr)oxide fraction, and the organic matter surfaces become important only at high pH. A high pH condition is not typical for these tropical volcanic-derived soils.

The pH is well recognized as the principal factor that modifies the solubility of boron in soils. This fact was also demonstrated by the modeling results reported in Chapter 2. For our soil, the pH has important consequences for boron adsorption under alkaline conditions (i.e., pH higher than 7.0), but as our modeling results suggest, the pH changes have little influence on the total boron adsorption at the pH range between 4 to 6.

Due to the high solubility of the boric acid in these volcanic soil systems, it is recommended to evaluate other boron sources aiming for higher retention of this nutrient in Andosols. The application of borate (oxyanion) sources will probably be retained to a greater extent than the boric acid. Additionally, considering the high solubility of boric acid in this system, decreasing the rate of boron applied and increasing the frequency of application could improve the boron nutrient status for the crops developed in these types of systems. On the other hand, we tried to clarify the cause of boron deficiency in these acid volcanic soils. With the results obtained from the boron adsorption experiments, we assume that the cause of boron deficiency in this volcanic soil is the increased leaching; as for the boron applied treatments, most of the boron remained in solution (68 to 70%), independent of the boron solution concentration. Furthermore, the sampled region is characterized by high precipitation and extreme events (see Figure S.3.1. from Chapter 3), and the volcanic soils by high permeability. These factors (high solubility, permeable soil, and high precipitation) could promote the continuous boron leaching from these volcanic soils.

In Chapter 3, we aimed to understand better the possible side effects of high potassium chloride fertilizer additions on the availability and leaching of zinc. For the zinc batch adsorption experiments, we demonstrated that zinc adsorption in volcanic soils depends on the ionic strength and the solution pH; this behavior agrees with results observed in other soils (Casagrande et al., 2004; Van Eynde et al., 2022a). In the same way, adding potassium chloride at high rates for the column transport experiments modified the ionic strength of both volcanic soils and changed the pH of the leachate solution for one of the volcanic soils. The modifications of pH and ionic strength induced by the potassium chloride additions increased the zinc leaching rates in these volcanic soil systems. Also, the increased DOC content observed at increased

potassium chloride rates could also affect the partition (more desorption) between the solution and the solid soil surfaces.

We tried to model the zinc batch adsorption experiments' results using the CD-MUSIC-NICA-Donnan approach. However, the agreement between model calculations and experimental results was not very good at these extremely low micromolar zinc concentrations. Consequently, it was not possible to interpret the zinc adsorption data based on model simulations. Therefore, implementing a mechanistic modeling approach is still a remaining but very useful task. The correct implementation of a mechanistic multi-surface adsorption model for zinc will help to understand and simulate the complex dynamics of zinc adsorption in volcanic soil systems, as simple and empirical approaches like linear adsorption isotherms are not applicable to the complexity of zinc interactions observed in our experiments

The following step in implementing mechanistic multi-surface models in volcanic soils would be the development of model parameters specific for nanoparticle oxide surfaces present in volcanic soils (e.g., to develop CD-MUSIC model parameters for allophane nanoparticles). In addition, the evaluation of the model performance to describe zinc adsorption in these volcanic soils should preferably determine the ionic zinc species (i.e., Zn^{2+}) in solution, for example, by using the Donnan-Membrane Technique as implemented by Duffner et al. (2014).

The typical pH range observed in these volcanic soils greatly influences the partition of zinc between the surfaces and the solution, which is different from the results obtained in Chapter 2. For boron, significant changes occur only at high pH.

In **Chapter 4,** we made a first step for applying a solute transport model to our breakthrough curves data. The original objective of developing the tracer transport experiments was to obtain by inverse modeling the complementary information required to apply a hydrological model to simulate the transport of boron and zinc in undisturbed soil columns. However, after observing the hysteresis phenomena between loading and unloading tracer breakthrough curves in preliminary experiments, we developed additional experiments to explain the causes of the observed hysteresis and elucidate the potential effects of the fertilizer additions (by increasing the salt concentration in the system) on the values of solute transport model parameters. With this additional experiment, we determined the influence of the soil solution concentration on the values of the parameters typically used for modeling solute transport in porous media with a consistent dataset (a robust time-series data). The additional experiment evaluated breakthrough curves that increased or decreased gradually by step inputs the solution concentration, determining the different parameters commonly used for solute transport modeling for each sub-experiment.

This set of experiments showed an important variation between loading and unloading the solute to the columns and the parameter-dependence on concentration for the most common solute transport models (e.g., Convection-Dispersion Equation). These results advise that these models at least should consider a range of these parameter values when simulating the transport of fertilizer solutions through the soil, but preferably implement alternative modeling approaches that consider the interactions between chemical and physical processes. The effect of the solution concentration on transport parameters probably is not crucial for the transport of solutes that move into the soil system at low concentrations (for instance, pesticides, pharmaceuticals, and nanoparticles) because of the low solute concentrations that move through the soil. However, for fertilizer solutions, the changes in solution concentration are significant and can promote variations in the model parameters of solute transport models. The effect of the transport of concentrated solutions on the movement of solutes present in the soil at low concentrations (e.g., pharmaceuticals, pesticides, and nanoparticles) is a still-pending task that was out of the objectives of the present work.

The findings of this chapter suggest that hydrological and geochemical processes occur simultaneously, and results do not depend on specific isolated processes. Consequently, simulation models should also be able to simultaneously describe the complex interaction of chemistry as flow through unsaturated systems occurs. Several examples of coupled geochemical and hydrological models are available, for instance, the different versions of the HYDRUS-PHREEQC (HPx) (Jacques et al., 2018a). However, implementing specific chemical models in reactive transport codes like our boron adsorption or our zinc desorption data would require the implementation of additional modules that are not already available in these software codes. For instance, the CD-MUSIC model with the extended Stern approach, as far as I am concerned, is not available at the PHREEQC code. A new version of HP1 is under development (D. Jacques) which combines the HYDRUS hydrological model with the ORCHESTRA chemical module, which can simulate all the chemical models presented here.

The principal conclusion of this chapter is that the hysteresis phenomena and the parameter dependence on concentration are produced by a combination of physical and chemical processes like the direction in which advective and diffusive processes occur (as suggested by Peters et al. (2019) and Chen et al. (2021)), plus the charge-related processes like the expansion and contraction of the Donnan volume and differences in the diffusive rate product of the concentration differences.

5.2 Discussion

Boric acid adsorption and interactions with phosphate:

Although boron deficiency is a common issue for agricultural production in volcanic soils, there is limited information available about its correct management. In recent years, a few efforts have been developed to comprehend the boron dynamics in volcanic soil systems. Terraza Pira et al. (2018) recently contributed to understanding this problem, evaluating boron adsorption in different Guatemalan volcanic soils. However, before this study aforementioned, there was no explicit attempt to understand the boron adsorption process in volcanic soils for more than four decades despite the common appearance of boron deficiencies in these soils.

Terraza Pira et al. (2018) suggested that boron adsorbs strongly in volcanic soils and that this strong adsorption is mainly related to high contents of short-range ordered minerals like allophane, imogolite, and ferrihydrite. In contrast, the results obtained in our adsorption experiments showed moderate boric acid adsorption in the evaluated andosol, as, on average, only thirty percent of the boron adsorbed to the soil surfaces. The causes of the contrasting results obtained between both volcanic soil experiments are unclear but could be related to methodological differences or different characteristics of the volcanic soils. For example, Terraza Pira et al. (2018) evaluated higher boron concentrations than those assessed in our experiments, and they reported the pH determined in NaF for their volcanic soils to evidence the volcanic characteristics of these soils but did not show the pH determined in water which gives essential information for the interpretation of boron solubility. Therefore, it is not clear whether their soils are acid or not. As shown by modeling simulations in Figure 2.3, the pH of the solution has a predominant impact on boron solubility.

The conclusions provided by Terraza Pira et al. (2018) were based on the results of batch adsorption experiments obtained for a big group of soils (25 volcanic ash-derived soils) and their correlation with different soil properties. However, these results did not consider the possible adsorption mechanisms and their relationship with the different soil adsorption surfaces (for instance (hydr)oxides, aluminosilicates, organic matter, and clay).

More recently, Van Eynde et al. (2020) made an important contribution while simulating by CD-MUSIC modeling the different boron adsorption mechanisms to pure ferrihydrite suspension nanoparticles. In addition, Goli et al. (2019) developed the necessary parameters to model boron adsorption to humic acids using the NICA-Donnan model. The availability of these model parameters allowed the interpretation of our boron adsorption isotherms, employing an additive multisurface modeling approach which constitutes an advance for the interpretation of boron adsorption in volcanic soils. Furthermore, the availability of these

model parameters allowed the interpretation of our boron adsorption results employing a mechanistic approach for our volcanic soil system.

The CD-MUSIC-NICA-Donnan modeling approach previously predicted boron adsorption in multisurface soil systems from temperate and tropical weathered soils (Van Eynde et al., 2020b), but it has not been implemented in volcanic soils. Therefore, the application of the CD-MUSIC-NICA-Donnan model for the interpretation of boron adsorption in volcanic soils has two significant contributions: First, testing the recently developed model parameters for volcanic soils, and second, a better understanding of the boron adsorption mechanisms in volcanic soils, which were not assessed in previous studies. Terraza Pira et al. (2018) emphasized that boron adsorption in volcanic soils differs strongly from its adsorption to other types of soils and the correction of boron deficiency in these soils requires differentiated management. However, according to the low boron adsorption observed for our volcanic soil, we assume this result could vary depending on the characteristics of the solution (e.g., at low pH conditions).

The model parameters developed by Van Eynde et al. (2020a) agree with the spectroscopic results provided by Su and Suarez (1995), which suggest boron adsorption by inner- and outer-sphere species. Furthermore, our modeling results consistently agree with the presence of both surface-adsorbed boron species and with the interpretation of the boron interactions with phosphate. This last was possible due to the implementation of a state-of-the-art model that considers the boron adsorption by both surface species (inner- and outer-sphere). The possibility of simulating boron adsorption using both adsorbed species (using the CD-MUSIC approach) provides an advantage over other boron adsorption modeling approaches. For instance, the Constant Capacitance model (Goldberg et al., 2005; Goldberg and Glaubig, 1985; Vaughan and Suarez, 2003) assumes boron adsorption only as inner-sphere species, which makes cumbersome the interpretation of boron adsorption data and its interaction with phosphate adsorbed ions, as the addition of phosphate to our volcanic soil system displaces the boron adsorbed at the inner-sphere sites, and therefore, the principal boron adsorbed species in our multi-component volcanic soils system correspond to outer-sphere species. The successful interpretation of the boron adsorption isotherms with the CD-MUSIC model allows the interpretation of the adsorption data in agreement with the results of different boron adsorbed species (inner- and outer-sphere species). In addition, the good agreement between measured and modeled adsorption data encourages its implementation to test by modeling different boron fertilization strategies to correct its deficiency in volcanic soils.

Multicomponent interactions of potassium fertilizer on zinc availability and leaching:

For the case of highly fertilized volcanic systems, other results show different adsorption interactions for zinc, a micronutrient that also constrains yields in Andosols. The zinc interaction with

fertilizer has been studied for phosphate sources, which reported that phosphate additions increase zinc sorption (Selim, 2016). However, the interaction of zinc with other fertilizer sources like potassium is less studied; therefore, we evaluated whether the high potassium chloride solution concentrations affect zinc adsorption in two volcanic soil systems. As explained in Chapter 3, potassium chloride applications at high rates strongly modify zinc availability (increased solubility) in these volcanic soil systems, which is a contrasting process compared to the zinc-phosphate interaction. Unfortunately, we could not simultaneously evaluate the overall effect of adding potassium, phosphate, and nitrogen to check for the complete set of possible interactions that could affect zinc sorption processes in these highly fertilized volcanic soil systems. However, the proper evaluation of the complete set of interactions requires understanding individual processes, which can be complemented by developing adsorption experiments and interpreting the results using mechanistic modeling simulations.

For the case of zinc, it is clear that adsorption depends to a great extent on the soil solution pH (Arias et al., 2005; Barrow, 1993; Casagrande et al., 2004; Dyer et al., 2004; Fest et al., 2005; Nomaan et al., 2021; Van Eynde et al., 2022b, 2022a) and on the solution ionic strength (Casagrande et al., 2004; Dyer et al., 2004; Shuman, 1986). For our volcanic soils, the batch adsorption experiments also showed the important effect of both chemical variables (pH and ionic strength) on zinc adsorption. The pH dependence of zinc sorption in these volcanic soils could be related to the effect of pH on zinc sorption to both adsorption surfaces (the mineral (aluminosilicates and (hydr)oxides) fraction and the organic matter surfaces), while the ionic strength does not modify the zinc adsorption to pure (hydr)oxide systems. For example, for pure ferrihydrite systems, Trivedi et al. (2004) and Van Eynde et al. (2022b) showed the key role of pH on zinc sorption, but an irrelevant effect of the ionic strength for zinc adsorption to pure ferrihydrite systems. Also, Trivedi and Axe (2001) did not find an effect of the ionic strength on zinc adsorption to goethite. For our volcanic soils, the ionic strength showed relevant effects on zinc adsorption, indicating important participation of the organic matter for the sorptionof zinc sorption.

Organic matter is an important soil sorbent surface for zinc (Gurpreet-Kaur et al., 2013), and organic matter is typically present in high quantities in volcanic soils, as shown in Table 2.1. In this regard, Buurman et al. (2007) emphasize that the volcanic ash-derived soils from this tropical region accumulate and preserve substantial quantities of secondary organic matter particles (Buurman et al., 2007). According to their results, the incorporation and accumulation of high quantities of organic matter in these volcanic soils (located in warm and per-humid conditions) could relate to the incorporation of decomposition products and microbial soil organic matter in very fine aggregates that remain saturated and thus protected for degradation under the per-humid conditions of the Atlantic region of Costa Rica. Therefore, the high accumulation of organic matter in these soils could result in an important contribution to zinc adsorption

and consequently, the ionic strength could be an important factor in evaluating and modeling zinc adsorption in tropical volcanic soils from humid regions, mainly considering that about 60% of the Andosols of the world are located in tropical regions (Takahashi and Shoji, 2002).

Our results also showed that the addition of concentrated potassium chloride solutions to the volcanic soils modifies the pH and the ionic strength. This result suggests an important side effect of high potassium fertilization on the availability and leaching of zinc in volcanic soils, evidenced in our batch adsorption experiments and in the column transport experiments.

Furthermore, the addition of highly concentrated solutions (i.e., high quantities of fertilizer) to volcanic soils promotes the interaction of physical and chemical processes that could result in different parameter values for the commonly used solute transport models (e.g., Convection-Dispersion equation) as discussed in the following section.

The effect of solution chemistry and flow rate on apparent solute transport parameters:

Several authors have suggested the importance of chemical and physical interactions for the transport of solutes (Chen et al., 2021; Erfani et al., 2021; Muniruzzaman and Rolle, 2021; Rolle et al., 2013b, 2013a). However, solute transport models that consider these interactions are still scarce. Our results corroborated that physical-chemical interactions are essential for simulating nutrient transport in undisturbed volcanic soils and under unsaturated conditions. In addition, our results demonstrated that simple approaches typically used for the simulation of nutrient transport in soils (e.g., the implementation of linear or non-linear sorption isotherms and their respective calculation of retardation factors or the implementation of the Convection Dispersion Equation (CDE) under conditions with contrasting concentration gradients) should be reconsidered. For example, Peters et al. (2019) showed by numerical simulations that the dispersive term of the CDE is not applicable for conditions with strong concentration gradients. These results agree with the different dispersion coefficients we obtained under different concentrations for our NaCl transport experiments and with the hysteresis directly measured by Chen et al. (2021) in a repacked sand system.

Despite the evidence that geochemical and physical interactions play an essential role in the transport of nutrients, the implementation of conventional approaches disregarding these interactions are widely available, and the options of models that consider these interactions are limited. A potential solution to these issues is the coupled versions of geochemical and hydrological models like HYDRUS-PHREEQC (Jacques et al., 2018b, 2002; Jacques and Simunek, 2005). This approach calculates the water flux for each cell at different timesteps employing the Richards equation, and then the geochemical model calculates the equilibrium concentration for each cell, avoiding simplifications of the modeled system. Peters et al. (2019)

also suggested other alternative model options for the description of solute transport under variable concentration gradients that produce unrealistic direction and magnitude of the dispersive flux of the CDE, for example, random-walk particle tracking methods implementing dispersion as an anisotropic random process, or Navier–Stokes related approaches. However, these alternative model options should still be tested against experimental data.

Implementing the CD-MUSIC-NICA-Donnan models coupled with hydrological steady-state or variably saturated models (e.g., with HYDRUS) still requires advances currently under development.

5.3 Application of the research findings:

Chapter 2:

The excellent modeling results of Chapter 2 provided a better understanding of the boron adsorption process in a volcanic soil system. A better comprehension of the boron adsorption process helps to establish better management practices for improving the plant boron nutrient status, increasing nutrient use efficiency, and reducing leaching losses in volcanic soil systems.

In addition, the good match between boron modeled and experimental data encourages the coupling of the CD-MUSIC-NICA-Donnan model with hydrological models, which could simulate the boron transport under multi-component conditions in volcanic soils, as well as in other complex soil systems.

Furthermore, the high solubility of boric acid in the acid volcanic ash-derived soils suggests the need for splitting the applications of this boron source to increase the boron use efficiency and provide the crops with the correct boron amounts according to the crop requirements. Another possible solution to the boron leaching problem could be the usage of different boron sources

Chapter 3:

The information obtained in Chapter 3 about the increased solubility and leaching of zinc under the application of high rates of potassium chloride brings clues about the better management of zinc in these volcanic soil systems. For example, some growers currently apply potassium and zinc fertilizer simultaneously, but considering the increased zinc availability produced by the potassium chloride application, it is not necessary to increase the zinc concentrations even more during periods of increased zinc availability. After the potassium chloride concentration has decreased in the soil (e.g., from the root

zone area), the zinc concentrations in the solution return to limiting conditions for plant uptake in these volcanic soils, which is the right moment for supplying zinc to the crops.

Additionally, the increased leaching of zinc under the addition of high potassium chloride rates indicates that the tropical volcanic soil systems from humid regions require careful zinc management to avoid current zinc deficiencies and to avoid its future appearance by applying very high potassium fertilizer rates.

A better understanding of the fertilizer interactions and side effects is very helpful for increasing nutrient use efficiency and avoiding the excessive solubility and leaching of micronutrients and undesired elements such as heavy metals.

Chapter 4:

The results of Chapter 4 gave important information for future modeling of nutrient transport in volcanic soil systems, and it is clear that concentration matters for nutrient transport in volcanic soils. Furthermore, Chapter 4 emphasizes the need for developing and applying modeling approaches considering the coupled interaction between physical and chemical processes.

These new findings on the concentration dependence of transport processes enhance our understanding of fertilizer movement in soil systems, in which transport times are considerably larger for low concentration conditions, and hysteresis between the solute loading and unloading modifies the values of solute transport model parameters.

5.4 Critical analysis of the obtained results:

First, our work still has several limitations in predicting the effect of high fertilizer rates in volcanic soil systems. For zinc adsorption, we were not able to implement an entirely mechanistic modeling approach, and this issue limits the implementation of future mechanistic reactive transport model simulations for zinc.

Second, in the current advance of our research in volcanic soils, we are paying more attention to the chemical processes and just an incipient incursion in the transport processes. However, our current approach did not consider other processes like root water and nutrient uptake, crop growth processes, plant metabolism, or environmental forcing to describe the real availability and transport of a nutrient in an agricultural production system. In this case, a better understanding of the transport of solutes and a reliable

enhancement in nutrient management requires the integrated evaluation of soil-driven processes with plant and atmospheric-driven processes. For example, the integration of geochemical, hydrological, root water and nutrient uptake models, crop growth models, and atmospheric or environmental models. However, each of these model modules has particular complexities that difficult its implementation in a general modeling framework. Despite the complex reality of natural production systems, it is essential to comprehend individual processes that may affect production or threaten the environment.

For Chapter 4, the hydrodynamic parameters of our transport systems were fitted to breakthrough curve data. According to several authors (Chen et al., 2021; Erfani et al., 2021; Karadimitriou et al., 2017), the results of optimization methods for two-phase transport systems (e.g., by CXTFIT optimization) differ strongly from directly measured data. For future research on the effect of solution concentrations on the hydrodynamic solute transport parameters, it would be desirable to incorporate more advanced techniques to measure these parameters directly. For the present research, the lack of access to specialized equipment and the financial aspects did not allow incorporate these state-of-the-art techniques (e.g., fast 4D synchrotron x-ray imaging) into our experiments. For future related experiments, the combination of the simple techniques implemented in our experiments with more advanced ones may bring more robust and conclusive data.

5.5 Future advancements:

The improvement of fertilizer management practices for highly fertilized agricultural systems could be strongly beneficiated by implementing mechanistic modeling approaches to test different practices related to the 4R-stewardship (practices to increase the nutrient use efficiency) (Johnston and Bruulsema, 2014). The good results obtained for boron adsorption with the CD-MUSIC-NICA-Donnan approach encourage the implementation of this model coupled with a hydrological model.

For the case of zinc transport in these volcanic soils, the results obtained in this thesis by empirical adsorption models showed the need to implement mechanistic approaches to calculate zinc sorption. The zinc retardation factor estimated by the linear adsorption isotherms differed strongly from the zinc transport data obtained by applying the highly concentrated potassium chloride solution to our column transport experiments (potassium breakthrough curves). Therefore, to estimate the zinc desorption and transport from these soils, it is necessary to include modeling approaches that account for the multi-component interactions between ionic strength, pH, DOC, and concentrations of different ions that could interact with the reactive zinc fractions. However, implementing the CD-MUSIC model for zinc adsorption in these volcanic soils still requires evaluating the zinc adsorption process at higher solution concentrations; as for the

concentrations obtained in our current batch adsorption experiments, the geochemical model was not able to simulate the obtained results and overestimated the zinc adsorbed fraction.

Therefore, a logical step I should take after the conclusion of this thesis is the validation of coupled reactive transport models (hydrological and geochemical), starting with controlled steady-state water fluxes and then, depending on the results, implementing the models under field transient conditions. The Multi-Step Flux Transport setup implemented for column transport experiments complies with the assumption of steady-state water flow. Therefore, this experimental setup will allow the evaluation of the geochemical model performance when coupled to water movement processes in soil column experiments.

A second step is validating coupled hydrological distributed and geochemical models under field conditions. This kind of coupled code already exists (e.g., HYDRUS-PHREEQC), but as far as the author is concerned, the available codes do not include the last version of the CD-MUSIC model. Therefore, the upcoming software versions that include the ORCHESTRA coupled with hydrological models will be advantageous for incorporating the last version of the CD-MUSIC model into reactive transport models.

Regarding the excess of N-P-K fertilizers applied to intensive agricultural production systems, to avoid the fertilizer excess is necessary to estimate the kinetics of root nutrient uptake for highly demanding crops to supply the correct amounts of fertilizer according to the root nutrient uptake capacity. For example, implementing the Michaelis-Menten kinetics (Epstein and Hagen, 1951) or the Flow-Force model (Le Deunff et al., 2016; Le Deunff and Malagoli, 2014; Malagoli and Le Deunff, 2014; Thellier, 1971, 1970) for the estimation of root nutrient uptake. Such kind of Michaelis-Menten kinetics data is available for extensive grain crops like wheat, barley, and rice (Botella et al., 1994; Fageria, 1976; Hasegawa and Ichii, 1994; Nielsen and Schjorring, 1983; Raman et al., 1995; Youngdahl et al., 1982), but it is scarce for uncommon and highly demanding crops like papaya. In this way, the knowledge of root nutrient uptake kinetics will define critical concentrations for each specific nutrient (e.g., the Cmin or Km parameters from the Michaelis-Menten approach). The definition of critical concentrations for root nutrient uptake integrated with the calculation of soil solution concentrations in the root zone area (by coupled geochemical and hydrological models) should improve fertilizer dosage and timing, reducing the side environmental risks and increasing the fertilizer use efficiency.

5.6 References:

Arias, M., Pérez-Novo, C., Osorio, F., López, E., Soto, B., 2005. Adsorption and desorption of copper and zinc in the surface layer of acid soils. J. Colloid Interface Sci. 288, 21–29. https://doi.org/10.1016/j.jcis.2005.02.053

Barrow, N.J., 1993. Mechanisms of Reaction of Zinc with Soil and Soil Components BT - Zinc in Soils and Plants: Proceedings of the International Symposium on 'Zinc in Soils and Plants' held at The University of Western Australia, 27–28 September, 1993, in: Robson, A.D. (Ed.), . Springer Netherlands, Dordrecht, pp. 15–31. https://doi.org/10.1007/978-94-011-0878-2_2

Botella, M.A., Cerdá, A., Lips, S.H., 1994. Kinetics of NO3− and NH4+ Uptake by Wheat Seedlings. Effect of Salinity and Nitrogen Source. J. Plant Physiol. 144, 53–57. https://doi.org/10.1016/S0176-1617(11)80992-2

Buurman, P., Peterse, F., Almendros Martin, G., 2007. Soil organic matter chemistry in allophanic soils: A pyrolysis-GC/MS study of a Costa Rican Andosol catena. Eur. J. Soil Sci. 58, 1330–1347. https://doi.org/10.1111/j.1365-2389.2007.00925.x

Casagrande, J.C., Alleoni, L.R.F., De Camargo, O.A., Arnone, A.D., 2004. Effects of pH and ionic strength on zinc sorption by a variable charge soil. Commun. Soil Sci. Plant Anal. 35, 2087–2095. https://doi.org/10.1081/LCSS-200028914

Chen, Y., Steeb, H., Erfani, H., Karadimitriou, N.K., Walczak, M.S., Ruf, M., Lee, D., An, S., Hasan, S., Connolley, T., Vo, N.T., Niasar, V., 2021. Nonuniqueness of hydrodynamic dispersion revealed using fast 4D synchrotron x-ray imaging. Sci. Adv. 7, 1–7. https://doi.org/10.1126/sciadv.abj0960

Duffner, A., Weng, L., Hoffland, E., Van Der Zee, S.E.A.T.M., 2014. Multi-surface modeling to predict free zinc ion concentrations in low-zinc soils. Environ. Sci. Technol. 48, 5700–5708. https://doi.org/10.1021/es500257e

Dyer, J.A., Trivedi, P., Scrivner, N.C., Sparks, D.L., 2004. Surface complexation modeling of zinc sorption onto ferrihydrite. J. Colloid Interface Sci. 270, 56–65. https://doi.org/10.1016/S0021-9797(03)00618-0

Epstein, E., Hagen, C.E., 1951. A kinetic study of the absorption of alkali cations by barley roots. Plant Physiol. 27, 457–474. https://doi.org/doi: 10.1104/pp.27.3.457

Erfani, H., Karadimitriou, N.K., Nissan, A., Walczak, M.S., An, S., Berkowitz, B., Niasar, V., 2021. Process-Dependent Solute Transport in Porous Media. Transp. Porous Media 140, 421–435. https://doi.org/10.1007/s11242-021-01655-6

Fageria, N.K., 1976. Kinetics of magnesium uptake by rice plants. Biol. Plant. 18, 169–172. https://doi.org/10.1007/BF02922795

Fest, E.P.M.J., Temminghoff, E.J.M., Griffioen, J., Van Riemsdijk, W.H., 2005. Proton buffering and metal leaching in sandy soils. Environ. Sci. Technol. 39, 7901–7908. https://doi.org/10.1021/es0505806

Goldberg, S., Corwin, D.L., Shouse, P.J., Suarez, D.L., 2005. Prediction of Boron Adsorption by Field Samples of Diverse Textures. Soil Sci. Soc. Am. J. 69, 1379–1388. https://doi.org/10.2136/sssaj2004.0354

Goldberg, S., Glaubig, R.A., 1985. Boron Adsorption on Aluminum and Iron Oxide Minerals. Soil Sci.

Soc. Am. J. 49, 1374–1379.

Goli, E., Hiemstra, T., Rahnemaie, R., 2019. Interaction of boron with humic acid and natural organic matter: Experiments and modeling. Chem. Geol. 515, 1–8. https://doi.org/10.1016/j.chemgeo.2019.03.021

Gurpreet-Kaur, Sharma, B.D., Sharma, S., 2013. Effects of Organic Matter and Ionic Strength of Supporting Electrolyte on Zinc Adsorption in Benchmark Soils of Punjab in Northwest India. Commun. Soil Sci. Plant Anal. 44, 922–938. https://doi.org/10.1080/00103624.2012.747602

Hasegawa, H., Ichii, M., 1994. Variation in Michaelis-Menten kinetic parameters for nitrate uptake by the young seedlings in rice (Oryza sativa L.). Breed. Sci. 44, 383–386.

Jacques, D., Mallants, D., Genuchten, M.T. Van, 2018a. The HPx software for multicomponent reactive transport during variably-saturated flow: Recent developments and applications 1–16. https://doi.org/10.1515/johh-2017-0049

Jacques, D., Simunek, J., 2005. User Manual of the Multicomponent Variably- Saturated Flow and Transport Model HP1.

Jacques, D., Simunek, J., Mallants, D., van Genuchten, M.T., 2002. Multicomponent transport model for variably-saturated porous media: application to the transport of heavy metals in soils, in: Hassanizadeh, S.M., Schotting, R.J., Gray, W.G., Pinder, G.F. (Eds.), Developments in Water Science. Elsevier, pp. 555–562. https://doi.org/https://doi.org/10.1016/S0167-5648(02)80108-3.

Jacques, D., Šimůnek, J., Mallants, D., Van Genuchten, M.T., 2018b. The HPx software for multicomponent reactive transport during variably-saturated flow: Recent developments and applications. J. Hydrol. Hydromechanics 66, 211–226. https://doi.org/10.1515/johh-2017-0049

Johnston, A.M., Bruulsema, T.W., 2014. 4R nutrient stewardship for improved nutrient use efficiency. Procedia Eng. 83, 365–370. https://doi.org/10.1016/j.proeng.2014.09.029

Karadimitriou, N.K., Joekar-Niasar, V., Brizuela, O.G., 2017. Hydro-dynamic Solute Transport under Two-Phase Flow Conditions. Sci. Rep. 7, 1–7. https://doi.org/10.1038/s41598-017-06748-1

Le Deunff, E., Malagoli, P., 2014. An updated model for nitrate uptake modelling in plants. I. Functional component: Cross-combination of flow-force interpretation of nitrate uptake isotherms, and environmental and in planta regulation of nitrate influx. Ann. Bot. 113, 991–1005. https://doi.org/10.1093/aob/mcu021

Le Deunff, E., Tournier, P.H., Malagoli, P., 2016. The thermodynamic flow-force interpretation of root nutrient uptake kinetics: A powerful formalism for agronomic and phytoplanktonic models. Front. Physiol. 7, 1–18. https://doi.org/10.3389/fphys.2016.00243

Malagoli, P., Le Deunff, E., 2014. An updated model for nitrate uptake modelling in plants. II. Assessment of active root involvement in nitrate uptake based on integrated root system age: Measured versus modelled outputs. Ann. Bot. 113, 1007–1019. https://doi.org/10.1093/aob/mcu022

Mendez, J.C., Hiemstra, T., 2020. High and low affinity sites of ferrihydrite for metal ion adsorption: Data and modeling of the alkaline-earth ions Be, Mg, Ca, Sr, Ba, and Ra. Geochim. Cosmochim. Acta 286, 289–305. https://doi.org/10.1016/j.gca.2020.07.032

Muniruzzaman, M., Rolle, M., 2021. Impact of diffuse layer processes on contaminant forward and back diffusion in heterogeneous sandy-clayey domains. J. Contam. Hydrol. 237, 103754. https://doi.org/10.1016/j.jconhyd.2020.103754

Nielsen, N.E., Schjorring, J.K., 1983. Efficiency and kinetics of phosphorus uptake from soil by various barley genotypes. Plant Soil 72, 225–230.

Nomaan, S.M., Stokes, S.N., Han, J., Katz, L.E., 2021. Application of spectroscopic evidence to diffuse layer model (DLM) parameter estimation for cation adsorption onto ferrihydrite in single- and bi-solute systems. Chem. Geol. 573, 120199. https://doi.org/10.1016/j.chemgeo.2021.120199

Peters, A., Iden, S.C., Durner, W., 2019. Local Solute Sinks and Sources Cause Erroneous Dispersion Fluxes in Transport Simulations with the Convection–Dispersion Equation. Vadose Zo. J. 18, 190064. https://doi.org/10.2136/vzj2019.06.0064

Raman, D.R., Spanswick, R.M., Walker, L.P., 1995. The kinetics of nitrate uptake from flowing solutions by rice: Influence of pretreatment and light. Bioresour. Technol. 53, 125–132. https://doi.org/10.1016/0960-8524(95)98138-E

Rolle, M., Chiogna, G., Hochstetler, D.L., Kitanidis, P.K., 2013a. On the importance of diffusion and compound-specific mixing for groundwater transport: An investigation from pore to field scale. J. Contam. Hydrol. 153, 51–68. https://doi.org/10.1016/j.jconhyd.2013.07.006

Rolle, M., Muniruzzaman, M., Haberer, C.M., Grathwohl, P., 2013b. Coulombic effects in advection-dominated transport of electrolytes in porous media: Multicomponent ionic dispersion. Geochim. Cosmochim. Acta 120, 195–205. https://doi.org/10.1016/j.gca.2013.06.031

Selim, H.M., 2016. Competitive sorption of heavy metals in soils: Experimental evidence, in: Selim, H.M. (Ed.), Competitive Sorption and Transport of Heavy Metals in Soils and Geological Media. CRC Press, pp. 1–48. https://doi.org/10.1201/b13041-8

Shuman, L.M., 1986. Effect of Ionic Strength and Anions on Zinc Adsorption by Two Soils. Soil Sci. Soc. Am. J. 50, 1438–1442. https://doi.org/10.2136/sssaj1986.03615995005000060012x

Su, C., Suarez, D.L., 1995. Coordination of Adsorbed Boron: A FTIR Spectroscopic Study. Environ. Sci. Technol. 29, 302–311. https://doi.org/10.1021/es00002a005

Takahashi, T., Shoji, S., 2002. Distribution and Classification of Volcanic Ash Soils. Glob. Environ. Res. 6, 83–97.

Terraza Pira, M.F., Sumner, M.E., Cabrera, M.L., Thompson, A., 2018. Boron Adsorption and Desorption on Volcanic Ash–Derived Soils. Soil Sci. Soc. Am. J. 82, 66–75. https://doi.org/10.2136/sssaj2016.08.0264

Thellier, M., 1971. Non-equilibrium thermodynamics and electrokinetic interpretation of biological systems. J. Theor. Biol. 31, 389–393. https://doi.org/10.1016/0022-5193(71)90017-8

Thellier, M., 1970. An Electrokinetic Interpretation of the Functioning of Biological Systems and its Application to the Study of Mineral Salts Absorption. Ann. Bot. 34, 983–1009.

Trivedi, P., Axe, L., 2001. Ni and Zn sorption to amorphous versus crystalline iron oxides: Macroscopic studies. J. Colloid Interface Sci. 244, 221–229. https://doi.org/10.1006/jcis.2001.7970

Trivedi, P., Dyer, J.A., Sparks, D.L., Pandya, K., 2004. Mechanistic and thermodynamic interpretations of zinc sorption onto ferrihydrite. J. Colloid Interface Sci. 270, 77–85. https://doi.org/10.1016/S0021-9797(03)00586-1

Van Eynde, E., Groenenberg, B.J., Hoffland, E., Comans, R.N.J., 2022a. Solid-solution partitioning of micronutrients Zn, Cu and B in tropical soils: mechanistic and empirical models. Geoderma 414, 115773. https://doi.org/10.1016/j.geoderma.2022.115773

Van Eynde, E., Hiemstra, T., Comans, R.N.J., 2022b. Interaction of Zn with ferrihydrite and its cooperative binding in the presence of PO4. Geochim. Cosmochim. Acta 320, 223–237. https://doi.org/10.1016/j.gca.2022.01.010

Van Eynde, E., Mendez, J.C., Hiemstra, T., Comans, R.N.J., 2020a. Boron Adsorption to Ferrihydrite with Implications for Surface Speciation in Soils: Experiments and Modeling. ACS Earth Sp. Chem. 4, 1269–1280. https://doi.org/10.1021/acsearthspacechem.0c00078

Van Eynde, E., Weng, L., Comans, R.N.J., 2020b. Boron speciation and extractability in temperate and tropical soils: A multi-surface modeling approach. Appl. Geochemistry 123, 104797. https://doi.org/10.1016/j.apgeochem.2020.104797

Vaughan, P.J., Suarez, D.L., 2003. Constant Capacitance Model Computation of Boron Speciation for Varying Soil Water Content. Methods 253–258. https://doi.org/10.2113/2.2.253

Youngdahl, L.J., Pacheco, R., Street, J.J., Vlek, P.L.G., 1982. The kinetics of ammonium and nitrate uptake by young rice plants. Plant Soil 69, 225–232.

SUMMARY

Volcanic ash-derived soils are important for agricultural production and sustain large populations worldwide. The main reason for this is their favorable physical properties like low bulk density, high water storage capacity, and high water permeability. Many of these volcanic soils are located in tropical and subtropical regions under high precipitation (udic) regimes. Under such conditions, where leaching of elements can be significant, the mobility of fertilizers in soil and their interaction with other nutrients is an important factor to consider for the optimal fertilization management. In this Ph.D. thesis, we evaluated the effect of high phosphate and high potassium solution concentration on the sorption interaction with micronutrients (B and Zn), and the effect of high potassium solution concentration on the zinc transport in alluvial volcanic ash soils. Additionally, we evaluated whether the increased saline concentrations in the solution modify the values of the hydrodynamic solute transport parameters used for modeling solute transport in porous soil systems.

In Chapter 2, we evaluated the effect of high phosphate solution concentration on boric acid adsorption. For this experiment, we collected an alluvial volcanic ash soil from San Bosco, Pococí, Costa Rica, and developed a series of batch adsorption experiments with and without the addition of phosphate and employing boric acid as a boron source. To gain more insight into the process and mechanisms of boron adsorption in these volcanic soils, we implemented a state-of-the-art multi-surface adsorption model (CD-MUSIC-NICA-Donnan), employing adsorption parameters recently determined in pure suspension systems (i.e., ferrihydrite and humic acids) and considering the directly optimized reactive surface area of this soil. This experiment and the model results showed that the high phosphate rates commonly applied to this volcanic soil have minor effects on boron adsorption at the typical low boron concentrations observed in the sampled region. In addition, the experimental results showed a slight competition between the added phosphate with boric acid only at high boron concentrations. The modeling results suggest that phosphate does not affect the boric acid adsorption due to the difference in the principal adsorption mechanisms when both nutrients are present in the soil system. Phosphate is adsorbed as inner-sphere species. In contrast, boric acid can be adsorbed by both mechanisms (inner-sphere or outer-sphere), but under the presence of phosphate, boric acid adsorbs as outer-sphere species, and due to its neutral charge, it is not affected by the charge generated by inner-sphere adsorption of phosphate.

In chapter 3, we evaluated the effect of high potassium chloride (KCl) concentrations on the zinc sorption process and its transport in undisturbed soil column experiments under unsaturated conditions. For this experiment, we collected two volcanic ash soils from San Bosco and La Sonia, Pococí, Costa Rica. First, considering that KCl additions modify the pH and the salt concentration in solution, we developed

zinc batch adsorption experiments at different pH and different solution ionic strengths. For this experiment, we found that a lower pH and a higher ionic strength promote increased zinc solution concentrations in both volcanic soils. Also, we developed a zinc desorption-transport experiment using undisturbed soil cores where we applied several pore volumes of the following treatments: 1). Initially, the columns were saturated with a 0.001M $CaCl_2$. 2). We loaded the KCl into the column by the addition of the 0.001M $CaCl_2$ + 0.064 M KCl solution. 3). We unloaded the potassium chloride from the column by applying a 0.001M $CaCl_2$ solution. 4). We loaded the KCl solution to the column again by applying the 0.001M $CaCl_2$ + 0.064 M KCl. 5) We unloaded the KCl solution from the soil column by applying the 0.001M $CaCl_2$ solution. This set of experiments showed that adding highly concentrated potassium chloride solutions promotes zinc desorption and leaching from these alluvial volcanic ash soils, which was related to the changes in solution pH, ionic strength, and DOC content.

Chapter 4 evaluated the effect of solution concentration and flux rate on the values of the hydrodynamic solute transport parameters using sodium chloride as a tracer solution and measuring the changes in the raw electric conductivity (mV/V). For the experiment about the effect of flow rate, we used undisturbed soil columns where we increased or decreased the solution concentration at different flow rates. For this experiment, we found different values of hydrodynamic solute transport parameters at the different flow rates and a strong hysteresis effect between the loading and unloading of the saline solution from the columns. Consequently, we explored the effect of solution concentration on the hysteresis phenomena and the effect of the solution concentration on the values of hydrodynamic solute transport parameters. For this additional set of experiments, we started our experiments with undisturbed soil columns with an increased sodium chloride concentration which was decreased by the application of sequential step inputs of a lower concentration solution until the final application of deionized water. Later, we increased the concentrations sequentially in the column, developing step inputs of NaCl breakthrough curves. The results of these experiments showed that hydrodynamic parameters depend on the concentration of the solution flowing through the column. Therefore, knowing these effects and the range of fitted parameter values is essential when modeling and predicting soil nutrient transport.

The results of these experiments showed important physical-chemical interactions of nutrients when applied at high rates in volcanic ash soil systems. These interactions should be considered for the proper fertilization management in volcanic ash soil systems.

Acknowledgments:

First of all, my profound gratitude is to Prof. Sjoerd van der Zee for his kindness and for accepting me as a Ph.D. student under his supervision, and therefore I extend my gratitude to his wife Gemma. Also, my profound gratitude to J.C.L. (Hans) Meeussen, who supervised and corrected my work during this last stage and made important contributions since the beginning of this Ph.D. project. Hans also made possible the implementation of the programming changes required for running the state-of-the-art version of the CD-MUSIC model into the ORCHESTRA code and patiently explained to me how to run the models in ORCHESTRA. To Harm Gooren for his valuable help in building the transport devices, and for the explanations about electronic issues.

To Prof. Violette Geissen for accepting to be my promotor and helping me to finalize the thesis, and to Prof. Coen Ritsema, for the help in solving the difficult situations faced during the last stage of my Ph.D.

Furthermore, my gratitude to Juan Carlos Méndez, that explained to me geochemical processes and modeling issues that I could not understand by self-learning. To Manuel Camacho for the correction of grammar mistakes and explanations about how to improve my poor writing skills. I also appreciate the unconditional help received from Bryan Alemán-Montes (University of Costa Rica) regarding the additional ongoing work related to this thesis.

To my wife Laura and to my daughters Leonela and Lourdes.

To our family friends in The Netherlands and the people of CNS-basisschool Wilhelmina in Bennekom, all of you hold a special place in our hearts.

To Marnella van der Tol, your kindness inspires other people!

To my colleagues from UCR and WUR, and for all the people that helped with different situations during these years that allowed the conclusion of this project. No one accomplishes goals alone!

To the Ministry of Science and Technology of Costa Rica, for the funds received (irresponsibly delayed and interrupted during the development of the Ph.D.)

I thank the University of Costa Rica for providing complementary funds for developing this thesis.

To my family, and specially to my father.

Netherlands Research School for the
Socio-Economic and Natural Sciences of the Environment

D I P L O M A

for specialised PhD training

The Netherlands research school for the
Socio-Economic and Natural Sciences of the Environment
(SENSE) declares that

Róger Armando Fallas Corrales

born on 12th June 1985 in Vuelta de Jorco, San José, Costa Rica

has successfully fulfilled all requirements of the
educational PhD programme of SENSE.

Wageningen, 1st November 2022

Chair of the SENSE board

Prof. dr. Martin Wassen

The SENSE Director

Prof. Philipp Pattberg

The SENSE Research School has been accredited by the Royal Netherlands Academy of Arts and Sciences (KNAW)

KONINKLIJKE NEDERLANDSE
AKADEMIE VAN WETENSCHAPPEN

The SENSE Research School declares that **Róger Armando Fallas Corrales** has successfully fulfilled all requirements of the educational PhD programme of SENSE with a work load of 38.6 EC, including the following activities:

SENSE PhD Courses

- Environmental research in context (2018)
- Research in context activity: 'Dissemination of knowledge to inter- and transdisciplinary groups' (2022)

Other PhD and Advanced MSc Courses

- Fundamentals of Crop Physiology in a Changing World, PE&RC and University of Florida (2018)
- ABC/J Summer School 'Hydrogeophysics', Geoverbund (2018)
- Grand Paradisso Summer School 'Critical Zone and Ecosystem Dynamics', National Research Council of Italy (2018)
- Subsurface Solute Transport, Wageningen University (2018)
- Summer School for Flow and Transport in Terrestrial Systems, TU Clausthal (2018)
- Nutritional Physiology of Crop Plants, Universidad de Costa Rica & Hohenheim University (2019)
- The Art of Modelling, PE&RC and WIMEK (2019)
- Dynamic Models in R, PE&RC (2019)
- ORCHESTRA workshop, SLM chair group Wageningen University (2019)
- Vegetable Growing in a Climate Change Conditions, Universidad de Costa Rica & Hohenheim University (2019)
- Python Programming for Scientists (Programación en Python para Científicos), Colaboratorio Nacional de Computación Avanzada, Centro Nacional de Alta Tecnología (2019)
- Machine Learning with Python, Colaboratorio Nacional de Computación Avanzada, Centro Nacional de Alta Tecnología (2020)

Oral Presentations

- *Boron adsorption and competition with phosphate in a volcanic ash-derived soil*. AGU Fall Meeting, 13-17 December 2021, New Orleans, LA, United states

SENSE coordinator PhD education

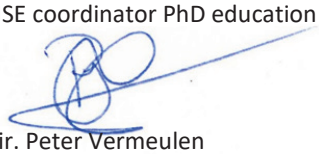

Dr. ir. Peter Vermeulen

The research described in this thesis was financially supported by The Ministry of Science, Technology and Telecommunications of Costa Rica (MICITT), under the PINN-MICITT program (contract 2-1-4-17-1-014), and by the University of Costa Rica (contract OAICE 53-2018).

Financial support from Wageningen University for printing this thesis is gratefully acknowledged.

Cover design by Edgar Díaz Mora

Printed by ProefschriftMaken || DigiForce